DISSERTATION

# MICROCHIP CAPILLARY ELECTROPHORESIS: IMPROVEMENTS USING DETECTION GEOMETRY, ON-LINE PRECONCENTRATION AND SURFACE MODIFICATION

Submitted by

Qian Guan

Department of Chemistry

In partial fulfillment of the requirements

For the Degree of Doctor of Philosophy

Colorado State University

Fort Collins, Colorado

Summer 2012

Doctoral Committee:

Advisor: Charles S. Henry

Steven H. Strauss
Alan K Van Orden
Amber Krummel
William H. Hanneman

ABSTRACT

MICROCHIP CAPILLARY ELECTROPHORESIS: IMPROVEMENTS USING DETECTION GEOMETRY, ON-LINE PRECONCENTRATION AND SURFACE MODIFICATION

Capillary electrophoresis and related microfluidic technologies have been utilized with great success for a variety of bioanalytical applications. Microchip capillary electrophoresis (MCE) has the advantages of decreased analysis time, integrated sample processing, high portability, high throughput, minimal reagent consumption, and low analysis cost. This thesis will focus on the optimization of our previous microchip capillary electrophoresis coupled electrochemical detection (MCE-ECD) design for improved separation and detection performance using detection geometry, on-line preconcentration and surface modification.

The first effort to improve detection sensitivity and limits of detection (LODs) of our previous MCE-ECD system is established by an implementation of a capillary expansion (bubble cell) at the detection zone. Bubble cell widths were varied from 1× to 10× the separation channel width (50 μm) to investigate the effects of electrode surface area on detection sensitivity, LOD, and separation efficiency. Improved detection sensitivity and decreased LODs were obtained with increased bubble cell width, and LODs of dopamine and catechol detected in a 5× bubble cell were 25 nM and 50 nM respectively. In addition, fluorescent imaging results demonstrate ~8% to ~12% loss in separation efficiency in 4× and 5× bubble cell, respectively. Another effort for enhancing detection sensitivity and reducing LODs involves using field amplified sample injection and field amplified sample stacking. Stacking effects were shown for both methods using DC amperometric and pulsed amperometric detections. Decreased LODs of dopamine were achieved using both on-line sample preconcentration methods.

The use of mixed surfactants to affect electroosmotic flow (EOF) and alter separation selectivity for electrophoretic separations in poly(dimethylsiloxane) (PDMS) is also presented in this thesis. First the effect of surfactant concentration on EOF was studied using the current monitoring method for a single anionic surfactant (sodium dodecyl sulfate, SDS), a single zwitterionic surfactant (N-tetradecylammonium-N,N-dimethyl-3-ammonio-1-propane sulfonate, TDAPS), and a mixed ionic/zwitterionic surfactant system (SDS/TDAPS). SDS increases the EOF as reported previously while TDAPS shows an initial increase in EOF followed by a reduction in EOF at higher concentrations. The addition of TDAPS to a solution containing SDS makes the EOF decrease in a concentration dependent manner. The mixed SDS/TDAPS surfactant system allows tuning of the EOF across a range of pH and concentration conditions. After establishing EOF behavior, the adsorption/desorption rates were measured and show a slower adsorption/desorption rate for TDAPS than SDS. Next, capacitively coupled contactless conductivity detection ($C^4D$) is introduced for EOF measurements on PDMS microchips as an alternative to the current monitoring method to improve measurement reproducibility. EOF measurements as a function of the surfactant concentration were performed simultaneously using both methods for three nonionic surfactants, (polyoxyethylene (20) sorbitan monolaurate (Tween 20), polyoxyethylene octyl phenyl ether (Triton X-100), polyethylene glycol, (PEG 400)), mixed ionic/nonionic surfactant systems (SDS/Tween 20, SDS/Triton X-100, and SDS/PEG 400) and mixed zwitterionic/nonionic surfactant systems (TDAPS/Tween 20, TDAPS/Triton X-100, and TDAPS/PEG 400). EOF for the nonionic surfactants decreases with increasing surfactant concentration. The addition of SDS or TDAPS to a nonionic surfactant increases EOF relative to the pure nonionic surfactant. Next, separation and electrochemical detection of two groups of model analytes were explored using mixed surfactant systems. Similar analyte resolution with

greater peak heights was achieved with mixed surfactant systems relative to the single surfactant system. Finally, the utility of mixed surfactant systems to achieve improved separation chemistry of biologically relevant compounds in complex sample matrixes was demonstrated in two applications, which include the detection of catecholamine release from rat pheochromocytoma (PC12) cells by stimulation with 80 mM $K^+$ and the detection of reduced glutathione (GSH) in red blood cells (RBCs) exposed to fly ash suspension as a model environmental oxidant.

# ACKNOWLEDGEMENTS

It is my pleasure to thank the assistance and contributions of various individuals during my Ph.D. studying period. First I would like to express my profound gratitude to: my supervisor, Prof. Charles S. Henry for giving me the opportunity to work on my thesis in his group. I greatly appreciate his immense help to get my projects off the ground and running and his guidance throughout the entire process.

Many thanks to Dr. Jon Vickers, Dr. Ryan E. Holcomb and Dr. James R. Kraly, who gave me valuable aids on the instrument running of microchip capillary electrophoresis coupled with electrochemical detection and conventional capillary electrophoresis with UV detection. Dr. Scott D. Noblitt is acknowledged for his enthusiastic help on providing useful insight and a variety of discussion throughout my projects. Also many thanks to Dr. Jason Emory for the many resources he provided for my research and assistance with manuscript preparation. I also express my gratitude to all group members present and past for their cooperative spirit and contribution to the friendly atmosphere prevalent in the group.

Many thanks go to my committee members for guidance and advice along the way.

Funding for my two projects came from the National Institutes of Health grant EB 004876-01A1 and 2R44HL083579-02A1 through a sub-contract from Advanced MicroLabs, LLC.

I would like to thank all my friends who have encouraged me and had nice time with me. Finally, I would like to appreciate my husband Dr. Kai Li and my parents. Their encouragements gave me so much strength to complete my study.

TABLE OF CONTENTS

ABSTRACT..... ……ii

ACKNOWLEDGEMENTS ……v

LIST OF FIGURES……ix

.

CHAPTERS

1. INTRODUCTION .....1
1.1 Dissertation overview .....1
1.2 Capillary electrophoresis .....3
1.2.1 Modes of CE .....3
1.2.2 Electroosmotic Flow and Electrophoretic Mobility.....5
1.2.3 EOF Measurement Methods .....7
1.3 MCE-ECD.....9
1.4 On-line Sample Preconcentration Methods .....14
1.5 Surface Modification .....15
1.6 Important Electrochemically Active Analytes.....18
1.6.1 Catecholamines.....18
1.6.2 Thiols .....19
1.7 References.....22

2. INCORPORTION OF A BUBBLE CELL IN DETECTION ZONE FOR IMPROVING THE DETECTION SENSITIVITY AND LODS OF MCE-ECD .....29
2.1 Introduction.....29
2.2 Experimental.....30
2.2.1 Chemicals.....30
2.2.2 PDMS Microchip Fabrication.....31
2.2.3 MCE-ECD.....34
2.3 Results and Discussion .....35
2.3.1 Bubble Cell Design .....35
2.3.2 Characterization of Bubble Cell Design with DC Amperometric Detection.....35
2.3.3 Impact of Bubble Cell Widths on Separation Efficiency.....38
2.4 Conclusions.....40
2.5 References.....42

3. FURTHER IMPROVEMENT IN DETECTION PERFORMANCE OF MCE-ECD USING FASI OR FASS.....43
3.1 Introduction.....43
3.2 Experimental.....45

3.2.1 Chemicals....45
3.2.2 PDMS Microchip Fabrication....46
3.2.3 MCE-ECD....47
3.3 Results and Discussion....48
3.3.1 Stacking Characterization with DC Amperometric Detection....49
3.3.2 Stacking Characterization with Pulsed Amperometric Detection....51
3.4 Conclusions....55
3.5 References....57

4. EOF MEASUREMANTS OF SINGLE AND MIXED SURFACTANT SYSTEMS USING BOTH CURRENT MONITORING AND $C^4D$ METHODS....58
4.1 Introduction....58
4.2 Experimental....62
4.2.1 Chemicals....62
4.2.2 EOF Measurements....64
4.2.3 Adsorption/Desorption Rates Study....67
4.3 Results and Discussion....67
4.3.1 Single SDS Surfactant System....67
4.3.2 Single TDAPS Surfactant System....68
4.3.3 Mixed SDS/TDAPS Surfactant System....72
4.3.4 Adsorption/Desorption Rates of Surfactants....76
4.3.5 EOF Measurements by $C^4D$ and Current Monitoring Methods....78
4.3.6 Single Nonionic Surfactant System....81
4.3.7 Mixed Anionic/Nonionic Surfactant Systems....83
4.3.8 Mixed Zwitterionic/Nonionic Surfactant Systems....86
4.4 Conclusions....92
4.5 References....94

5. ELECTROPHORETIC SEPARATIONS IN POLY(DIMETHYLSILOXANE) MICROCHIPS USING MIXTED SURFACTANT SYSTEMS....97
5.1 Experimental....97
5.1.1 Chemicals....97
5.1.2 Sample preparation and analysis....98
5.1.3 PDMS Microchip Fabrication....99
5.1.4 MCE-ECD....100
5.2 Results and Discussion....101
5.2.1 Separation Applications Using Mixed SDS/TDAPS Surfactant System....101
5.2.2 Separation and Detection of GSH in Human RBCs....109
5.2.3 Separation Applications Using Mixed SDS/Nonionic Surfactant Systems....110
5.2.4 Time Study of GSH in RBCs Exposed to Fly Ash Suspension/$H_2O_2$....116
5.2.5 Separation Application Using Mixed TDAPS/Tween 20 Surfactant System....118
5.2.6 Catecholamine Release from PC12 cells by Stimulation with 80 mM $K^+$....122
5.3 Conclusions....124
5.4 References....126

6. CONCLUSIONS AND FUTURE DIRECTIONS .....127
6.1 Dissertation summary .....127
6.2 Future directions .....130
6.3 References .....133

LIST OF FIGURES

Figure Page

**Figure 1.1:** **4**
(A) Capillary zone electrophoresis. The negatively charged silanols groups on capillary walls attract cations from buffer, creating an electric double layer. Once applying a voltage, an electroosmotic flow is created causing the bulk flow through the capillary. Based on their differing mobilities or velocities, all analytes are carried with buffer solutions towards the cathode, in a migration order of cations coming out first, anions the last, while all neutral compounds coelute with EOF without any resolution. (B) Micellar electrokinetic chromatography with anionic micelle. During separation, compounds are separated based upon their differing affinities for the micelles, which are formed by adding the surfactant to BGE above its critical micellar concentration.

**Figure 1.2:** **7**
(A) Plug-like electroosmotic flow through a capillary. (B) Pressure induced parabolic flow through a capillary.

**Figure 1.3:** **8**
Principle of electroosmotic mobility measurement of the channel wall with the current monitoring method.

**Figure 1.4:** **11**
ECD modes: (A) Amperometric detection, in which a constant potential is applied to the working electrode to facilitate the redox reactions of the analytes. (B) PAD, a potential waveform is applied to the working electrode. An oxidative cleaning potential (high positive) is followed by a reductive potential (negative) to regenerate the clean, oxide-free WE surface before a detection potential is applied to analyze the analyte of interest.

**Figure 1.5:** **13**
Three methods for aligning the working electrode that facilitate isolating the EC detector from the separation voltage. (A1) and (A2) End-channel detection, the working electrode is placed at the end of the separation channel either on or off chip. (B) In-channel detection, the working electrode is placed in the separation channel. (C) Off-channel detection, the working electrode is placed in the separation channel but the separation voltage is isolated from the amperometric current through the use of a decoupler.

**Figure 1.6:** **15**
Schematic showing FASS of anionic species. A long plug of sample prepared in a low-conductivity BGE, is injected into separation channel filled with high-conductivity BGE. Upon the application of high voltage, anionic analytes become stacked up in the back of the sample plug due to the faster migration of analytes in the sample BGE relative to the running BGE caused by the high electrical field strength in the sample zone.

**Figure 1.7:** **19**
The biosynthetic pathway of catecholamines and the chemical structures of catecholamines, catechol, ascorbic acid, and L-3,4-dihydroxyphenylalanine (L-DOPA).

**Figure 1.8:** **21**
The chemical structures of cysteine (Cys), homocysteine (Hcy), and reduced glutathione (GSH).

**Figure 2.1:** **33**
(A) Schematic of PDMS microchips (50 μm × 50 μm × 6 cm from buffer to waste reservoir) with a double T injector (250 μm, 625 pL) for pinched injection. The sample, buffer and sample waste side channels are all 1 cm in length. All reservoirs are 5 mm in diameter. (B) Bright field image of silicon mold with a bubble cell width 5× the separation channel width (50 μm). The gold color seen in this picture is the native color of the SU-8 photoresist when photographed. Electrode channels a, b and c are 50 μm wide with 125 μm spacing between the channels and used as alignment channels for placing a 25 μm Pd decoupler and two 25 μm Au working electrodes (WEs) respectively. 1, 2 and 3 are three positions chosen to measure separation efficiencies in the separation channel and the bubble cell detection zone, respectively.

**Figure 2.2:** **37**
(A) Example electropherograms for 100 μM dopamine and catechol detected on PDMS microchips at the upstream WE in 1× to 5× bubble cells. (B) Changes in peak heights (left Y axis label) of 100 μM dopamine and catechol and noise level (right Y axis label) at the upstream WE in 1× to 10× bubble cells. Experimental conditions: separation field strength: 200 V/cm; pinched injection time: 10 s; BGE: 20 mM TES, 1 mM SDS (pH 7.0); $E_{Det}$ = 1.4 V.

**Figure 2.3:** **39**
Separation efficiency comparisons among 1× to 5× bubble cells. Figure 2.1B shows three positions chosen in a bubble cell to collect electropherograms of 20 μM fluorescein on each PDMS microchip. Experimental conditions: separation field strength: 200 V/cm; pinched injection time: 7 s; BGE: 20 mM boric acid (pH 9.2).

**Figure 3.1:** **46**
Schematic of PDMS microchips (50 μm × 50 μm × 6 cm from buffer to waste reservoir) with a straight T injector for gated and hydrodynamic injections and a 4× bubble cell (its width is 4× the separation channel width (50 μm)) in the electrochemical detection zone. The sample, buffer and sample waste side channels are all 1 cm in length. All reservoirs are 5 mm in diameter. Electrode channels are 50 μm wide with 125 μm spacing between the channels and used as alignment guides for placing a 25 μm Pd decoupler and a 25 μm Au working electrode (WE) respectively.

**Figure 3.2:** **48**
BGE loading, voltage settings and flow diagrams of gated and hydrodynamic injections and their corresponding separation phases.

**Figure 3.3:** **50**
Example electropherograms for 50 μM dopamine, catechol, and ascorbic acid detected on PDMS microchips with 4× bubble cell using FASI (A) and FASS (B) sample preconcentration

techniques. Experimental conditions: separation field strength: 125 V/cm in FASI; 114 V/cm in FASS; running BGE: 20mM TES, 1mM SDS (pH 7.0); sample BGE: diluted running BGE with SF 1, 5, 10, and 100, respectively; $E_{Det}$: 1V. (C) Comparisons of detection sensitivity of dopamine using FASI and FASS under different stacking factors.

**Figure 3.4:** **52**
Example electropherograms for 50 μM dopamine, catechol, and ascorbic acid detected on PDMS microchips with 4× bubble cell using FASI (A) and FASS (B) sample preconcentration techniques. Experimental conditions: 5-s gated injection in FASI, 25-s or 60-s hydrodynamic injection in FASS; separation field strength: 125 V/cm in FASI; 114 V/cm in FASS; running BGE: 20mM TES, 1mM SDS (pH 7.0); sample BGE: diluted running BGE with SF 1, 5, 10, and 100, respectively; $E_{Det}$ = 1V. (C) Comparisons of detection sensitivity of dopamine using FASI and FASS under different stacking factors.

**Figure 3.5:** **54**
(A) Example electropherograms for 250 μM Ty, Hcy, Cys and GSH on a PDMS microchip with 4× bubble cell under nonstacking (SF 1) and FASI, FASS two stacking conditions. Experimental conditions: separation field strength: 5-s gated injection in FASI, 25-s hydrodynamic injection in FASS; 125 V/cm in FASI; 114 V/cm in FASS; running BGE: 20 mM boric acid (pH 9.2); sample BGE: 20 mM boric acid (pH 9.2) for SF 1, 4 mM boric acid (pH 9.2) for SF 5, respectively; $E_{Det}$ = 1.6 V. (B) Comparisons of peaking heights and HPWs of Tyr, Hcy, Cys and GSH using nonstacking, FASI and FASS sample preconcentration techniques. (C) Comparisons of detection sensitivity of four analytes at the concentration range of 20 to 500 μM under nonstacking (SF 1) and FASI, FASS two stacking conditions.

**Figure 4.1:** **61**
Principle of a $C^4D$ system. (A) Schematic drawing of the sensing electrodes (B) Simplified equivalent circuitry for $C^4D$.

**Figure 4.2:** **64**
Chemical structures of the selected surfactants. (A) SDS, (B) TDAPS, (C) DDAPS, (D) Tween 20, (E) Triton X-100, (F) PEG 400.

**Figure 4.3:** **66**
Instrument setup for EOF measurements simultaneously using both current monitoring and $C^4D$ methods, which includes a PDMS microchip being placed on a ET121 $C^4D$ microfluidic platform, a laboratory built high-voltage power supply (HVPS) facilitating voltage control, and a EA120 $C^4D$ Amp. as well as a ER280 PowerChrom system for data collecting.

**Figure 4.4:** **68**
EOF as a function of concentration in TES buffer (20 mM) at pH 7.0 and phosphate buffer (20 mM) at pH 4.0, 7.0 and 10.0 for an anionic surfactant SDS.

**Figure 4.5:** **71**
(A) EOF as a function of concentration in TES buffer (20 mM) at pH 7.0 and phosphate buffer (20 mM) at pH 4.0, 7.0 and 10.0 for a zwitterionic surfactant TDAPS. The inserted panel

describes the hypothesized surfactant molecule interaction with the PDMS surface. (B) EOF as a function of concentration in TES buffer (20 mM) at pH 7.0 for a zwitterionic surfactant DDAPS.

**Figure 4.6:** **72**
(A) EOF as a function of concentration for a zwitterionic surfactant DDAPS in fused silica capillary. (B) Proposed hemimicelle model.

**Figure 4.7:** **74**
(A) EOF as a function of SDS concentration using TDAPS in TES buffer (20 mM) at pH 7.0. (B) EOF as a function of the ratio of SDS/TDAPS concentration in TES buffer (20 mM) at pH 7.0.

**Figure 4.8:** **75**
EOF as a function of SDS concentration using TDAPS in phosphate buffer (20 mM) at (A) pH 4.0, (B) pH 7.0, and (C) pH 10.0.

**Figure 4.9:** **76**
EOF as a function of the ratio of SDS/TDAPS concentration in phosphate buffer (20 mM) at (A) pH 4.0, (B) pH 7.0, and (C) pH 10.0.

**Figure 4.10:** **78**
Adsorption/desorption experiments of surfactants. The mark* denotes the point when the surfactant was added and the arrow denotes the point when the surfactant was removed from the solution reservoirs.

**Figure 4.11:** **80**
(A) EOF measurements using both current monitoring and $C^4D$ methods. The mark* denotes the time point at which the polarity is reversed. Field strength: 200 V/cm; BGE: TES buffer (20 mM) at pH 7.0. (B) EOF as a function of difference in ionic strength between the BGEs used in both current monitoring and $C^4D$ methods.

**Figure 4.12:** **82**
EOF as a function of concentration in boric acid buffer (20 mM) at pH 9.2 for nonionic surfactants (A) Tween 20 and Triton X-100, and (B) PEG 400.

**Figure 4.13:** **85**
EOF as a function of SDS concentration using (A) Tween 20, (B) Triton X-100, and (C) PEG 400 in boric acid buffer (20 mM) at pH 9.2.

**Figure 4.14:** **86**
EOF as a function of the ratio of (A) SDS/Tween 20, (B) SDS/Triton X-100, and (C) SDS/PEG 400 concentration in boric acid buffer (20 mM) at pH 9.2.

**Figure 4.15:** **89**
EOF as a function of TDAPS concentration using (A) Tween 20, (B) Triton X-100, and (C) PEG 400 in boric acid buffer (20 mM) at pH 9.2.

**Figure 4.16:** **90**
EOF as a function of the ratio of (A) TDAPS/Tween 20, (B) TDAPS/Triton X-100, and (C) TDAPS/PEG 400 concentration in boric acid buffer at (20 mM) pH 9.2.

**Figure 4.17:** **91**
EOF as a function of TDAPS concentration using (A) Tween 20, (B) Triton X-100, and (C) PEG 400 in TES buffer (20 mM) at pH 7.0.

**Figure 4.18:** **92**
EOF as a function of the ratio of (A) TDAPS/Tween 20, (B) TDAPS/Triton X-100, and (C) TDAPS/PEG 400 concentration in TES buffer (20 mM) at pH 7.0.

**Figure 5.1:** **103**
Example electropherograms for 50 μM dopamine, catechol, and ascorbic acid in 20 mM TES buffer at pH 7.0 with various surfactant conditions. Experimental conditions: separation field strength: 123 V/cm, 1-s gated injection; detection: DC Amp., $E_{det}$ = 1.2 V.

**Figure 5.2:** **104**
Comparisons of resolution results of dopamine, catechol and ascorbic acid calculated form peak information in electropherograms under different conditions. Resolution ($R$) is calculated based on the following equation where $t_1$, $t_2$ are the migration time of two analytes, respectively, and $W_{h1}$, $W_{h2}$ are the half peak widths of two analytes in seconds, respectively. $R = [2\ln(2)]^{0.5}(t_2 — t_1)/(W_{h1}+W_{h2})$, which will be used for all resolution calculations in this thesis.

**Figure 5.3:** **107**
Example electropherograms for 200 μM Tyr, Hcy, Cys and 600 μM GSH in 20 mM boric acid buffer at pH 9.2 with various surfactant conditions (mixed SDS/TDAPS system). Experimental conditions: separation field strength: 123 V/cm, 3-s gated injection; detection: PAD, $E_{det}$ = 1.6 V.

**Figure 5.4:** **108**
Comparison of resolution results of Tyr, Hcy, Cys and GSH calculated from peak information in electropherograms under different surfactant conditions.

**Figure 5.5:** **110**
Electropherograms of 4× diluted hemolysate samples of RBCs without and with the standard solution containing 100 μM GSH. BGE: 20 mM Boric acid, 0.1 mM SDS, 0.5 mM TDAPS, pH 9.2. Experimental conditions: separation field strength: 123 V/cm, 3-s gated injection; Detection: PAD, $E_{det}$ = 1.6 V.

**Figure 5.6:** **113**
Example electropherograms for 50 μM Tyr, Hcy, Cys and 150 μM GSH in 20 mM boric acid buffer at pH 9.2 with various surfactant conditions (mixed SDS/PEG 400 system). Experimental conditions: separation field strength: 123 V/cm; 3-s gated injection; Detection: PAD, $E_{det}$ = 1.6 V.

**Figure 5.7:** **114**
Example electropherograms for 50 μM Tyr, Hcy, Cys and 150 μM GSH in 20 mM boric acid buffer at pH 9.2 with various surfactant conditions (mixed SDS/Tween 20 system). Experimental conditions: separation field strength: 123 V/cm; 3-s gated injection; Detection: PAD, $E_{det}$ = 1.6 V.

**Figure 5.8:** **115**
Example electropherograms for 50 μM Tyr, Hcy, Cys and 150 μM GSH in 20 mM boric acid buffer at pH 9.2 with various surfactant conditions (mixed SDS/Triton X-100 system). Experimental conditions: separation field strength: 123 V/cm; 3-s gated injection; Detection: PAD, $E_{det}$ = 1.6 V.

**Figure 5.9:** **116**
Normalized peak area ratios of four analytes in three specific mixed SDS/nonionic surfactant (Tween 20, Triton X-100, or PEG 400) conditions.

**Figure 5.10:** **117**
Time study of GSH concentration in RBCs exposed to fly ash suspension with or without $H_2O_2$.

**Figure 5.11:** **121**
Example electropherograms for 20 μM DA, NE, E and 40 μM CA and L-DOPA in 20 mM TES buffer at pH 7.0 as a function of surfactant composition. Experimental conditions: separation field strength: 150 V/cm; 10-s hydrodynamic injection; Detection: DC Amp., $E_{det}$ = 1.2 V.

**Figure 5.12:** **122**
The resolutions between analytes for all tested surfactant systems.

**Figure 5.13:** **124**
Electropherograms of catecholamine release from PC12 cells by stimulation with 80 mM $K^+$ in 2× diluted sample and with the standard solution containing 5 μM DA, NE, E and 10 μM CA and L-DOPA. BGE: 20 mM TES, 0.5 mM Tween 20, 4 mM TDAPS, pH 7.0. Experimental conditions: separation field strength: 150 V/cm; 10-s Hydrodynamic injection; Detection: DC Amp., $E_{det}$ = 1.2 V.

# CHAPTER 1. INTRODUCTION

## 1.1 DISSERTATION OVERVIEW

Microchip capillary electrophoresis (MCE) has been established as an important sub-section of traditional capillary electrophoresis (CE) and has found widespread use in academic laboratories and more recently in commercial products.[1-3] MCE has the advantages of decreased analysis time (seconds time scale), integrated sample processing, high portability, high throughput, minimal reagent consumption (pL injection volumes), and low analysis cost, which make it an attractive separation method, especially for point-of-care applications.[4-6] However, one major limitation of CE and also MCE analyses is the poor concentration sensitivity caused by the limited volume of injected samples and the low absorption path-length if UV detection is used. Moreover, while MCE provides fast separations, the short separation channels make resolving multiple compounds challenging.

Our ultimate goal is to develop a lab-on-a-chip device for direct, sensitive detection of multiple redox markers with highly efficient separation, which has the potential to be used for metabolic profiling. The focus of the research contained within this dissertation was on the optimization of our previous microchip capillary electrophoresis coupled electrochemical detection (MCE-ECD) design for improved separation and detection performance by using detection geometry, on-line preconcentration and mixed surfactant pseudo-stationary phase. The first part of this thesis focuses on the use of a bubble cell to improve detection sensitivity and LODs (Chapter 2). Bubble cell widths were varied from 1× to 10× the separation channel width (50 μm) and the effects of electrode surface area on detection sensitivity and LODs were

characterized using DC amperometry for the detection of model analytes. The impact of bubble cell widths on separation efficiency was examined using fluorescence imaging. The second part focuses on the use of two on-line sample preconcentration techniques for further enhancing detection sensitivity and reducing LODs. Stacking effects are demonstrated in chapter 3 for both FASI (for gated injection) and FASS (for hydrodynamic injection) methods using DC amperometric detection and PAD. The third and final part of this project was to explore the electroosmotic flow (EOF) and separation behavior of representative anionic, zwitterionic and non-ionic surfactants and the different combinations of these surfactants using PDMS microchips. EOF measurements were performed as a function of the surfactant concentration using both current monitoring and capacitively coupled contactless conductivity detection ($C^4D$) methods (Chapter 4). Next, separation and electrochemical detection of two groups of model analytes were performed using the mixed surfactant systems and are discussed in chapter 5. Expanded ability to control EOF and enhanced peak heights and/or analyte resolution was achieved in some mixed surfactants relative to single surfactants. Following these, in the same chapter, catecholamine release from rat pheochromocytoma (PC12) cells by stimulation with 80 mM $K^+$ and detection of reduced glutathione (GSH) in red blood cells (RBCs) exposed to fly ash suspension as a model environmental oxidant using mixed surfactant background electrolytes was studied to demonstrate the ability for improved separation chemistry of biologically relevant compounds in complex sample matrixes.

The rest of this chapter serves as a cursory introduction to these topics and the impetus behind research presented in this thesis. More in depth discussions of specific topics and techniques are given in the following chapters.

## 1.2 CAPILLARY ELECTROPHORESIS

CE is an analytical technique that separates ions based on their electrophoretic mobility with the use of an applied voltage. In 1981 Jorgenson and Lukacs[7, 8] first described the use of a fused silica capillary column and aqueous buffer to separate charged compounds, indicating the potential of CE as a new analytical separation technique. CE exhibits an ability to produce high resolution separation of both charged and non-charged molecules in short analysis time (minutes) while using very small sample and reagent volumes (μL). These attractive features make it both competitive and a good alternative to the traditional techniques such as high pressure liquid chromatography (HPLC) or gas chromatography (GC).

### 1.2.1 Modes of CE

As a rapidly growing separation technique, CE has diverse application areas, including food analysis,[9, 10] pharmaceutical analysis,[11, 12] bioanalysis,[13] and environmental pollutants analysis.[14, 15] The versatility of CE is partially originated from its various modes of operation. Based on the separation mechanism, the main modes encompassed by CE can be classified as follows: capillary zone electrophoresis (CZE) (separating anlytes via their different electrophoretic mobilities)[7, 16, 17] (Figure 1.1A), micellar electrokinetic chromatography (MEKC) (separation of compounds based on their partitioning between the background electrolyte (BGE) and the micelles that serve as a pseudo-stationary phase)[18, 19] (Figure 1.1B), capillary gel electrophoresis (CGE) (the adaptation of traditional gel electrophoresis into the capillary using polymers in solution to create a molecular sieve),[20, 21] capillary isoelectric focusing (CIEF) (a high-resolution technique for protein separation based on differences in isoelectric points (pI),[22] capillary isotachophoresis (CITP) (a “moving boundary” electrophoretic technique in which

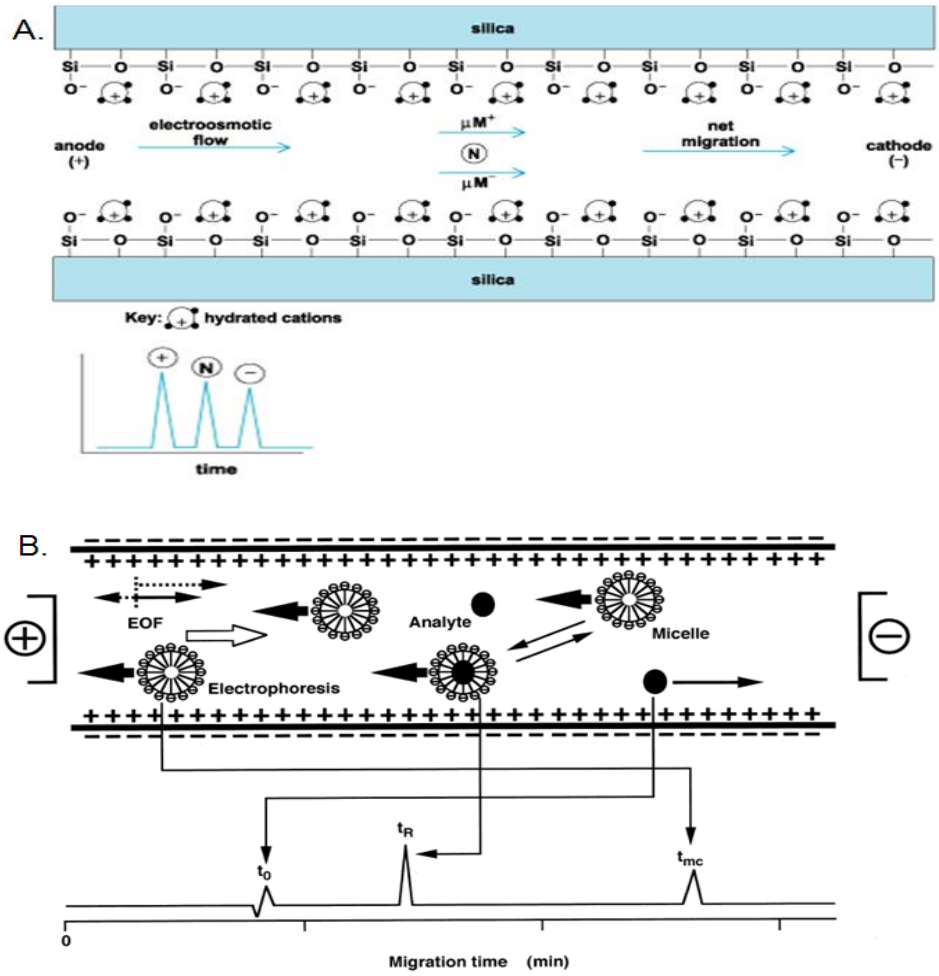


**Figure 1.1:** (A) Capillary zone electrophoresis. The negatively charged silanols groups on capillary walls attract cations from buffer, creating an electric double layer. Once applying a voltage, an electroosmotic flow is created causing the bulk flow through the capillary. Based on their differing mobilities or velocities, all analytes are carried with buffer solutions towards the cathode, in a migration order of cations coming out first, anions the last, while all neutral compounds coelute with EOF without any resolution. (B) Micellar electrokinetic chromatography with anionic micelle.[23] During separation, compounds are separated based upon their differing affinities for the micelles, which are formed by adding the surfactant to BGE above its critical micellar concentration.

sample components condense between leading and terminating constituents, producing a steady-state migrating configuration composed of consecutive sample zones,[24] and capillary electrochromatography (CEC) (an emerging hybrid separation technique that combined advantages of both electrophoretic and chromatographic processes for the separation of neutral compound mixtures in columns packed with a chromatographic stationary phase).[25, 26] CZE is the most widely used mode because it is applicable to separations of both anions and cations, and from small ions to particles. The development of MEKC is a major advancement in CE because it has provided a method for separation of electrically neutral compounds. Schematic representations of the separation mechanism of CZE and MEKC[23] are shown in Figure 1.1 since these two separation modes were used in the following work.

### 1.2.2 Electroosmotic Flow and Electrophoretic Mobility

EOF plays a vital role in CE and in analytical methods in microfabricated devices based on electrophoresis.[27, 28] EOF is generated at the surface-solution interface in a capillary or microfabricated channel, where an electrical double layer is formed by attracting the mobile cations from BGE to the negatively charges on the inner wall of the capillary.[16] Once applying a voltage, the cations in the diffuse portion of double layer migrate towards the cathode, carrying water with them, and finally resulting in a net flow of bulk BGE moving to the same direction. Since the EOF is generally greater than the electrophoretic flow of analytes, all analytes are carried with BGE towards the cathode. In the case of the reversed surface charge of the capillary, anions associate with the capillary wall and the resulting EOF moves to the opposite way. The relative flat flow profile (Figure 1.2) for EOF results in high-efficiency separation with significantly less deleterious dispersive effects than the parabolic one encountered in HPLC,

which relies on high pressure pumps to induce flow.[8, 29-31] The mobility of the EOF ($\mu_{eof}$) is defined in equation 1.1, and is related to the zeta potential ($\zeta$) (governed by the charge on the capillary surface) across the double layer, the viscosity ($\eta$) and the dielectric constant ($\varepsilon$) of the BGE as shown in equation 1.2. The magnitude of EOF will change due to changes in the chemical composition of the surface, changes in the pH and BGE composition, and changes in temperature.[29, 32-34]

$$\mu_{eof} = \frac{v_{eof}}{E} \tag{1.1}$$

Here, $v_{eof}$ is the linear velocity of EOF, and $E$ is the electrical field strength.

$$\mu_{eof} = \frac{\varepsilon \xi}{4\pi\eta r} \tag{1.2}$$

Here $r$ is the capillary radius.

In normal polarity CZE, charged analytes are separated in the BGE based upon their individual electrophoretic mobilities in an applied electrical field. The resulting analyte velocities in this field are described by equation 1.3 in which velocity ($v_{ep}$) is equal to the intrinsic electrophoretic mobility of an analyte ($\mu_{ep}$) multiplied by the field strength ($E$).

$$v_{ep} = \frac{q}{f}E = \mu_{ep}E \tag{1.3}$$

Electrophoretic mobility ($\mu_{ep}$) is governed by the analyte's charge ($q$) and frictional coefficient ($f$) as defined by the Stokes equation (1.4).

$$f = 6\pi\eta r \tag{1.4}$$

This equation describes the frictional coefficient ($f$) for a spherical particle having a hydrodynamic radius $r$ in a solution of viscosity ($\eta$).

In the presence of EOF, a new, apparent velocity ($v_{app}$) which is proportional to the sum of both

the electrophoretic ($\mu_{ep}$) and electroosmotic mobilities ($\mu_{eof}$) is observed and described in equation 1.5.

$$v_{app} = \mu_{app}E \equiv (\mu_{ep} + \mu_{eof})E \quad (1.5)$$

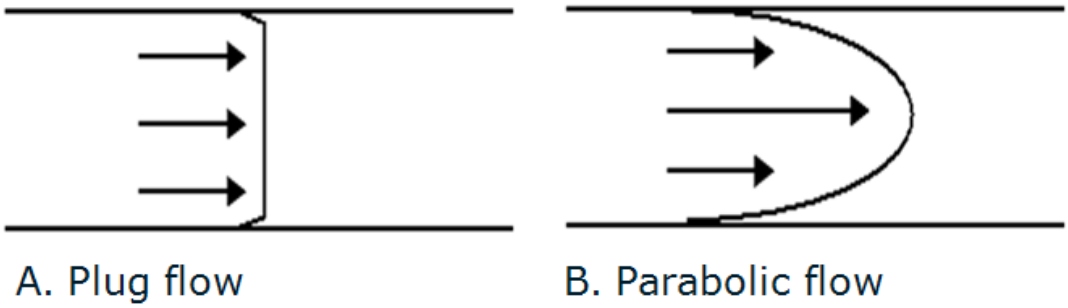


**Figure 1.2** (A) Plug-like electroosmotic flow through a capillary. (B) Pressure induced parabolic flow through a capillary.

### 1.2.3 EOF measurement methods

Given the importance of EOF, accurate and precise methods for its measurement are useful. Many EOF measurement methods have been reported for CE and its microchip format.[35] The neutral marker method is the earliest reported method for measuring EOF in CE,[7, 36] which relies on the injection of an electrically neutral compound followed by recording its migration time through capillaries. This method have no interaction with the electrolyte or the capillary wall and provides only an average EOF that cannot compensate for the effects of EOF changes during the measurement. As an alternative, the fluorescent marker method involves the introduction of a fluorescent agent downstream in the EOF direction and monitoring its movement at the end of the capillary.[37] However, this method is less widely used due to the use of a bulky fluorescence detection system and the contamination possibility caused by fluorescent agent. The average EOF rate can also be measured by weighing the effluent from a capillary with

an analytical balance.[38, 39] A potential difficulty with this method is the mass loss by evaporation; therefore, it is not available for operating in microchips because of less liquid mass transmitted by EOF. As the most widely used method, the current monitoring method measures the electrophoretic current change as an electrolyte of different ionic strength fills the capillary or channel (Figure 1.3).[40] The time required to reach a steady state separation current can then be used to calculate EOF. Reported precision for average EOF rates measured by this method in CE and microchip CE ranges between 5% and 15%.[40-42] Based on a similar measurement principle, conductivity detection monitors the change in bulk solution conductivity between two electrodes when an analyte band passes through the electrode gap.[43] More reproducible EOF measurements (relative standard deviation (RSD) 1.9%) were reported using this method than the current monitoring method (RSD 5.9%) by Henry's group.[44]

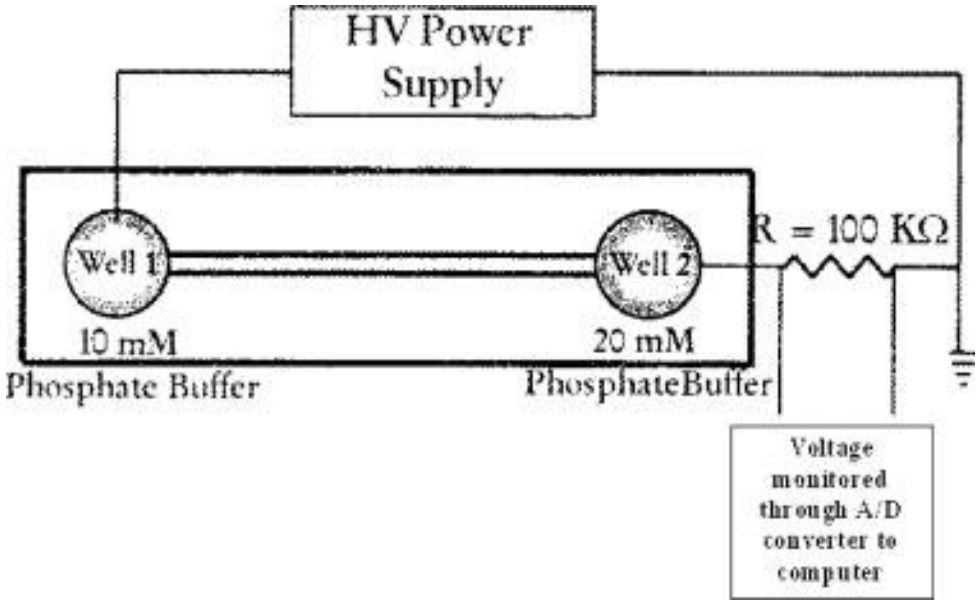


**Figure 1.3** Principle of electroosmotic mobility measurement of the channel wall with the current monitoring method.[42]

## 1.3 MCE-ECD

As the interest and use of MCE grows, several types of detection modes have been coupled with MCE to monitor analyte separation in these devices, including laser-induced fluorescence (LIF),[45, 46] mass spectrometry (MS),[47, 48] absorbance,[49] electrochemical techniques[50, 51] and other methods.[52-54] LIF is the most frequently used mode for MCE due to its inherent high sensitivity, low limits of detection (LODs), and relative ease of implementation with MCE system.[55-57] However, most compounds are not naturally fluorescent and must be derivatized with a fluorophore to be detected by LIF, which increase the time and complexity of analysis. MS has also been employed as a detection mode for miniaturized devices. The primary advantage of coupling MS with microchip CE devices is increased throughput of samples.[62, 63] Unfortunately, commercially available MS systems are costly, not inherently portable, and less sensitive than LIF.

Electrochemical detection (ECD) is an attractive alternative to optical detection for microfludic and lab-on-a-chip applications,[58-60] because it not only offers detection limit comparable to fluorescence, but is also less expensive and complex.[61, 62] There are several advantages of ECD over other detection modes, including the fact that many compounds can be detected without derivatization and the ability to miniaturize both the detector and control instrumentation. Microelectrodes can be fabricated directly onto the microchip device using common photolithographic techniques, producing a fully integrated system. Although microelectrodes generate extremely small currents, the background current is reduced even further, resulting in an increased signal-to-noise ratio and potentially better LODs.[63, 64] Furthermore, based on the electroactivity difference of analytes, ECD has the advantages of specificity through redox chemistry, and selectivity through potential control.[65, 66] By increasing

the total number of working electrodes and thus the total number of applied detection potentials, MCE-ECD has the potential to meet the goal for increasing the amount of detected analytes in a single metabolic profiling analysis.[67]

Amperometry is the most extensively reported ECD method to be coupled with MCE due to its ease of operation and minimal background-current contributions.[2, 58-60] It is accomplished by applying a constant potential to the working electrode (WE) and measuring the current as a function of time as shown in Figure 1.3A. In the conventional three-electrode setup, a reference and auxiliary electrode are also present. In some cases, only a working and counter electrode may be employed in a two-electrode configuration.[68] The applied potential facilitates the redox reactions of the analytes, while the current output is directly proportional to the number of moles of analyte oxidized or reduced at the WE surface.[69] The optimal potential can be selected by constructing a hydrodynamic voltammogram.[69] However, one drawback to the use of amperometry is the fact that electrodes become fouled when they interact with analytes such as phenols, thiols or carbohydrates.[70-72] The accumulation of absorbed carbonaceous material on the WE causes an unstable signal.[70, 72] To overcome problems associated with electrode fouling without the need for electrode polishing or pretreatment, a potential waveform referred to as pulsed amperometric detection (PAD) is used (Figure 1.3B).[73-75] In PAD, a larger positive potential is first applied to the WE, where an oxide layer is formed on the surface and any adsorbed organic material is simultaneously stripped off from the surface. Next, a reducing potential is applied to the WE to dissolve the oxide layer. This redox cycle serves to regenerate the clean, oxide-free noble metal (typically Pt or Au) surface. Finally, a third potential is applied for detection. PAD has been used in combination with HPLC, CE and MCE for quantification of

a wide number of analytes in various samples.[76-80] In this thesis, MCE coupled with DC amperometry or PAD is employed to analyze the analyte of interest.

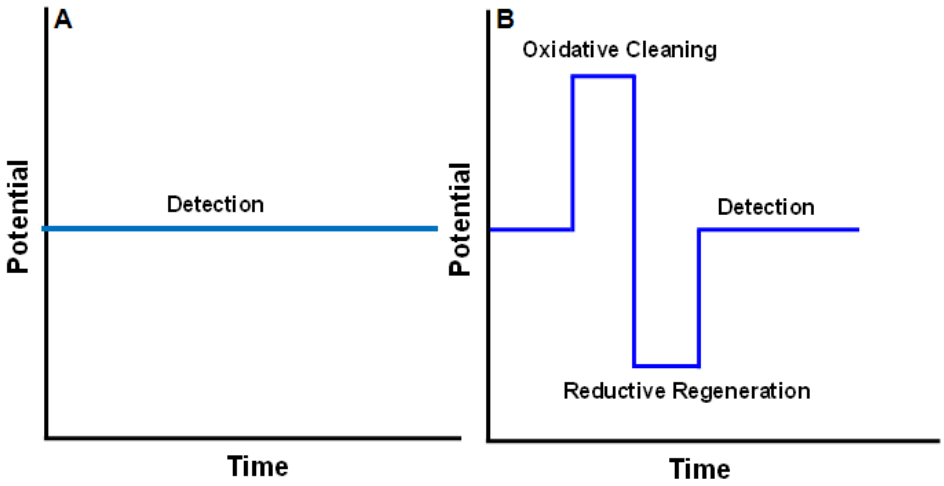


**Figure 1.4:** ECD modes: (A) Amperometric detection, in which a constant potential is applied to the working electrode to facilitate the redox reactions of the analytes. (B) PAD, a potential waveform is applied to the working electrode. An oxidative cleaning potential (high positive) is followed by a reductive potential (negative) to regenerate the clean, oxide-free WE surface before a detection potential is applied to analyze the analyte of interest.

One major issue when utilizing amperometry detection with MCE is the isolation of the high-voltage separation field from the detection system since it would interfere with the detection system and harm the grounded potentiostat. Three different approaches, which are termed end-channel detection,[81-85] in-channel detection,[86-89] and off-channel detection,[90-93] have been developed for this purpose and depicted in Figure 1.4. End-channel detection has been widely used in conventional and microchip CE,[81-85] where the WE is placed tens of microns from the separation channel and the counter electrode is grounded and placed behind the WE. In this

configuration, the WE feels nearly ground potential since the resistance drops dramatically at the interface between the narrow separation channel and the big waste reservoir.[2] However, this detection mode suffers from the poor separation efficiency due to serious band broadening and decreased detector response due to diffusion.[2] Significant improvements in detection sensitivity can be achieved if the separation current is grounded before reaching the WE by either using in-channel detection mode equipped with an electrically isolated potentiostat[86, 94] or simply placing a decoupler in front of WE in the off-channel detection mode.[95, 96] Our group has reported a sensitive detection of a wide range of analytes by incorporating a simple Pd microwire decoupler with Au pr Pt WEs into a MCE-ECD device.[67, 97, 98] Recently, surface modification of the WEs with nanomaterials, such as carbon nanotubes (CNTs),[99-101] gold nanoparticles,[102] and nanowires,[103] have been shown to be another way to improve detection sensitivity and LODs in MCE-ECD system. Significant improvements in the performance of MCE-ECD were observed using a carbon nanotube (CNT)-modified WE for the detection of several classes of hydrazine, phenol, purine, and amino acid compounds.[104] The broad and significant catalytic activity exhibited by the CNT electrode indicates great promise for a wide range of bioanalytical and environmental applications.

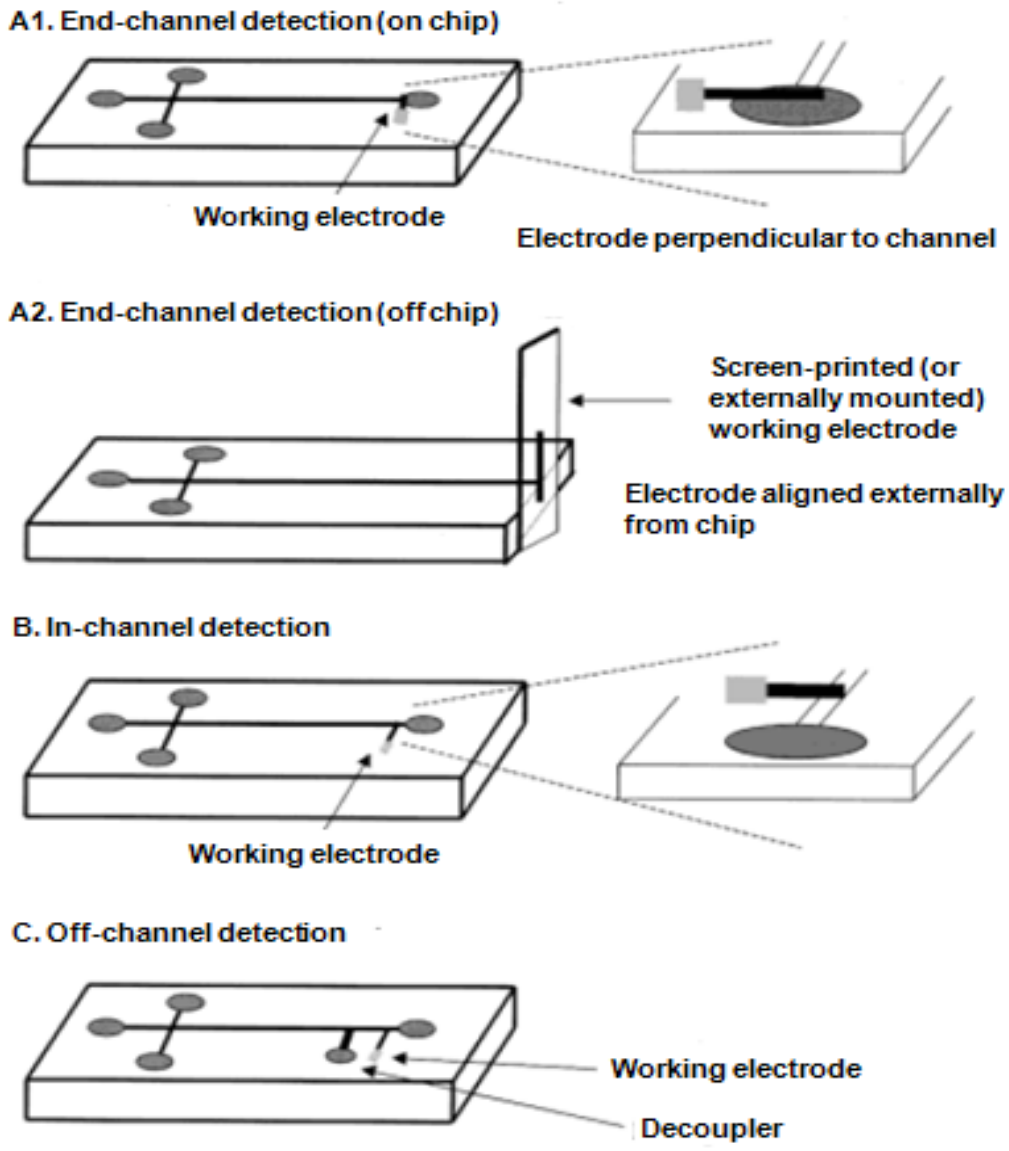


**Figure 1.5.** Three methods for aligning the working electrode that facilitate isolating the EC detector from the separation voltage.[2] (A1) and (A2) End-channel detection, the working electrode is placed at the end of the separation channel either on or off chip. (B) In-channel detection, the working electrode is placed in the separation channel. (C) Off-channel detection, the working electrode is placed in the separation channel but the separation voltage is isolated from the amperometric current through the use of a decoupler.

## 1.4 ON-LINE SAMPLE PRECONCENTRATION METHODS

An additional means of improving detection limits in CE and MCE is to employ sample preconcentration methods.[105-109] The most widely adapted approaches for on-line sample pretreatment include isotachophoresis (ITP),[110, 111] sample stacking,[6, 45, 112, 113] solid phase extraction (SPE),[114-116] and sweeping techniques.[117-120] Field amplified sample injection (FASI) and field amplified sample stacking (FASS) are two widely used sample preconcentration techniques in traditional CE, and preconcentration factors from 10 to 1000 have been achieved.[6, 35, 102, 103] Compared to ITP which uses a binary buffer system to confine the sample between a leading and a terminating BGE, FASI and FASS are more convenient techniques to incorporate with electrophoretic analysis because of the simple requirement of the manipulation of just two streams, the running and sample BGEs. For both FASI and FASS techniques, a long plug of sample, prepared in a low-conductivity BGE, is injected into the separation channel filled with a higher-conductivity BGE by either electrokinetic forces or hydrodynamic flow.[45] Upon the application of high voltage, the analytes become stacked at the boundary between the sample BGE (low-conductivity) and the running BGE (high-conductivity) due to the higher electric field strength and hence faster migration of the analytes in the sample BGE relative to the running BGE. The formed thin zone of analytes then moves through the separation channel and separates into individually zones according to conventional free zone electrophoresis. The stacking mechanism occurs for ionic analytes, with the positively and negatively charged analytes stacking up in front of and in back of the sample plug, respectively.[121] The neutral compounds are left in the sample plug and coelute.[121, 122] Schematic showing FASS of anionic species is in Figure 1.5. Theoretically, the amount of sample being stacked is simply proportional to the resistivities between the sample buffer and the running buffer. However, the mismatched

conductivity at the boundary will generate a laminar flow, causing band broadening. Therefore, sample stacking and laminar broadening work against each other to yield a point with the optimal stacking effect.

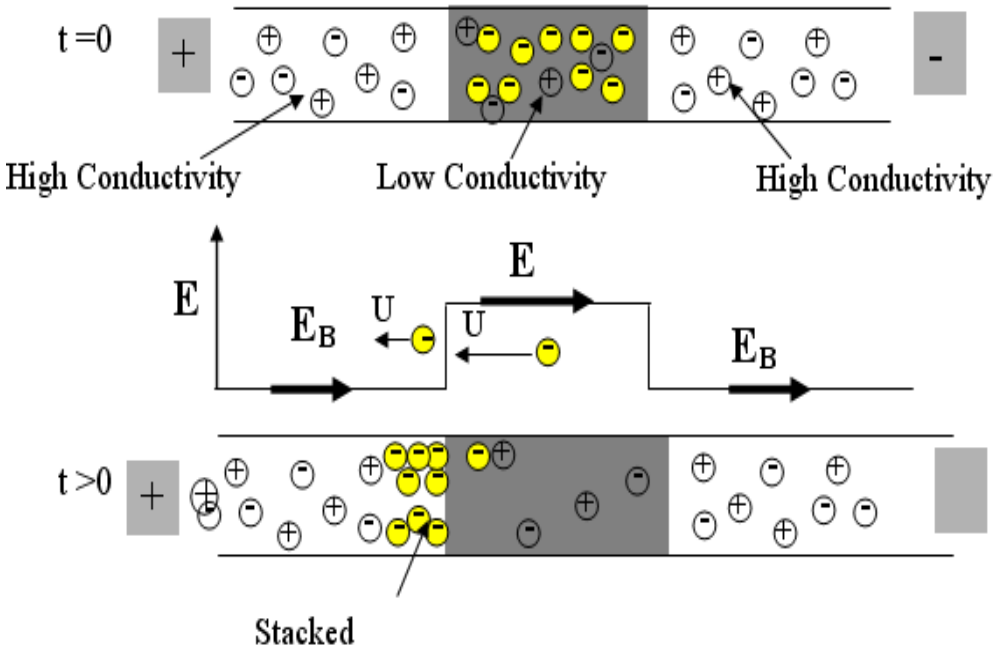


**Figure 1.6** Schematic showing FASS of anionic species. A long plug of sample prepared in a low-conductivity BGE, is injected into separation channel filled with high-conductivity BGE. Upon the application of high voltage, anionic analytes become stacked up in the back of the sample plug due to the faster migration of analytes in the sample BGE relative to the running BGE caused by the high electrical field strength in the sample zone.

## 1.5 SURFACE MODIFICATION

The manipulation of fluids in channels with dimensions of tens of micrometers, microfluidics, has emerged as a distinct new field.[123] As an important characteristic of fluids in CE and microchip CE, EOF plays an important role in the analyte separations and microfluidic

transport.[27, 28] EOF control in MCE has proven more challenging than in traditional CE in part because of the strong adsorption and surface effects in variety of materials used to make these devices. EOF within microfluidic devices made from polymers such as poly(dimethylsiloxane) (PDMS),[124] poly(methyl methacrylate) (PMMA),[125, 126] polycarbonate,[127] and polystyrene (PS)[127, 128] can vary widely due to the diversity of the surface-exposed functional groups. In addition, because of the low surface charge density, the zeta potential of these materials that gives rise to the EOF is much lower than that for the glass-based fluidic chips, thus less than optimal for specific separations.[129] To meet the requirement of microfluidic applications, chemical modification of microchannel surface is commonly used to minimize unwanted analyte-wall interactions and manipulate EOF. Demonstrated modifiers include inorganic anions,[130] divalent metals,[131] polyamines,[132] polyelectrolytes,[133-137] covalent modifications,[138-140] variations in the bonding method,[141] and the addition of surfactants to the BGE.[41, 142, 143]

Surface coatings can be divided into three categories, permanent coatings based on covalent reactions between the modifying agent and the surface, adsorbed coatings based typically on ionic interactions between a polymer and the surface, and dynamic coatings which rely on the equilibrium between the modifier in solution and the surface.[144, 145] While permanent coatings have demonstrated remarkable stability and migration time reproducibility, they also require longer capillary preparation times and can be susceptible to chemical degradation, particularly at alkaline pH.[146] Adsorbed coatings are attractive because they do not require the modifier be present in the solution and tend to be more stable at alkaline pH relative to covalent coatings. A successive multiple-ionic-layer approach[147-149] for adsorbed coatings has been applied to both microfluidic PDMS[134] and thermoset polyester (TPE)[98] channels. In these studies, polyelectrolyte multilayers are created by exposing the surface to the cationic polymer Polybrene

(PB) followed by a layer of dextran sulfate (DS) as the anionic polymer. Unfortunately, most adsorbed coatings provide little adjustability of the EOF. Dynamic coatings are the easiest surface modification method for both conventional and microchip CE because of their low cost, simplicity, and versatility.[144, 150] In this method, solution-phase modifiers are added to the BGE or are applied within a rinsing step prior to analysis, and interact with the capillary surface, changing the zeta potential[27, 28] and therefore the EOF and the separation. Depending on the modifying agents' charges, the EOF can be suppressed, increased, or reversed. Applications of single surfactants in dynamic coatings to control EOF in both traditional and microchip CE have been published. These surfactants include anionic surfactants (sodium dodecyl sulfate (SDS)),[41, 151] cationic surfactants (cetyltrimethylammonium bromide (CTAB),[152, 153] tetradecyltrimethylammonium bromide (TTAB),[154] and didodecyldimethylammonium bromide (DDAB)[155]), and zwitterionic surfactants (dodecyldimethyl (2-hydroxy-3-sulfopropyl) ammonium (DSB),[156] N-hexadecyl-N,N-dimethyl-3-ammonio-1-propane sulfonate (HDAPS) and N-tetradecyl-N,N-dimethyl-3-ammonio-1-propane sulfonate (TDAPS)[157, 158]). Successful applications of nonionic surfactants, such as polyoxyethylene ether (Brij 35), polyoxyethylene (20) sorbitan monolaurate (Tween 20), polyoxyethylene octyl phenyl ether (Triton X-100), to suppress EOF and minimize surface adsorption of biomolecules in CE and microfluidic system have also been reported.[159-162] Furthermore, mixed surfactant systems represent an interesting alternative to single surfactant systems. The use of different combinations of mixed surfactants, such as mixed cationic/zwitterionic,[156, 163, 164] cationic/anionic,[165] ionic/nonionic,[142] and zwitterionic/nonionic[166] surfactants, have been discussed for both better control of EOF and separation chemistry in fused silica capillaries and glass microchips. Despite these advances, the

application of mixed surfactants systems for surface modification on polymeric microdevices has been limited.

## 1.6 IMORPTANT ELECTROCHEMICALLY ACTIVE ANALYTES

### 1.6.1 Catecholamines

Catecholamines are a group of compounds with a catechol nucleus consisting of benzene with two hydroxyl side groups, and a side-chain amine. Three catecholamine compounds, dopamine (DA), norepinephrine (NE) and epinephrine (E) are widely distributed in vivo, and are important as neurotransmitters and hormones in mammalian species.[167] As shown in the biosynthetic pathway of these compounds (Figure 1.6), tyrosine hydroxylase converts tyrosine to L-3,4-dihydroxyphenylalanine (L-DOPA) for the production of catecholamines and DA is produced from L-DOPA by DOPA decarboxylase, acting as a precursor of E and NE. The production and regulation of catecholamines has a profound effect on the sympathetic and parasympathetic nervous system, cardiovascular system, metabolic rate and body temperature.[168] Catecholamines have most frequently been determined by using amperometric detection coupled with separation methods such as HPLC[169-172] and CE or microchip CE,[173-176] since they are easily converted into quinone species by electrochemical oxidation. In this thesis, catecholamines, catechol (CA), ascorbic acid (AA), and L-DOPA will be used as model analytes in DC amperometry experiment and their chemical structures are shown in Figure 1.6.

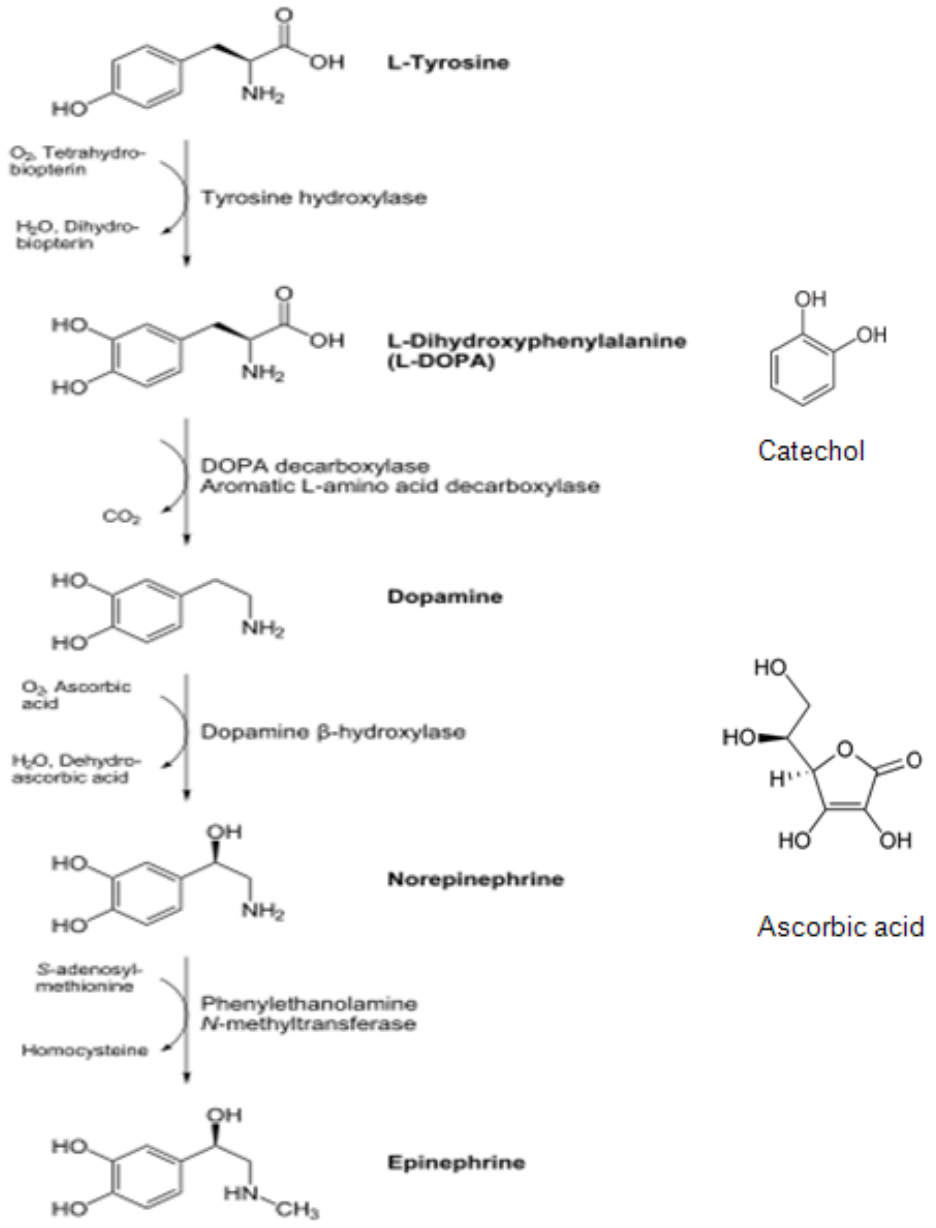


**Figure 1.7** The biosynthetic pathway of catecholamines and the chemical structures of catecholamines, catechol, ascorbic acid, and L-3,4-dihydroxyphenylalanine (L-DOPA).

### 1.6.2 Aminothiols

Thiols have been of continuing interest for many years because of their clinical, biological, and pharmaceutical importance in several biological processes.[177, 178] A specific group

of thiols, the sulfhydryl thiols (R-SH), such as homocysteine (Hcy), cysteine (Cys), and reduced glutathione (GSH), are the most often considered in biological analysis. Attention to these compounds has come about because of their association with oxidative stress and damage in the body. There is also increasing evidence for the involvement of these thiols in metabolic regulation, signal transduction and regulation of gene expression.[179-181] Moreover, oxidants and antioxidants are proposed to participate in this redox regulation by shifting the balance between reduced and oxidized cellular thiols.[182] For example, GSH is a key endogenous antioxidant, and the ratio of oxidized to reduced GSH has been shown to be an effective measure of oxidative stress. As another example, the normal physiological level of plasma Hcy is in the range of 5 to15 μM, so when present at elevated levels, this compound can be used as an indicator for diagnosis of Alzheimer's,[183] folate and cobalamin (vitamin B12) deficiency,[184, 185] and cardiovascular diseases.[3] Cys deficiency is also involved in many syndromes, such as slow growth in children, hair depigmentation, edema, lethargy, liver damage, loss of muscle and fat, and weakness.[186] Due to the extensive inter-conversion between these compounds in the intracellular sulfur metabolism, various conventional techniques such as HPLC[187-189] and CE and its microchip format[190-192] separations coupled with different detection methods have been employed to determine their concentrations in body fluids. In this thesis, Hcy, Cys, and GSH (Figure 1.7) will be used as model analytes to demonstrate the ability of our MCE-PAD system to provide resolution of biologically relevant compounds in complex sample matrixes by using appropriate mixed surfactants.

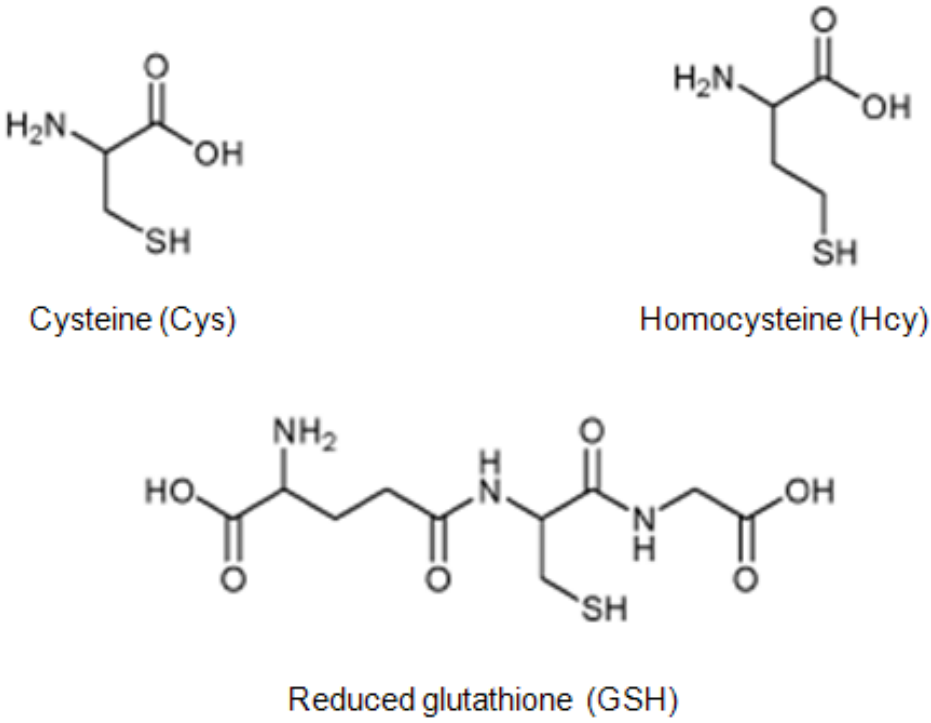


**Figure 1.8** Structures of cysteine (Cys), homocysteine (Hcy) and reduced glutathione (GSH).

## 1.7 REFERENCES


(1) Auroux, P. A., Iossifidis, D., Reyes, D. R., Manz, A., *Analytical Chemistry* **2002**, *74*. 2637-2652.
(2) Vandaveer, W. R., Pasas, S. A., Martin, R. S., Lunte, S. M., *Electrophoresis* **2002**, *23*. 3667-3677.
(3) Refsum, H., Ueland, P. M., Nygard, O., Vollset, S. E., *Annual review of medicine* **1998**, *49*. 31-62.
(4) Dolnik, V., Liu, S. R., Jovanovich, S., *Electrophoresis* **2000**, *21*. 41-54.
(5) Vilkner, T., Janasek, D., Manz, A., *Analytical Chemistry* **2004**, *76*. 3373-3385.
(6) Beard, N. R., Zhang, C. X., deMello, A. J., *Electrophoresis* **2003**, *24*. 732-739.
(7) Jorgenson, J. W., Lukacs, K. D., *Analytical Chemistry* **1981**, *53*. 1298-1302.
(8) Jorgenson, J. W., Lukacs, K. D., *Clinical chemistry* **1981**, *27*. 1551-1553.
(9) Cieslik, E., Niedospial, A., Mickowska, B., *Zywnosc-Nauka Technologia Jakosc* **2008**, *15*. 5-14.
(10) Dong, Y. Y., *Trends in Food Science & Technology* **1999**, *10*. 87-93.
(11) Marsh, A., Broderick, M., Altria, K., Power, J., Donegan, S., Clark, B., *Methods in molecular biology* **2008**, *384*. 205-245.
(12) Rabel, S. R., Stobaugh, J. F., *Pharmaceutical research* **1993**, *10*. 171-186.
(13) Kostal, V., Katzenmeyer, J., Arriaga, E. A., *Analytical Chemistry* **2008**, *80*. 4533-4550.
(14) Fukushi, K., Takeda, S., Chayama, K., Wakida, S., *Journal of Chromatography A* **1999**, *834*. 349-362.
(15) Fung, Y. S., Tung, H. S., *Electrophoresis* **1999**, *20*. 1832-1841.
(16) Jorgenson, J. W., Lukacs, K. D., *Science* **1983**, *222*. 266-272.
(17) Jorgenson, J. W., *Science* **1984**, *226*. 254-261.
(18) Terabe, S., Otsuka, K., Ichikawa, K., Tsuchiya, A., Ando, T., *Analytical Chemistry* **1984**, *56*. 111-113.
(19) Terabe, S., Otsuka, K., Ando, T., *Analytical Chemistry* **1985**, *57*. 834-841.
(20) Paulus, A., Ohms, J. I., *Journal of chromatography* **1990**, *507*. 113-123.
(21) Cohen, A. S., Najarian, D. R., Karger, B. L., *Journal of chromatography* **1990**, *516*. 49-60.
(22) Wehr, T., Zhu, M., Rodriguez, R., Burke, D., Duncan, K., *American biotechnology laboratory* **1990**, *8*. 22-29.
(23) Watanabe, T., Terabe, S., *Journal of chromatography. A* **2000**, *880*. 311-322.
(24) Gebauer, P., Bocek, P., *Electrophoresis* **1997**, *18*. 2154-2161.
(25) Yan, C., Dadoo, R., Zhao, H., Zare, R. N., Rakestraw, D. J., *Analytical Chemistry* **1995**, *67*. 2026-2029.
(26) Pretoriu.V, Hopkins, B. J., Schieke, J. D., *Journal of chromatography* **1974**, *99*. 23-30.
(27) Kirby, B. J., Hasselbrink, E. F., *Electrophoresis* **2004**, *25*. 187-202.
(28) Kirby, B. J., Hasselbrink, E. F., *Electrophoresis* **2004**, *25*. 203-213.
(29) Rice, C. L., Whitehea.R, *Journal of Physical Chemistry* **1965**, *69*. 4017-&.
(30) Tsuda, T., Ikedo, M., Jones, G., Dadoo, R., Zare, R. N., *Journal of chromatography* **1993**, *632*. 201-207.
(31) Tallarek, U., Rapp, E., Scheenen, T., Bayer, E., Van As, H., *Analytical Chemistry* **2000**, *72*. 2292-2301.
(32) Effenhauser, C. S., Bruin, G. J. M., Paulus, A., *Electrophoresis* **1997**, *18*. 2203-2213.

(33) Fletcher, P. D. I., Haswell, S. J., Paunov, V. N., *Analyst* **1999**, *124*. 1273-1282.
(34) Knox, J. H., Mccormack, K. A., *Chromatographia* **1994**, *38*. 207-214.
(35) Wang, W., Zhou, F., Zhao, L., Zhang, J. R., Zhu, J. J., *Journal of chromatography. A* **2007**, *1170*. 1-8.
(36) Lukacs, K. D., Jorgenson, J. W., *Journal of High Resolution Chromatography & Chromatography Communications* **1985**, *8*. 407-411.
(37) Lee, T. T., Dadoo, R., Zare, R. N., *Analytical Chemistry* **1994**, *66*. 2694-2700.
(38) Fanali, S., Bocek, P., *Electrophoresis* **1996**, *17*. 1921-1924.
(39) Altria, K. D., Filbey, S. D., *Analytical Proceedings* **1993**, *30*. 363-365.
(40) Huang, X. H., Gordon, M. J., Zare, R. N., *Analytical Chemistry* **1988**, *60*. 1837-1838.
(41) Ocvirk, G., Munroe, M., Tang, T., Oleschuk, R., Westra, K., Harrison, D. J., *Electrophoresis* **2000**, *21*. 107-115.
(42) Locascio, L. E., Perso, C. E., Lee, C. S., *Journal of chromatography. A* **1999**, *857*. 275-284.
(43) Wanders, B. J., Vandegoor, T. A. A. M., Everaerts, F. M., *Journal of Chromatography A* **1993**, *652*. 291-294.
(44) Liu, Y., Wipf, D. O., Henry, C. S., *The Analyst* **2001**, *126*. 1248-1251.
(45) Jacobson, S. C., Ramsey, J. M., *Electrophoresis* **1995**, *16*. 481-486.
(46) Jakeway, S. C., de Mello, A. J., Russell, E. L., *Fresenius' journal of analytical chemistry* **2000**, *366*. 525-539.
(47) Ramsey, R. S., Ramsey, J. M., *Analytical Chemistry* **1997**, *69*. 2617-2617.
(48) Xue, Q. F., Foret, F., Dunayevskiy, Y. M., Zavracky, P. M., McGruer, N. E., Karger, B. L., *Analytical Chemistry* **1997**, *69*. 426-430.
(49) Liang, Z. H., Chiem, N., Ocvirk, G., Tang, T., Fluri, K., Harrison, D. J., *Analytical Chemistry* **1996**, *68*. 1040-1046.
(50) Mayrhofer, K., Zemann, A. J., Schnell, E., Bonn, G. K., *Analytical Chemistry* **1999**, *71*. 3828-3833.
(51) Wang, J., Polsky, R., Tian, B. M., Chatrathi, M. P., *Analytical Chemistry* **2000**, *72*. 5285-5289.
(52) Mogensen, K. B., Klank, H., Kutter, J. P., *Electrophoresis* **2004**, *25*. 3498-3512.
(53) Ocvirk, G., Tang, T., Harrison, D. J., *Analyst* **1998**, *123*. 1429-1434.
(54) Burggraf, N., Krattiger, B., de Mello, A. J., de Rooij, N. F., Manz, A., *Analyst* **1998**, *123*. 1443-1447.
(55) Roulet, J. C., Volkel, R., Herzig, H. P., Verpoorte, E., de Rooij, N. F., Dandliker, R., *Analytical Chemistry* **2002**, *74*. 3400-3407.
(56) Qin, J. H., Fung, Y. S., Zhu, D. R., Lin, B. C., *Journal of Chromatography A* **2004**, *1027*. 223-229.
(57) Johnson, M. E., Landers, J. P., *Electrophoresis* **2004**, *25*. 3513-3527.
(58) Woolley, A. T., Lao, K. Q., Glazer, A. N., Mathies, R. A., *Analytical Chemistry* **1998**, *70*. 684-688.
(59) Gavin, P. F., Ewing, A. G., *Analytical Chemistry* **1997**, *69*. 3838-3845.
(60) Lacher, N. A., Lunte, S. M., Martin, R. S., *Analytical Chemistry* **2004**, *76*. 2482-2491.
(61) Wang, J., Pumera, M., *Analytical Chemistry* **2002**, *74*. 5919-5923.
(62) Wallingford, R. A., Ewing, A. G., *Analytical Chemistry* **1987**, *59*. 1762-1766.
(63) Wightman, R. M., *Science* **1988**, *240*. 415-420.
(64) Wightman, R. M., *Analytical Chemistry* **1981**, *53*. 1125-&.

(65) Matson, W. R., Langlais, P., Volicer, L., Gamache, P. H., Bird, E., Mark, K. A., *Clinical chemistry* **1984**, *30*. 1477-1488.
(66) Gamache, P., Ryan, E., Svendsen, C., Murayama, K., Acworth, I. N., *Journal of chromatography* **1993**, *614*. 213-220.
(67) Holcomb, R. E., Kraly, J. R., Henry, C. S., *The Analyst* **2009**, *134*. 486-492.
(68) Schwarz, M. A., Galliker, B., Fluri, K., Kappes, T., Hauser, P. C., *The Analyst* **2001**, *126*. 147-151.
(69) Lunte, S. M., Lunte, C. E., Kissinger, P. T., in: Kissinger, P. T., Heineman, W. R. (Eds.). Marcel Dekker: New York, 2nd ed. edn., 1996, pp 813–853.
(70) Garcia, C. D., De Pauli, C. P., Ortiz, P. I., *Journal of Electroanalytical Chemistry* **2001**, *510*. 115-119.
(71) Garcia, G., Garcia, C. D., Ortiz, P. I., De Pauli, C. P., *Journal of Electroanalytical Chemistry* **2002**, *519*. 53-59.
(72) Fanguy, J. C., Henry, C. S., *Analyst* **2002**, *127*. 1021-1023.
(73) Hompesch, R. W., Garcia, C. D., Weiss, D. J., Vivanco, J. M., Henry, C. S., *The Analyst* **2005**, *130*. 694-700.
(74) Garcia, C. D., Henry, C. S., *Analytical Chemistry* **2003**, *75*. 4778-4783.
(75) Garcia, C. D., Henry, C. S., *Analytica Chimica Acta* **2004**, *508*. 1-9.
(76) Garcia, C. D., Henry, C. S., *Electroanalysis* **2005**, *17*. 1125-1131.
(77) Garcia, C. D., Henry, C. S., *Electroanalysis* **2005**, *17*. 223-230.
(78) Zhong, M., Lunte, S. M., *Analytical Chemistry* **1996**, *68*. 2488-2493.
(79) Weber, P. L., Lunte, S. M., *Electrophoresis* **1996**, *17*. 302-309.
(80) Oshea, T. J., Lunte, S. M., Lacourse, W. R., *Analytical Chemistry* **1993**, *65*. 948-951.
(81) Vandaveer, W. R. t., Pasas-Farmer, S. A., Fischer, D. J., Frankenfeld, C. N., Lunte, S. M., *Electrophoresis* **2004**, *25*. 3528-3549.
(82) Wang, J., Siangproh, W., Blasco, A. J., Chailapakul, O., Escarpa, A., *Analytica Chimica Acta* **2006**, *556*. 301-305.
(83) Shin, D. C., Sarada, B. V., Tryk, D. A., Fujishima, A., *Analytical Chemistry* **2003**, *75*. 530-534.
(84) Klett, O., Bjorefors, F., Nyholm, L., *Analytical Chemistry* **2001**, *73*. 1909-1915.
(85) Klett, O., Nischang, I., Nyholm, L., *Electrophoresis* **2002**, *23*. 3678-3682.
(86) Martin, R. S., Ratzlaff, K. L., Huynh, B. H., Lunte, S. M., *Analytical Chemistry* **2002**, *74*. 1136-1143.
(87) Liu, Y., Vickers, J. A., Henry, C. S., *Analytical Chemistry* **2004**, *76*. 1513-1517.
(88) Xu, J. J., Bao, N., Xia, X. H., Peng, Y., Chen, H. Y., *Analytical Chemistry* **2004**, *76*. 6902-6907.
(89) Klett, O., Nyholm, L., *Analytical Chemistry* **2003**, *75*. 1245-1250.
(90) Qian, J., Wu, Y., Yang, H., Michael, A. C., *Analytical Chemistry* **1999**, *71*. 4486-4492.
(91) Zhang, S. S., Yuan, Z. B., Liu, H. X., Zou, H., Wu, Y. J., *Journal of Chromatography A* **2000**, *872*. 259-268.
(92) Osbourn, D. M., Lunte, C. E., *Analytical Chemistry* **2001**, *73*. 5961-5964.
(93) Osbourn, D. M., Lunte, C. E., *Analytical Chemistry* **2003**, *75*. 2710-2714.
(94) Lai, C. C. J., Chen, C. H., Ko, F. H., *Journal of Chromatography A* **2004**, *1023*. 143-150.
(95) Wu, C. C., Wu, R. G., Huang, J. G., Lin, Y. C., Hsien-Chang, C., *Analytical Chemistry* **2003**, *75*. 947-952.

(96) Kim, J. H., Kang, C. J., Jeon, D., Kim, Y. S., *Microelectronic Engineering* **2005**, *78-79*. 563-570.
(97) Vickers, J. A., Henry, C. S., *Electrophoresis* **2005**, *26*. 4641-4647.
(98) Vickers, J. A., Dressen, B. M., Weston, M. C., Boonsong, K., Chailapakul, O., Cropek, D. M., Henry, C. S., *Electrophoresis* **2007**, *28*. 1123-1129.
(99) Xu, J., Zhang, H., Chen, G., *Talanta* **2007**, *73*. 932-937.
(100) Chen, G., *Talanta* **2007**, *74*. 326-332.
(101) Crevillen, A. G., Pumera, M., Gonzalez, M. C., Escarpa, A., *Electrophoresis* **2008**, *29*. 2997-3004.
(102) Shiddiky, M. J., Shim, Y. B., *Analytical Chemistry* **2007**, *79*. 3724-3733.
(103) Yogeswaran, U., Chen, S. M., *Sensors* **2008**, *8*. 290-313.
(104) Wang, J., Chen, G., Chatrathi, M. P., Fujishima, A., Tryk, D. A., Shin, D., *Analytical Chemistry* **2003**, *75*. 935-939.
(105) Osbourn, D. M., Weiss, D. J., Lunte, C. E., *Electrophoresis* **2000**, *21*. 2768-2779.
(106) Shihabi, Z. K., *Journal of chromatography. A* **2000**, *902*. 107-117.
(107) Quirino, J. P., Terabe, S., *Journal of chromatography. A* **2000**, *902*. 119-135.
(108) Beckers, J. L., Bocek, P., *Electrophoresis* **2000**, *21*. 2747-2767.
(109) Chien, R. L., *Electrophoresis* **2003**, *24*. 486-497.
(110) Shihabi, Z. K., *Electrophoresis* **2002**, *23*. 1612-1617.
(111) Xu, Z. Q., Hirokawa, T., Nishine, T., Arai, A., *Journal of chromatography. A* **2003**, *990*. 53-61.
(112) Maeso, N., Cifuentes, A., Barbas, C., *Journal of chromatography. B, Analytical technologies in the biomedical and life sciences* **2004**, *809*. 147-152.
(113) Chen, Z., Naidu, R., *Journal of chromatography. A* **2004**, *1023*. 151-157.
(114) Strausbauch, M. A., Landers, J. P., Wettstein, P. J., *Analytical Chemistry* **1996**, *68*. 306-314.
(115) Li, J., Thibault, P., Martin, A., Richards, J. C., Wakarchuk, W. W., van der Wilp, W., *Journal of chromatography. A* **1998**, *817*. 325-336.
(116) Zhang, P., Xu, G. W., Xiong, J. H., Zheng, Y. F., Shi, X. Z., Yang, Q., Wei, F. S., *Journal of separation science* **2003**, *26*. 1527-1532.
(117) Quirino, J. P., Terabe, S., *Science* **1998**, *282*. 465-468.
(118) Sera, Y., Matsubara, N., Otsuka, K., Terabe, S., *Electrophoresis* **2001**, *22*. 3509-3513.
(119) Monton, M. R., Quirino, J. P., Otsuka, K., Terabe, S., *Journal of chromatography. A* **2001**, *939*. 99-108.
(120) Wu, C. H., Chen, M. C., Su, A. K., Shu, P. Y., Chou, S. H., Lin, C. H., *Journal of chromatography. B, Analytical technologies in the biomedical and life sciences* **2003**, *785*. 317-325.
(121) Burgi, D. S., Chien, R. L., *Analytical Chemistry* **1991**, *63*. 2042-2047.
(122) Sueyoshi, K., Kitagawa, F., Otsuka, K., *Analytical Chemistry* **2008**, *80*. 1255-1262.
(123) Whitesides, G. M., *Nature* **2006**, *442*. 368-373.
(124) Duffy, D. C., McDonald, J. C., Schueller, O. J. A., Whitesides, G. M., *Analytical Chemistry* **1998**, *70*. 4974-4984.
(125) Henry, A. C., Tutt, T. J., Galloway, M., Davidson, Y. Y., McWhorter, C. S., Soper, S. A., McCarley, R. L., *Analytical Chemistry* **2000**, *72*. 5331-5337.
(126) Johnson, T. J., Waddell, E. A., Kramer, G. W., Locascio, L. E., *Applied Surface Science* **2001**, *181*. 149-159.

(127) Roberts, M. A., Rossier, J. S., Bercier, P., Girault, H., *Analytical Chemistry* **1997**, *69*. 2035-2042.
(128) Barker, S. L. R., Tarlov, M. J., Canavan, H., Hickman, J. J., Locascio, L. E., *Analytical Chemistry* **2000**, *72*. 4899-4903.
(129) Muck, A., Svatos, A., *Talanta* **2007**, *74*. 333-341.
(130) Fujimoto, C., *Electrophoresis* **2002**, *23*. 2929-2937.
(131) Pietrzyk, D. J., Chen, S., Chanthawat, B., *Journal of Chromatography A* **1997**, *775*. 327-338.
(132) Bai, Y. L., Koh, C. G., Boreman, M., Juang, Y. J., Tang, I. C., Lee, L. J., Yang, S. T., *Langmuir* **2006**, *22*. 9458-9467.
(133) Doherty, E. A. S., Meagher, R. J., Albarghouthi, M. N., Barron, A. E., *Electrophoresis* **2003**, *24*. 34-54.
(134) Liu, Y., Fanguy, J. C., Bledsoe, J. M., Henry, C. S., *Analytical Chemistry* **2000**, *72*. 5939-5944.
(135) Hu, S., Ren, X., Bachman, M., Sims, C. E., Li, G. P., Allbritton, N., *Analytical Chemistry* **2002**, *74*. 4117-4123.
(136) Belder, D., Deege, A., Kohler, F., Ludwig, M., *Electrophoresis* **2002**, *23*. 3567-3573.
(137) Pittman, J. L., Henry, C. S., Gilman, S. D., *Analytical Chemistry* **2003**, *75*. 361-370.
(138) Miyaki, K., Zeng, H. L., Nakagama, T., Uchiyama, K., *Journal of chromatography. A* **2007**, *1166*. 201-206.
(139) Wang, A. J., Feng, J. J., Fan, J., *Journal of chromatography. A* **2008**, *1192*. 173-179.
(140) Feng, J. J., Wang, A. J., Fan, J., Xu, J. J., Chen, H. Y., *Analytica chimica acta* **2010**, *658*. 75-80.
(141) Duffy, D. C., McDonald, J. C., Schueller, O. J., Whitesides, G. M., *Analytical Chemistry* **1998**, *70*. 4974-4984.
(142) Badal, M. Y., Wong, M., Chiem, N., Salimi-Moosavi, H., Harrison, D. J., *Journal of chromatography. A* **2002**, *947*. 277-286.
(143) Kato, M., Gyoten, Y., Sakai-Kato, K., Toyo'oka, T., *Journal of chromatography. A* **2003**, *1013*. 183-189.
(144) Pallandre, A., de Lambert, B., Attia, R., Jonas, A. M., Viovy, J. L., *Electrophoresis* **2006**, *27*. 584-610.
(145) Ludwig, M., Belder, D., *Electrophoresis* **2003**, *24*. 2481-2486.
(146) Schmalzing, D., Piggee, C. A., Foret, F., Carrilho, E., Karger, B. L., *Journal of chromatography. A* **1993**, *652*. 149-159.
(147) Decher, G., *Science* **1997**, *277*. 1232-1237.
(148) Katayama, H., Ishihama, Y., Asakawa, N., *Analytical Chemistry* **1998**, *70*. 5272-5277.
(149) Katayama, H., Ishihama, Y., Asakawa, N., *Analytical Chemistry* **1998**, *70*. 2254-2260.
(150) Belder, D., Ludwig, M., *Electrophoresis* **2003**, *24*. 3595-3606.
(151) Roman, G. T., Carroll, S., McDaniel, K., Culbertson, C. T., *Electrophoresis* **2006**, *27*. 2933-2939.
(152) Vrouwe, E. X., Luttge, R., Olthuis, W., van den Berg, A., *Journal of chromatography. A* **2006**, *1102*. 287-293.
(153) Wang, W., Zhao, L., Zhang, J. R., Zhu, J. J., *Journal of chromatography. A* **2007**, *1142*. 209-213.
(154) Gong, M., Wehmeyer, K. R., Limbach, P. A., Heineman, W. R., *Journal of chromatography. A* **2007**, *1167*. 217-224.

(155) Han, B., Xu, Y., Zhang, L., Yang, X., Wang, E., *Talanta* **2009**, *79*. 959-962.
(156) Wei, W., Ju, H., *Electrophoresis* **2005**, *26*. 586-592.
(157) Noblitt, S. D., Schwandner, F. M., Hering, S. V., Collett, J. L., Jr., Henry, C. S., *Journal of chromatography. A* **2009**, *1216*. 1503-1510.
(158) Gertsch, J. C., Noblitt, S. D., Cropek, D. M., Henry, C. S., *Analytical Chemistry* **2010**, *82*. 3426-3429.
(159) Wang, A. J., Xu, J. J., Chen, H. Y., *Analytica Chimica Acta* **2006**, *569*. 188-194.
(160) Xu, Y., Jiang, H., Wang, E., *Electrophoresis* **2007**, *28*. 4597-4605.
(161) Towns, J. K., Regnier, F. E., *Analytical Chemistry* **1991**, *63*. 1126-1132.
(162) Dou, Y. H., Bao, N., Xu, J. J., Meng, F., Chen, H. Y., *Electrophoresis* **2004**, *25*. 3024-3031.
(163) Yeung, K. K., Lucy, C. A., *Analytical Chemistry* **1998**, *70*. 3286-3290.
(164) Cunliffe, J. M., Baryla, N. E., Lucy, C. A., *Analytical Chemistry* **2002**, *74*. 776-783.
(165) Wang, C., Lucy, C. A., *Electrophoresis* **2004**, *25*. 825-832.
(166) Mori, M., Hu, W. Z., Haddad, P. R., Fritz, J. S., Tanaka, K., Tsue, H., Tanaka, S., *Analytical and Bioanalytical Chemistry* **2002**, *372*. 181-186.
(167) Tsunoda, M., *Analytical and Bioanalytical Chemistry* **2006**, *386*. 506-514.
(168) Atuk, N. O., Hanks, J. B., Weltman, J., Bogdonoff, D. L., Boyd, D. G., Vance, M. L., *The Journal of clinical endocrinology and metabolism* **1994**, *79*. 1609-1614.
(169) Kumarathasan, P., Vincent, R., *Journal of chromatography. A* **2003**, *987*. 349-358.
(170) Sabbioni, C., Saracino, M. A., Mandrioli, R., Pinzauti, S., Furlanetto, S., Gerra, G., Raggi, M. A., *Journal of chromatography. A* **2004**, *1032*. 65-71.
(171) Talwar, D., Williamson, C., McLaughlin, A., Gill, A., O'Reilly, D. S., *Journal of chromatography. B, Analytical technologies in the biomedical and life sciences* **2002**, *769*. 341-349.
(172) Sastre, E., Nicolay, A., Bruguerolle, B., Portugal, H., *Journal of chromatography. B, Analytical technologies in the biomedical and life sciences* **2004**, *801*. 205-211.
(173) Chen, D. C., Zhan, D. Z., Cheng, C. W., Liu, A. C., Chen, C. H., *Journal of chromatography. B, Biomedical sciences and applications* **2001**, *750*. 33-39.
(174) Male, K. B., Luong, J. H., *Journal of chromatography. A* **2003**, *1003*. 167-178.
(175) Johirul, M., Shiddiky, A., Kim, R. E., Shim, Y. B., *Electrophoresis* **2005**, *26*. 3043-3052.
(176) Lacher, N. A., Lunte, S. M., Martin, R. S., *Analytical Chemistry* **2004**, *76*. 2482-2491.
(177) Martindale, W., in Reynolds, E. F. (Ed.). Pharmaceutical Press: London, 29th edition edn., 1989.
(178) Russoin, A., Glick, D. Wiley: New York, 1998, vol. Vol. 33.
(179) Moriarty-Craige, S. E., Jones, D. P., *Annual review of nutrition* **2004**, *24*. 481-509.
(180) Bayle, C., Causse, E., Couderc, F., *Electrophoresis* **2004**, *25*. 1457-1472.
(181) Chen, X., Zhou, Y., Peng, X., Yoon, J., *Chemical Society reviews* **2010**, *39*. 2120-2135.
(182) Winterbourn, C. C., Metodiewa, D., *Free radical biology & medicine* **1999**, *27*. 322-328.
(183) Seshadri, S., Beiser, A., Selhub, J., Jacques, P. F., Rosenberg, I. H., D'Agostino, R. B., Wilson, P. W., Wolf, P. A., *The New England journal of medicine* **2002**, *346*. 476-483.
(184) Savage, D. G., Lindenbaum, J., Stabler, S. P., Allen, R. H., *The American journal of medicine* **1994**, *96*. 239-246.
(185) Klee, G. G., *Clinical chemistry* **2000**, *46*. 1277-1283.
(186) Shahrokhian, S., *Analytical Chemistry* **2001**, *73*. 5972-5978.

(187) Ivanov, A. R., Nazimov, I. V., Baratova, L. A., *Journal of chromatography. A* **2000**, *870*. 433-442.
(188) Chwatko, G., Bald, E., *Talanta* **2000**, *52*. 509-515.
(189) Nolin, T. D., McMenamin, M. E., Himmelfarb, J., *Journal of chromatography. B, Analytical technologies in the biomedical and life sciences* **2007**, *852*. 554-561.
(190) Ivanov, A. R., Nazimov, I. V., Baratova, L. A., *Journal of chromatography. A* **2000**, *895*. 167-171.
(191) Chen, G., Zhang, L., Wang, J., *Talanta* **2004**, *64*. 1018-1023.
(192) Inoue, T., Kirchhoff, J. R., *Analytical Chemistry* **2002**, *74*. 1349-1354.

# CHAPTER 2. INCORPORTION OF A BUBBLE CELL IN DETECTION ZONE FOR IMPROVING THE DETECTION SENSITIVITY AND LODS OF MCE-ECD

## 2.1 INTRODUCTION

One major limitation of CE and also MCE analyses is the poor concentration sensitivity caused by the limited volume of injected samples and the low absorption path-length if UV detection is used. To address these issues, z- or u-shaped optical path and multi-reflection cells have been employed in traditional CE and MCE.[1-3] Also bubble-shaped detection cells in which the optical path length was increased have been utilized to enhance absorbance detection sensitivity and LOD.[4, 5] Increasing sensitivity for DC amperometry and PAD when coupled with MCE requires the isolation of the high-voltage separation field from the detection system in a process generally referred as current decoupling as discussed in more detail in Chapter 1. A significant improvement in detection sensitivity has been achieved when the separation current was grounded by using microfabricated Pd or Pt electrodes as a decoupler before reaching the working electrode.[6-8] Our group has developed a simple integrated Pd microwire decoupler and its coupling with DC for a sensitive detection of a wide range of analytes.[9-11] Based on this design, further increase in detection sensitivity will be explored and discussed in this chapter by expanding the exposed surface area of WE to the fluid flow in a bubble cell incorporated at the detection zone, since ECD is inherently surface derived phenomenon. Similar idea has been used to improve the absorbance detection performance in conventional[4] and microchip CE,[5] but never applied in MCE-ECD field in the range out of our research group. Several our group members

have already employed a bubble cell design in their MCE devices to improve the compatibility and applicability of contact conductivity detection in MCE.[12, 13]

Here, one effort on improving detection sensitivity and LODs by an implementation of a capillary expansion (bubble cell) at the detection zone is presented. Bubble cell widths were varied from 1× to 10× the separation channel width (50 μm) and the effects of electrode surface area on detection sensitivity and LODs were characterized for model analytes using DC amperometry coupled with MCE. In addition, the impact of bubble cell widths on separation efficiency was examined using fluorescent imaging. Improved detection sensitivity and decreased LODs were obtained with increased bubble cell width without losing much of separation efficiency, and LODs of dopamine and catechol detected in a 5× bubble cell were 25 nM and 50 nM, respectively.

## 2.2 EXPERIMENTAL

### 2.2.1 Chemicals

Hydrochloric acid (37%), N-tris[hydroxymethyl]methyl-2-aminoethane-sulfonic acid (TES), sodium dodecyl sulfate (SDS), 3,4-dihydroxyphenethylamine (dopamine), catechol, and propylene glycol methyl ether acetate were purchased from Sigma-Aldrich (St. Louis, MO). Sodium hydroxide and boric acid were purchased from Fisher (Pittsburgh, PA). Fluorescein was received from Eastman (Rochester NY, USA). Other reagents used for the fabrication of MCE-ECD include SU-8 2035 photoresist (Microchem, Newton, MA), Sylgard 184 elastomer and curing agent (PDMS) (Dow Corning, Midland, MI), 4-in. silicon wafers (University Wafer, South Boston, MA), and microwires made of 99.99% Pd (diameter 25 μm) and 99.99% Au (diameter 25 μm) (Goodfellow, Huntingdon, England). Solutions were prepared in 18.2 MΩ

water from a Millipore Milli-Q purification system (Milipore Corp., Billerica, MA). 10 mM stock solutions of dopamine and catechol were individually prepared weekly in 10 mM HCl. All stock solutions were stored at 4ºC. All BGEs were adjusted to their corresponding pH values with concentrated NaOH. A 20 mM boric acid buffer at pH 9.2 and a 20 mM TES buffer containing 1 mM SDS at pH 7.0 were used as BGEs for fluorescent imaging experiments and separations of dopamine and catechol, respectively.

### 2.2.2 PDMS Microchip Fabrication

The method used to fabricate PDMS microchips using incorporated microwires for detection has been published previously.[9, 14] Briefly, SU-8 2035, a negative photoresist was spun onto a 4-in. silicon wafer to a thickness of 50 μm. The coated wafer was baked at 65 ºC for 3 min and 95 ºC for 5 min. A digitally printed mask was used to define channel structures, and the system was exposed to a UV light source (364 nm, 400 W) for 9 sec. After exposure and post-baking at 65 ºC for 2 min and 95 ºC for 6 min, the wafer was developed in propylene glycol methyl ether acetate leaving a positive relief patter on the wafer. A degassed PDMS mixture (Sylgard 184 elastomer and curing agent (10:1)) was poured onto the resulting wafer and cured at 65 ºC for at least 2 h. The cured PDMS was peeled off the master and the reservoirs holes cut into the PDMS using a 5 mm diameter biopsy punch (Robbins Instruments, Chatham, NJ). The electrode microwires were aligned in pre-designated electrode channels. After plasma treatment of the molded and blank PDMS pieces (Harrick PDC-32G Plasma Cleaner/Sterilizer) for 45 s, the microchip was assembled to form an irreversible sealing by bringing two pieces into conformal contact. Instant adhesive was used to seal the ends of electrode alignment channels and glued the electrode leads which consist of insulated 1 mm diameter Cu wire to the assembled

device. Electrical contact between the electrode leads and electrodes was achieved using high purity silver paint (SPI Supplies, West Chester, PA). The exposed electrical contacts were insulated with half-cured PDMS mixture and allowed to dry for 24 hrs before use. Figure 2.1A shows a schematic drawing of PDMS microchips (50 μm × 50 μm × 6 cm), which has a double T injector with a 625 pL volume[15, 16] for pinched injection[17] and a bubble cell in the electrochemical detection zone. A bright field image of the silicon mold with a bubble cell width 5× the separation channel width (50 μm) is shown in Figure 2.1B. Each electrode channel is 50 μm wide and separated by 125 μm. A 25 μm Pd decoupler and two 25 μm Au working electrodes (WEs) are placed in the bubble cell using electrode alignment channels. The rectangular tapers connecting the electrode channels and the bubble cell are 20 μm × 56 μm and are shown in the red oval.

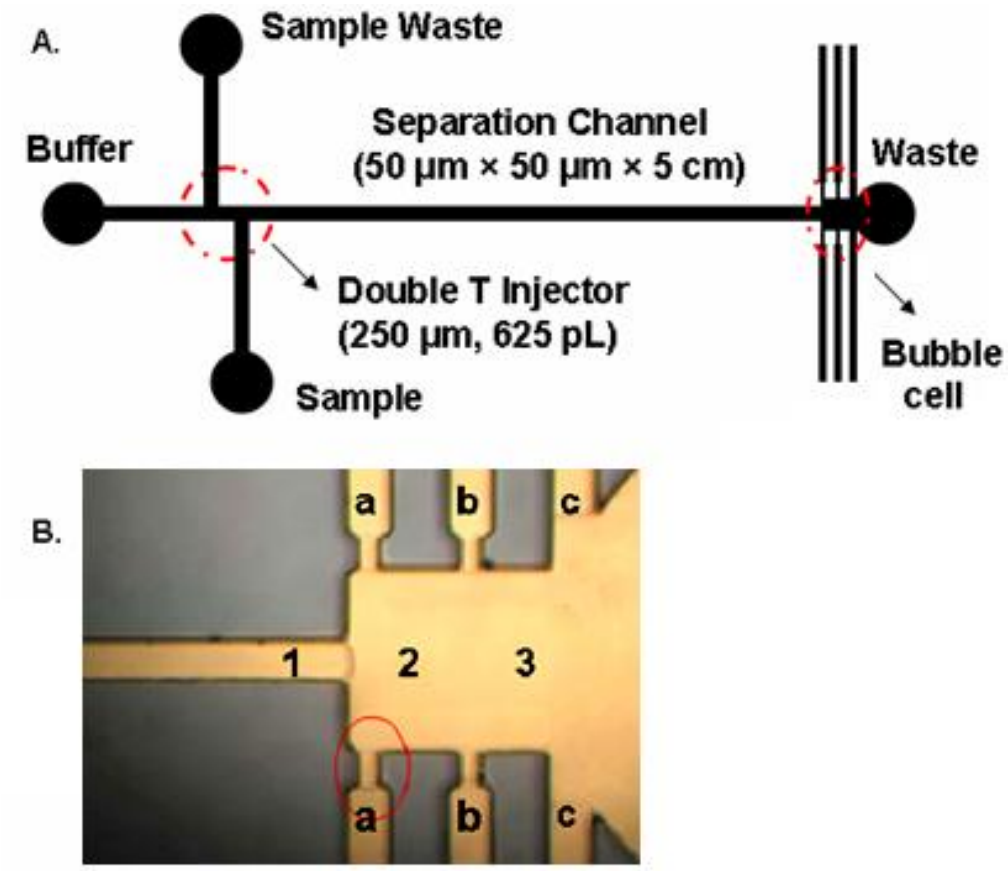


**Figure 2.1** (A) Schematic of PDMS microchips (50 µm × 50 µm × 6 cm from buffer to waste reservoir) with a double T injector (250 µm, 625 pL) for pinched injection. The sample, buffer and sample waste side channels are all 1 cm in length. All reservoirs are 5 mm in diameter. (B) Bright field image of silicon mold with a bubble cell width 5× the separation channel width (50 µm). The gold color seen in this picture is the native color of the SU-8 photoresist when photographed. Electrode channels a, b and c are 50 µm wide with 125 µm spacing between the channels and used as alignment channels for placing a 25 µm Pd decoupler and two 25 µm Au working electrodes (WEs) respectively. 1, 2 and 3 are three positions chosen to measure separation efficiencies in the separation channel and the bubble cell detection zone, respectively.

### 2.2.3 MCE-ECD

Channels and reservoirs were first rinsed with ultra-pure water and then filled with BGE for 30 min pretreatment by applying pressure to a reservoir containing the solution. The buffer in the sample reservoir was replaced with sample solution prior to running analyses. The corresponding positions of sample (SR), sample waste (SW), buffer (BR) and buffer waste (BW) reservoirs are shown in Figure 2.1A and equivalent volume of solutions were loaded in all reservoirs. Applied voltages were facilitated by a programmable high voltage power supply built in-house.[18] The Pd decoupler was always held at ground in both injection and separation phases to prevent exposing the detector electronics to high voltage. Pinched injection was performed by applying a high positive potential (450 V) to SR and BR, and a negative potential (–160 V) to SW. For its separation, a high positive potential (1,200 V) was applied to BR while SR and SW were held at 450 V, allowing only buffer to pass through the separation channel. DC amperometric detection was employed (CHI 1010A Electrochemical Analyzer, CH Instruments, Austin, TX) in a two-electrode configuration[9] for the detection of dopamine and catechol. A Pt wire (1 mm diameter) in the waste reservoir was acted as both auxiliary and psuedo-reference electrode.[9] Cleaning of Pd decoupler was done initially by running cyclic voltammetry (CV) from -1.0 V to 1.0 V at 0.1 V/s for 50 cycles. Two gold working electrodes were cleaned using CV by scanning from -0.5 V to 1.8 V at 0.5 V/s for 100 cycles while buffer flowed over the electrodes.

## 2.3 RESULTS AND DISCUSSION

### 2.3.1 Bubble Cell Design

A bubble cell design (Figure 2.1A and Figure 2.1B for detection zone details) was tested with PDMS microchips using a dual working electrode detection configuration. All microchips had one downstream Au WE placed at the exit of the separation channel, with a Pd decoupler and an upstream Au WE placed in the channel of the bubble cell. Bubble cell widths changing from 1× to 10× the separation channel width (50 μm) were chosen to investigate the effects of electrode surface area on detection sensitivity, LODs and separation efficiency at the upstream WE.

### 2.3.2 Characterization of Bubble Cell Design with DC Amperometric Detection

Dopamine and catechol were chosen as model analytes to characterize the new bubble cell design using DC amperometric detection. Figure 2.2A depicts example electropherograms for 100 μM dopamine and catechol detected on PDMS microchips at the upstream WE in 1× to 5× bubble cells. Significant increases in peak heights for both model analytes were observed at the upstream WE in the bubble cell as shown in Figure 2.2B. The peak heights of dopamine and catechol at the upstream WE increased approximately linearly from 1× to 5× bubble cell width ($R^2$ = 0.9658, $R^2$ = 0.9648, respectively), which can be attributed to the increase in the electrode surface area. Figure 2.2B also shows a roughly linear decrease in the noise at the upstream WE from 12.99 ± 0.34 pA (n = 4) in a 1× bubble cell to 2.786 ± 0.098 pA (n = 4) in a 5× bubble cell ($R^2$ = 0.9920). The decrease in noise is a result of a decrease in the resistance of the solution in the bubble cell. Lower resistance leads to a decreased voltage drop in the bubble cell, which is the major source of noise with ECD. However, when increasing the bubble cell from 5× to 10×,

increases in peak heights at the upstream WE were not as significant. These responses are probably caused by the increased band broadening produced in larger bubble cells. Furthermore, the noise in the bubble cell increased at 8× and 10× relative to 5× since two opposing phenomena are at work. As the bubble cell width increases, this source of noise decreases. Meanwhile, more noise arising from double-layer capacitance is noted in the bubble cell with larger electrode area. The 4× and 5× bubble cells appear to reach a minimum noise value at where these two phenomena are balanced. As shown in Table 2.1, approximate four-fold improvement was obtained for both analytes as the detection sensitivities of dopamine and catechol increased from 0.1213 and 0.0798 nA/μM in a 1× bubble cell to 0.4354 and 0.2904 nA/μM in a 5× bubble cell, respectively. Meanwhile, the LODs of dopamine and catechol decrease from 0.40 ± 0.01 and 0.60 ± 0.03 μM in a 1× bubble cell to 0.025 ± 0.002 and 0.050 ± 0.004 μM in a 5× bubble cell, respectively, showing a factor of 16 and 12 decreases in the LODs for both analytes (n = 4 and S/N = 3). The decreased LODs are the results of increased peak currents and decreased noise in the 5× bubble cell. The detection linear ranges for both analytes also correspondingly expanded to 0.1 to100 μM.

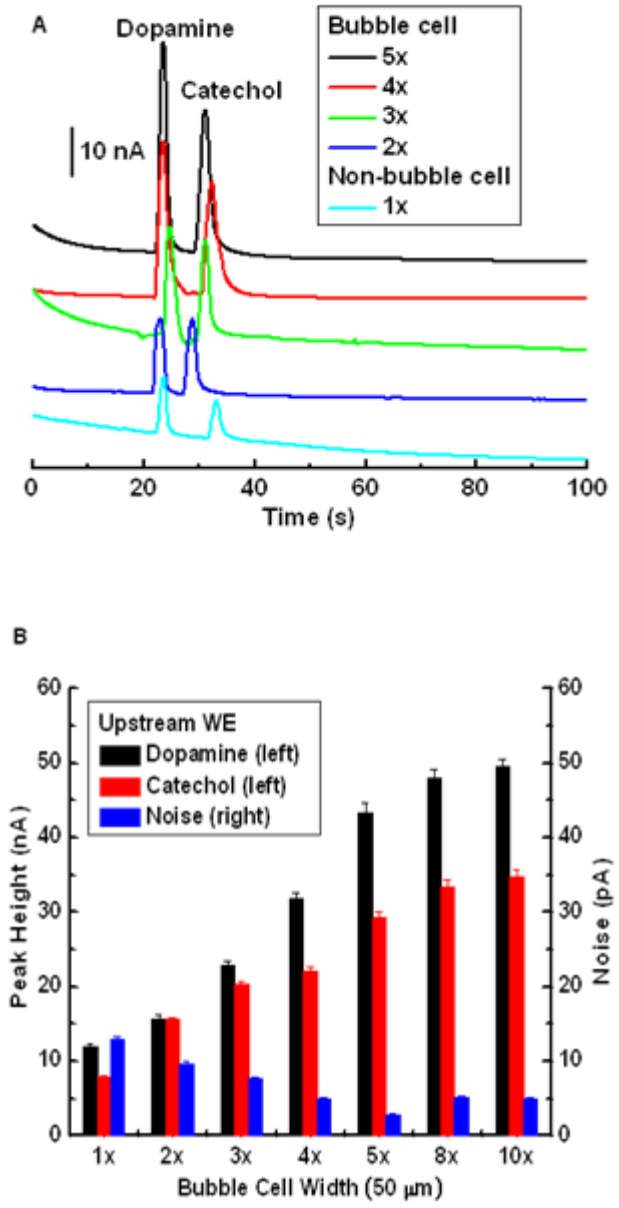


**Figure 2.2** (A) Example electropherograms for 100 μM dopamine and catechol detected on PDMS microchips at the upstream WE in 1× to 5× bubble cells. (B) Changes in peak heights (left Y axis label) of 100 μM dopamine and catechol and noise level (right Y axis label) at the upstream WE in 1× to 10× bubble cells. Experimental conditions: separation field strength: 200 V/cm; pinched injection time: 10 s; BGE: 20 mM TES, 1 mM SDS (pH 7.0); $E_{Det}$ = 1.4 V.

**Table 2.1** Detection sensitivities, LODs and separation efficiencies of dopamine and catechol detected on PDMS microchips at the upstream WE in 1× to 5× bubble cells, respectively. Separation efficiency ($N$ in plate) is calculated based on the following equation where $t_r$ is the migration time of the analyte, and $W_h$ is the half peak width. $N = 5.54(t_r/W_h)^2$, which will be used for all separation efficiency calculations in this thesis.

| Upstream WE | Dopamine | | | Catechol | | |
|---|---|---|---|---|---|---|
| | Sensitivity (nA/μM) | LOD (μM) | Separation efficiency (N/m) | Sensitivity (nA/μM) | LOD (μM) | Separation efficiency (N/m) |
| Bubble cell 1× | 0.1213 | 0.40±0.10 | 35,370 ± 1,800 | 0.0798 | 0.60±0.15 | 64,800 ± 3,100 |
| Bubble cell 2× | 0.1552 | 0.20±0.04 | 23,100 ± 14,00 | 0.1533 | 0.40±0.12 | 36,200 ± 1,700 |
| Bubble cell 3× | 0.2389 | 0.10±0.03 | 26,500 ± 1,550 | 0.2034 | 0.20±0.07 | 42,100 ± 2,000 |
| Bubble cell 4× | 0.3180 | 0.05±0.01 | 24,700 ± 1,450 | 0.2236 | 0.10±0.04 | 44,800 ± 1,950 |
| Bubble cell 5× | 0.4354 | 0.025±0.005 | 24,100 ± 1500 | 0.2904 | 0.05±0.02 | 41,860 ± 2,100 |

### 2.3.3 Impact of Bubble Cell Widths on Separation Efficiency

Next, separation efficiencies were measured as a function of bubble cell width using fluorescein. Figure 2.1B shows the three positions chosen to measure separation efficiencies in the separation channel and the bubble cell detection zone, respectively. Position 1 was located in the separation channel before the bubble cell, while positions 2 and 3 were selected between the decoupler and upstream WE and the upstream and downstream WE, respectively. The separation efficiencies at positions 2 and 3 relative to position 1 were monitored to determine the effect of bubble cell width on separation efficiency. Separation efficiencies were measured using the

decoupler and applying 1 V to both upstream and downstream WEs to replicate electrochemical experiments.

As depicted in Figure 2.3, separation efficiencies at positions 2 and 3 relative to position 1 decrease with increasing bubble cell width. Also, the separation efficiency at position 2 was higher than at position 3 for the same bubble cell width. As the bubble cell width increases, the velocity of fluid flow at the same position in the bubble cell decreases due to the larger channel

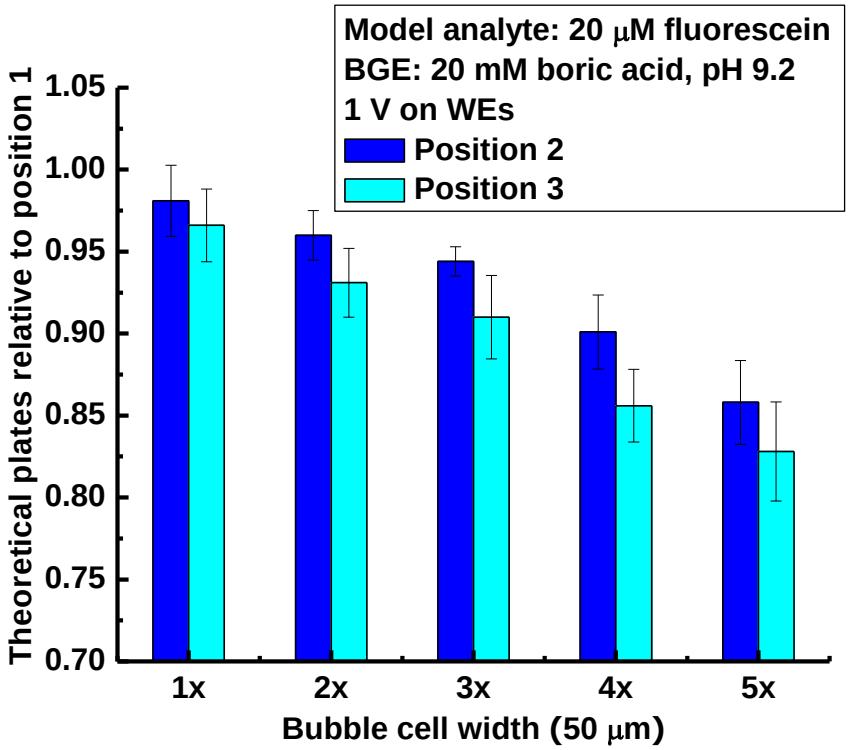


**Figure 2.3** Separation efficiency comparisons among 1× to 5× bubble cells. Figure 2.1B shows three positions chosen in a bubble cell to collect electropherograms of 20 μM fluorescein on each PDMS microchip. Experimental conditions: separation field strength: 200 V/cm; pinched injection time: 7 s; BGE: 20mM boric acid (pH 9.2).

volume. The decrease in fluid velocity causes an increase in the residence time of the analyte, resulting in band broadening of the analyte peak and a decrease in separation efficiency. In addition, separation efficiency decreases with increasing distance from the decoupler as fluid flow in this region is predominantly hydrodynamic. Compared with the 1× bubble cell, the loss in separation efficiencies at positions 2 and 3 relative to position 1 are 8.15% (position 2), 12.5% (position 3) in a 4× bubble cell, and 11.4% (position 2), 14.3% (position 3) in a 5× bubble cell, respectively. Therefore, as a compromise between the loss in separation efficiency and improved detection sensitivity as well as detection limit in a large bubble cell, microchips with a 4× bubble cell in the detection zone were selected for further experiments performed with sample stacking techniques.

## 2.4 CONCLUSIONS

Here, a simple implementation of a bubble cell detector for MCE-ECD was described. The surface area of WE exposed to the fluid flow entering into the detection zone increases with increasing bubble cell width. This ability affords improved detection sensitivity and lower LODs for model analytes with ~8% to ~12% loss in separation efficiency in 4× and 5× bubble cell, respectively. The lowest LODs of dopamine and catechol detected in a 5× bubble cell were 25 and 50 nM, showing a 16-fold and 12-fold decrease compared with the straight channel design, respectively. Considering the balance between the loss in separation efficiency and improved detection sensitivity as well as detection limit in a large bubble cell, microchips with a 4× bubble cell in the detection zone were selected for further experiments.

Besides using the incorporation of a bubble cell at the detection zone for improving detection sensitivity and detection limits in our previous MCE-ECD system, some on-line

sample preconcentration methods can be also employed for the same purpose since the low concentration detection sensitivity in MCE analyses is also caused by the limited volume of injected samples. In chapter 3, field amplified sample injection and field amplified sample stacking, two methods are investigated for their stacking effects using DC amperometric and pulsed amperometric detections in order to achieve a further enhancement in detection performance in our MCE-ECD system modified with a 4× bubble cell in the detection zone.

## 2.5 REFERENCES


(1) Chervet, J. P., Ursem, M., Salzmann, J. P., Vannoort, R. W., *Hrc-Journal of High Resolution Chromatography* **1989**, *12*. 278-281.
(2) Liang, Z. H., Chiem, N., Ocvirk, G., Tang, T., Fluri, K., Harrison, D. J., *Analytical Chemistry* **1996**, *68*. 1040-1046.
(3) Salimi-Moosavi, H., Jiang, Y. T., Lester, L., McKinnon, G., Harrison, D. J., *Electrophoresis* **2000**, *21*. 1291-1299.
(4) Xue, Q., Yeung, E. S., *Analytical Chemistry* **1994**, *66*. 1175-1178.
(5) Lu, Q., Copper, C. L., Collins, G. E., *Analytica chimica acta* **2006**, *572*. 205-211.
(6) Wu, C. C., Wu, R. G., Huang, J. G., Lin, Y. C., Hsien-Chang, C., *Analytical Chemistry* **2003**, *75*. 947-952.
(7) Kim, J. H., Kang, C. J., Jeon, D., Kim, Y. S., *Microelectronic Engineering* **2005**, *78-79*. 563-570.
(8) Lai, C. C. J., Chen, C. H., Ko, F. H., *Journal of Chromatography A* **2004**, *1023*. 143-150.
(9) Vickers, J. A., Henry, C. S., *Electrophoresis* **2005**, *26*. 4641-4647.
(10) Vickers, J. A., Dressen, B. M., Weston, M. C., Boonsong, K., Chailapakul, O., Cropek, D. M., Henry, C. S., *Electrophoresis* **2007**, *28*. 1123-1129.
(11) Holcomb, R. E., Kraly, J. R., Henry, C. S., *The Analyst* **2009**, *134*. 486-492.
(12) Noblitt, S. D., Henry, C. S., *Analytical Chemistry* **2008**, *80*. 7624-7630.
(13) Gertsch, J. C., Noblitt, S. D., Cropek, D. M., Henry, C. S., *Analytical Chemistry* **2010**, *82*. 3426-3429.
(14) McDonald, J. C., Duffy, D. C., Anderson, J. R., Chiu, D. T., Wu, H., Schueller, O. J., Whitesides, G. M., *Electrophoresis* **2000**, *21*. 27-40.
(15) Effenhauser, C. S., Manz, A., Widmer, H. M., *Analytical Chemistry* **1993**, *65*. 2637-2642.
(16) Koutny, L. B., Schmalzing, D., Taylor, T. A., Fuchs, M., *Analytical Chemistry* **1996**, *68*. 18-22.
(17) Jacobson, S. C., Hergenroder, R., Moore, A. W., Ramsey, J. M., *Analytical Chemistry* **1994**, *66*. 4127-4132.
(18) Garcia, C. D., Liu, Y., Anderson, P., Henry, C. S., *Lab on a Chip* **2003**, *3*. 324-328.

# CHAPTER 3. FURTHER IMPROVEMENT IN DETECTION PERFORMANCE OF MCE-ECD USING FASI OR FASS

## 3.1 INTRODUCTION

Since the sensitivity and limits of detection achieved in MCE analyses are restricted by the small volume of injected samples (for example, 625 pL in the microchip design with a double T injector for pinched injection (Figure 2.1A)), an additional means of improving detection sensitivity and LODs in MCE-ECD is to employ sample preconcentration methods. Field amplified sample injection (FASI) and field amplified sample stacking (FASS) are two widely used sample preconcentration techniques in traditional CE, with preconcentration factors from 10 to 1,000 being achieved.[1-4] Compared to isotachophoresis (ITP),[5, 6] FASI and FASS are more easily transferred into MCE because of the simple requirement of the manipulation of just two streams, the running and sample BGEs. For both methods, sample enrichment is based on the velocity change of the analytes between the sample and running BGEs, but subtle differences exist in the sample introduction in which electrokinetic and hydrodynamic injection are employed in FASI and FASS, respectively. The stacking mechanism occurs for ionic analytes, with the positively and negatively charged analytes stacking up in front of and in back of the sample plug, respectively,[7] while the neutral compounds are left in the sample plug and coelute.[7, 8] Detection performance is improved by increasing the amount of sample loaded onto the capillary and by narrowing the analyte bands in the capillary. The stacking of analytes in narrow bands causes reduced peak widths and increased peak heights of analytes, resulting in a greater signal-to-noise ratio and lower LODs. On the other hand, higher detection sensitivity can be

achieved without losing of separation efficiency due to the larger sample plug stacked with reduced analyte peak widths. The first application of FASI in MCE was reported by Jacobson and Ramsey,[2] resulting in no more than ~10-fold detection enhancement due to the pressure-driven peak broadening effects. To attain further enrichment, one approach made use of an additional branch channel, to load a large volume of low-conductivity sample solution, and then simultaneously pushed sample buffer out of the separation channel while stacking analytes.[9, 10] In another approach, an additional branch channel and a porous polymer structure was employed to stabilize the conductivity gradient boundaries to enhance detection sensitivity up to 1,000-fold.[11, 12] However, these sample stacking approaches were limited by more complicated MCE schemes, poorly controlled sample injection volumes and laborious analytical procedures. Furthermore, most analytes enriched in stacking techniques were detected with optical system or MS.[13-16] Shim et al. reported an on-chip electrochemical detection of trace DNA using microchip gel electrophoresis with FASI and FASS.[17] An ~25,000-fold improvement in detection sensitivity was achieved when gold nanoparticles were added to the stacking and separation buffers containing a hydroxypropyl cellulose matrix as well as a conducting polymer-modified electrode.

In this chapter, another effort for improving detection sensitivity and LODs using field amplified sample injection (FASI) and field amplified sample stacking (FASS) in MCE-ECD system is present here. FASS and FASI were employed to perform on-line sample preconcentration during the sample injection phase in our MCE-ECD system modified with a 4× bubble cell in the detection zone. Stacking effects were characterized for both FASI (for gated injection) and FASS (for hydrodynamic injection) methods using DC amperometric detection and PAD. A further enhancement in detection performance was obtained for some analytes of interests by using these two sample stacking methods.

## 3.2 EXPERIMENTAL

### 3.2.1 Chemicals

Hydrochloric acid (37%), N-tris[hydroxymethyl]methyl-2-aminoethane-sulfonic acid (TES), sodium dodecyl sulfate (SDS), 3,4-dihydroxyphenethylamine (dopamine), catechol, ascorbic acid, propylene glycol methyl ether acetate, DL-homocysteine (Hcy), and reduced glutathione (GSH) were purchased from Sigma-Aldrich (St. Louis, MO). L-tyrosine (Tyr) and L-cysteine (Cys) were obtained from Fluka (Buchs, Switerland). Sodium hydroxide and boric acid were purchased from Fisher (Pittsburgh, PA). Fluorescein was received from Eastman (Rochester NY, USA). Other reagents used for the fabrication of MCE-ECD include SU-8 2035 photoresist (Microchem, Newton, MA), Sylgard 184 elastomer and curing agent (PDMS) (Dow Corning, Midland, MI), 4 in. silicon wafers (University Wafer, South Boston, MA), and microwires made of 99.99% Pd (diameter 25 μm) and 99.99% Au (diameter 25 μm) (Goodfellow, Huntingdon, England). Solutions were prepared in 18.2 MΩ water from a Millipore Milli-Q purification system (Milipore Corp., Billerica, MA). 10 mM stock solutions of dopamine, catechol, ascorbic acid, Hcy, Cys and GSH were individually prepared weekly in 10 mM HCl, while 10 mM Tyr solution was prepared in 20 mM NaOH. All stock solutions were stored at 4ºC. A 20 mM TES buffer containing 1mM SDS was adjusted to pH 7.0 with concentrated NaOH and used as running BGE (high-conductivity) for the separation of dopamine, catechol and ascorbic acid. Running BGE was diluted to prepare each sample BGE (low-conductivity) for the appropriate stacking factor (SF): 20 mM TES, 1mM SDS (pH 7.0) for SF 1; 4 mM TES, 0.2 mM SDS (pH 7.0) for SF 5; 2 mM TES, 0.1mM SDS (pH 7.0) for SF 10; and 0.2 mM TES, 0.01mM SDS (pH 7.0) for SF 100. A 20 mM boric acid buffer was adjusted to pH 9.2 with concentrated NaOH and used as running BGE for the separation of Tyr, Hcy, Cys

and GSH. Again, sample BEGs were prepared for stacking experiments by dilution of running BGEs: 20 mM boric acid (pH 9.2) for SF 1; 10 mM boric acid (pH 9.2) for SF 2; 4 mM boric acid (pH 9.2) for SF 5; and 2 mM boric acid (pH 9.2) for SF 10.

### 3.2.2 PDMS microchip fabrication

The method used to fabricate PDMS microchips using incorporated microwires for detection has been published previously.[18, 19] Figure 3.1A is a schematic drawing of PDMS microchips (50 µm × 50 µm × 6 cm) used in stacking experiments. This design has a straight T injector suited for gated and hydrodynamic injection modes,[20, 21] and a 4× bubble cell (its width

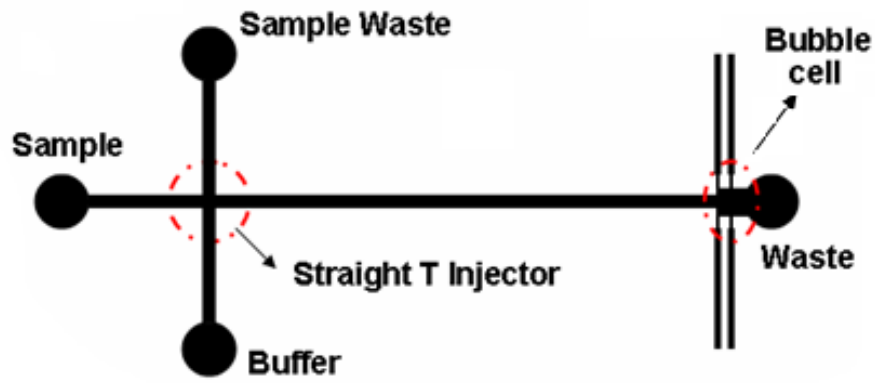


**Figure 3.1** Schematic of PDMS microchips (50 µm × 50 µm × 6 cm from buffer to waste reservoir) with a straight T injector for gated and hydrodynamic injections and a 4× bubble cell (its width is 4× the separation channel width (50 µm)) in the electrochemical detection zone. The sample, buffer and sample waste side channels are all 1 cm in length. All reservoirs are 5 mm in diameter. A Pd decoupler and Au working electrode (WE) were placed in the bubble cell using electrode alignment channels. Each electrode channel was 50 µm wide and separated by 125 µm. Au working electrode (WE) are placed in the bubble cell using electrode alignment channels. The rectangular tapers connecting the electrode channels and the bubble cell are 20 µm × 56 µm.

is 4× the separation channel width (50 μm)) in the electrochemical detection zone. Each electrode channel is 50 μm wide and separated by 125 μm. A 25 μm Pd decoupler and a 25 μm

### 3.2.3 MCE-ECD

Channels and reservoirs were first rinsed with ultra-pure water and then filled with BGE for 30 min pretreatment by applying pressure to a reservoir containing the solution. The buffer in the sample reservoir was replaced with sample solution prior to running analyses. The corresponding positions of sample (SR), sample waste (SW), buffer (BR) and buffer waste (BW) reservoirs are shown in Figure 3.1A. For gated injection using FASI technique, equivalent volume of sample BGE and running BGE were loaded in SR and other three reservoirs, while for hydrodynamic injection using FASS technique, the SR was filled with 80 μL of sample BGE and the remaining reservoir were filled with 50 μL of running BGE. Applied voltages were facilitated by a programmable high voltage power supply built in-house.[22] The Pd decoupler was always held at ground to isolate the potentiostat from high voltage. As shown in Figure 3.2, in gated mode, sample introduction was achieved by applying a high positive potential (1,050 V) to SR and keeping floating in BR, while in hydrodynamic mode, both SR and BR were held at grounding. Their following separation phases were performed by applying a proper high positive potential to BR while keeping voltage settings in all other reservoirs the same as their corresponding injection phases. DC amperometric detection and PAD were employed (CHI 1010A Electrochemical Analyzer, CH Instruments, Austin, TX) in a two-electrode configuration.[19] The former was used for the detection of dopamine, catechol, and ascorbic acid, while the latter was used for the detection of Tyr, Hcy, Cys and GSH. A Pt wire (1 mm diameter) in the waste reservoir was acted as both auxiliary and psuedo-reference electrode.[19] Cleaning of

Pd decoupler was done initially by running cyclic voltammetry (CV) from -1.0 V to 1.0 V at 0.1 V/s for 50 cycles. Two gold working electrodes were cleaned using CV by scanning from -0.5 V to 1.8 V at 0.5 V/s for 100 cycles while buffer was flowed over the electrodes.

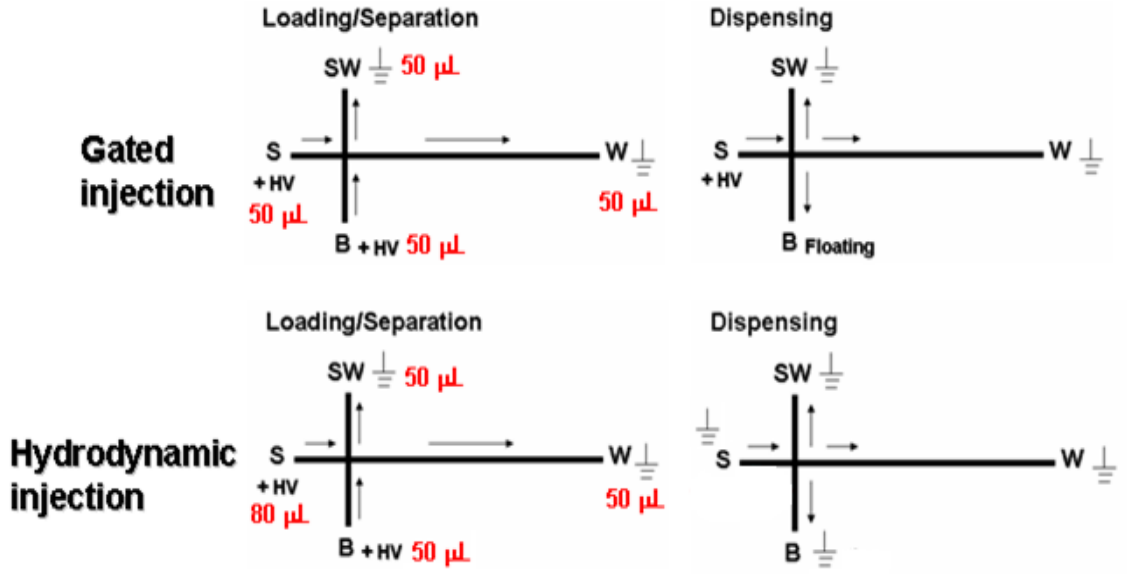


**Figure 3.2** BGE loading, voltage settings and flow diagrams of gated and hydrodynamic injections and their corresponding separation phases.

### 3.3 RESULTS AND DISCUSSION

In both FASI and FASS, the amount of sample being stacked is theoretically proportional to the resistivities between the sample BGE (low-conductivity) and the running BGE (high-conductivity). Since the ratio of resistivities is simply the inverse of the ratio of concentrations, in this thesis, stacking factor (SF) was defined as the ratio between the running and sample BGE concentrations. SFs of 1, 2, 5, 10, and 100, respectively, were chosen to investigate sample stacking effects in MCE-ECD.

### 3.3.1 Stacking Characterization with DC Amperometric Detection

Dopamine, catechol, and ascorbic acid were chosen as model analytes to characterize the stacking effects of FASS and FASI with DC amperometric detection. Figure 3.3A and 3.3B compares electropherograms of 50 μM analytes obtained with a straight T injector using FASI and FASS, respectively. Electropherograms for each stacking condition have been offset for clarity. First, significant sample stacking was achieved for positively charged dopamine when using a 5-s gated injection in FASI as evidenced by a significant peak height increase and peak width decrease with increasing SF. A similar trend was also observed for dopamine preconcentrated by using a 60-s hydrodynamic injection in FASS compared with a 25-s hydrodynamic injection under the nonstacking condition. The peak height enhancement of dopamine at SF 5, 10, and 100 relative to SF 1 are 2.84-, 3.63-, and 4.28-fold in FASI, and 1.71-, 2.92-, and 2.21-fold in FASS, respectively. Both FASI and FASS exhibited diminishing sample enhancement above a threshold SF. The reason for this behavior can be attributed to a laminar back flow inside the capillary generated by the difference in the EOF rate between sample and running buffers as noted by others.[7, 23] The laminar flow disturbs the original plug profile, reducing the stacking effectiveness. From these experiments, the lowest detection limit for dopamine of 8.02 ± 1.51 and 20.0 ± 3.5 nM (n = 4 and S/N = 3) were achieved with SF 100 in FASI and SF 10 in FASS, respectively. As expected, catechol, as a neutral analyte, did not stack in either FASI or FASS modes. Here, the broader peak and smaller peak height of catechol obtained from the stacking conditions relative to the nonstacking condition were the result of bandbroadening caused by a mobility mismatch between sample and running BGEs. Furthermore, the negatively charged analyte, ascorbic acid also did not achieve any obvious stacking. The smaller observed mobility of this analyte results in a much smaller sample plug volume being

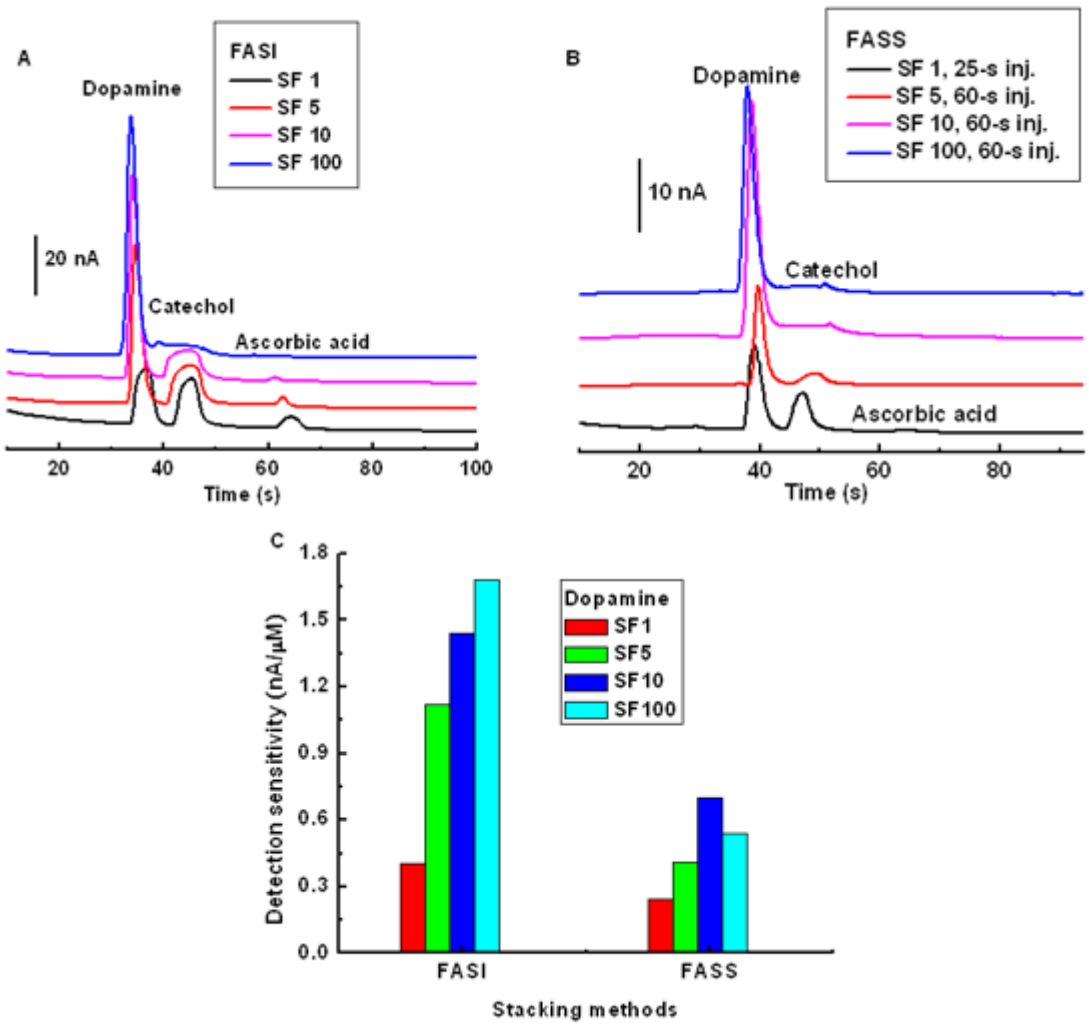


**Figure 3.3** Example electropherograms for 50 μM dopamine, catechol, and ascorbic acid detected on PDMS microchips with 4× bubble cell using FASI (A) and FASS (B) sample preconcentration techniques. Experimental conditions: 5-s gated injection in FASI, 25-s or 60-s hydrodynamic injection in FASS; separation field strength: 125 V/cm in FASI; 114 V/cm in FASS; running BGE: 20mM TES, 1mM SDS (pH 7.0); sample BGE: diluted running BGE with SF 1, 5, 10, and 100, respectively; $E_{Det}$ = 1V. (C) Comparisons of detection sensitivity of dopamine using FASI and FASS under different stacking factors.

injected and stacked than the positively charged analyte dopamine with a higher observed mobility. Furthermore, as shown in Figure 3.3 C, both stacking techniques improved detection sensitivity for dopamine in most stacking conditions, with a higher enhancement by using FASI relative to FASS probably due to a larger sample plug injected into the separation channel in gated injection than hydrodynamic injection.

### 3.3.2 Stacking Characterization with Pulsed Amperometric Detection

Several reports have shown the ability to stack negatively charged analytes using FASI and FASS.[9, 24, 25] This was not observed in the above results with ascorbic acid. Therefore, three negatively charged amino acids associated with oxidative stress in human disease, Tyr, Hcy, and Cys, were chosen as model analytes to further investigate the stacking effects of FASI and FASS coupled with pulsed amperometric detection (PAD). Integrating a self-cleaning cycle prior to the measurement, PAD has proven to be effective in the detection of a large number biomolecules with –OH, $–NH_2$, and –SH functional groups.[26-29] Example electropherograms of three analytes and the stacking effects by the comparison of their peak heights and half-peak widths (HPWs) using a 5-s FASI with different SF conditions are shown in Figure 3.4. Of the three analytes, Tyr has the highest observed mobility, inducing the longest sample plug injected into the separation channel. Therefore, Tyr was easily stacked by FASI, showing an increase in its peak height with SF 2 and reaching the largest increase with SF 5. There was no further increase in peak height when using SF higher than 5, as a result of the mobility mismatch between sample and running BGEs. The increased HPW of Tyr obtained from SF 5 to 10 also confirmed the existence of bandbroadening. Hcy, having a lower observed mobility, showed significant increase in peak height with SF greater than 2. For Cys with the lowest observed mobility, SF 2 produced

decreased peak heights compared with the nonstacking condition (SF 1); however, higher SFs showed improved peak heights. Since stacking and broadening functioned against each other, the optimal stacking effect on peak height showed analyte dependency for different SFs. In addition, all three analytes produced their smallest HPWs with SF 5. One more thing to note in Figure 3.4A is that an increasingly large fluctuation in the baseline appeared around 160 s where neutral analytes would elute when higher SFs were employed in FASI.

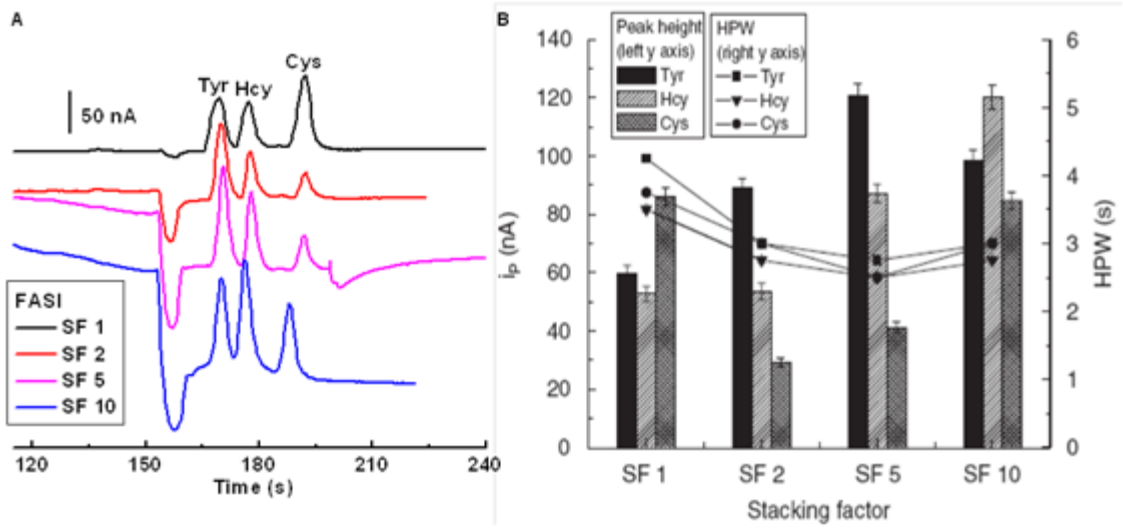


**Figure 3.4** (A) Example electropherograms for 250 μM Tyr, Hcy, and Cys detected on a PDMS microchip with 4× bubble cell using FASI. Experimental conditions: separation field strength: 125 V/cm in FASI; gated injection time: 5 s; running BGE: 20 mM boric acid (pH 9.2); sample BGE: diluted running BGE with SF 1, 2, 5, and 10, respectively; $E_{Det}$ = 1.6 V. (B) Comparisons of peaking heights (left y axis) and HPWs (right y axis) of analytes Tyr, Hcy, and Cys using different SFs in FASI.

Finally, comparisons of nonstacking, FASI (SF 5) using a 5-s gated injection, and FASS (SF 5) using a 25-s hydrodynamic injection were performed. Figure 3.5A and 3.5B shows their

example electropherograms and their comparisons on stacking effects in terms of peak heights and HPWs of analytes, respectively. Both FASS and FASI showed sample stacking for all four analytes. Due to the use of a longer injection time, FASS resulted in a larger increase in peak heights while keeping similar HPWs as FASI. Compared to the nonstacking condition, the peak heights of Tyr, Hcy, Cys and GSH increased 2.11-, 2.52-, 2.10- and 1.43-fold in FASI, and 2.45-, 3.23-, 3.76- and 4.67-fold in FASS, respectively. These results indicate that more efficient sample stacking occurred for more negatively charged analytes with FASS than with FASI, probably due to the decreased sampling bias produced with hydrodynamic injection. The LODs for Tyr, Hcy, Cys and GSH were 2.48 ± 0.15 μM, 4.04 ± 0.30 μM, 5.29 ± 0.55 μM, and 15.2 ±1.4 μM in FASI, and 2.52 ± 0.17 μM, 2.13 ± 0.20 μM, 3.26 ± 0.35 μM, and 13.1 ± 1.3 μM in FASS, respectively (n = 4 and S/N = 3). Although significant enhancement in peak heights were seen when detecting analytes at their relative high concentrations, improved detection limits were not achieved using FASI and FASS for these four analytes when compared to their LODs under nonstacking conditions (1.12 ± 0.12 μM, 1.05 ± 0.12 μM, 2.23 ± 0.31 μM, and 10.1 ± 1.6 μM, (n = 4 and S/N = 3) for Tyr, Hcy, Cys and GSH, respectively). The exact reason for this is not known at this time but may be a limitation of the increased baseline noise associated with the use of the PAD waveform. The methods do, however, increase the sensitivity of the analysis relative to nonstacking conditions when detecting the four analytes at the concentration range of 20 to 500 μM as depicted in Figure 3.5C.

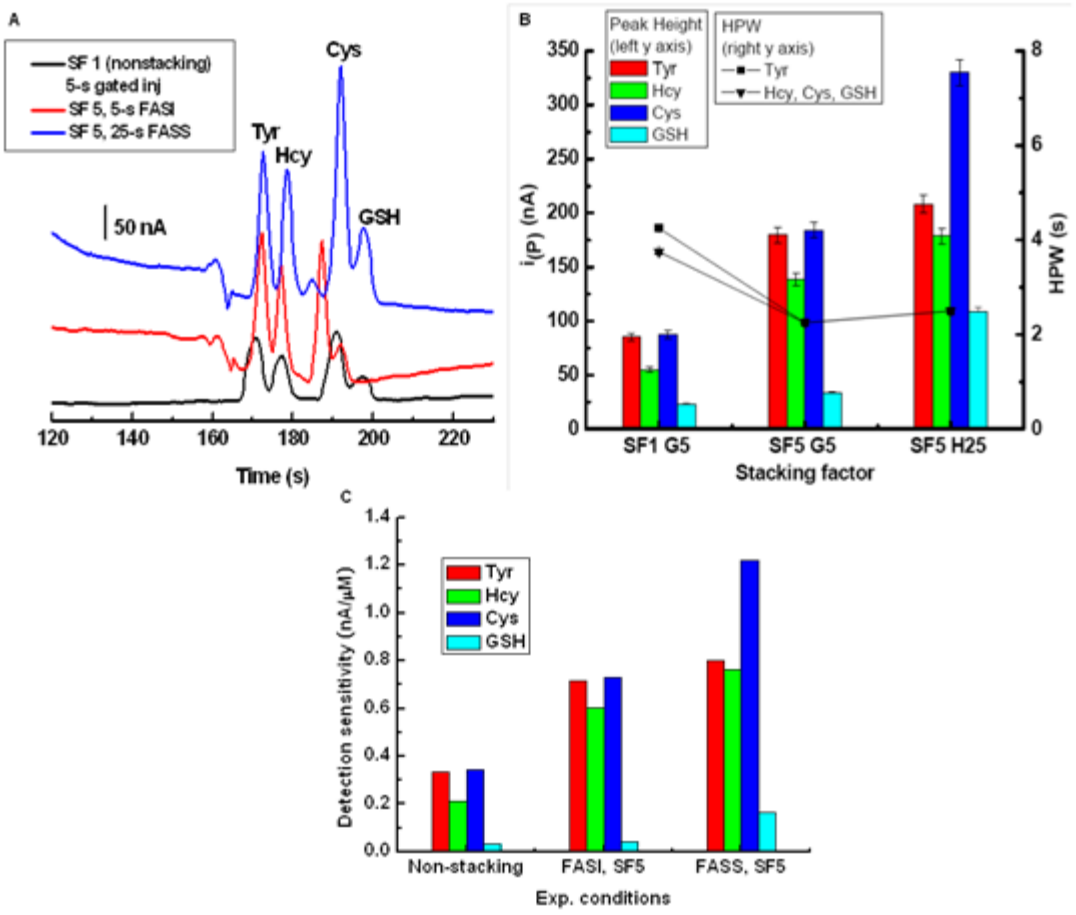


**Figure 3.5** (A) Example electropherograms for 250 μM Ty, Hcy, Cys and GSH on a PDMS microchip with 4× bubble cell under nonstacking (SF 1) and FASI, FASS two stacking conditions. Experimental conditions: separation field strength: 5-s gated injection in FASI, 25-s hydrodynamic injection in FASS; 125 V/cm in FASI; 114 V/cm in FASS; running BGE: 20 mM boric acid (pH 9.2); sample BGE: 20 mM boric acid (pH 9.2) for SF 1, 4 mM boric acid (pH 9.2) for SF 5, respectively; $E_{Det}$ = 1.6 V. (B) Comparisons of peaking heights and HPWs of Tyr, Hcy, Cys and GSH using nonstacking, FASI and FASS sample preconcentration techniques. (C) Comparisons of detection sensitivity of four analytes at the concentration range of 20 to 500 μM under nonstacking (SF 1) and FASI, FASS two stacking conditions.

## 3.4 CONCLUSIONS

In chapter 2, the improved detection sensitivity and LODs were achieved by modification our previous MCE-ECD system with an implementation of a capillary expansion (bubble cell) at the detection zone. Another effort to enhance the detection performance in MCE analyses involves employing some on-line sample preconcentration methods. Compared to other methods, FASS and FASI are more convenient techniques to incorporate with MCE analysis due to the easy manipulation of just two streams, the running and sample BGEs. Here, I demonstrated that FASS and FASI allow sample stacking on our MCE-ECD system with increased peak height, decreased HPW and improved detection sensitivity. Using stacking in conjunction with a 4× bubble cell, I obtained LODs of 8 and 20 nM for dopamine by using FASI and FASS, respectively. However, these stacking techniques did not significantly improve LODs for anionic analytes. Further optimization of our current MCE-ECD design may be necessary to enhance the stacking impact and improve LOD. This may include using either narrow channel, inversion of the applied electric field, or negative pressure for the introduction of large volume of low-conductivity sample solution. With the use of a bubble cell and sample stacking techniques, the improvement obtained on detection sensitivity in MCE-ECD has the potential to reach nanomolar detection limits for redox active biological molecules.

After improving the detection performance of our MCE-ECD system, the next step moves to the optimization of its separation performance by surface modification using surfactants. To systematically study EOF behaviors of representative single and mixed surfactant systems on poly(dimethylsiloxane) (PDMS) microchips, EOF measurements as a function of surfactant concentration were performed using both current monitoring and capacitively coupled contactless conductivity detection ($C^4D$) methods and are described in chapter 4. And then

electrophoretic separations and electrochemical detections of some biologically relevant compounds will be investigated using BGEs containing appropriate mixed surfactants to explore their abilities for a better EOF control and improved separation chemistry. This part of work will be discussed in chapter 5.

## 3.5 REFERENCES


(1) Beard, N. R., Zhang, C. X., deMello, A. J., *Electrophoresis* **2003**, *24*. 732-739.
(2) Jacobson, S. C., Ramsey, J. M., *Electrophoresis* **1995**, *16*. 481-486.
(3) Maeso, N., Cifuentes, A., Barbas, C., *Journal of chromatography. B, Analytical technologies in the biomedical and life sciences* **2004**, *809*. 147-152.
(4) Chen, Z., Naidu, R., *Journal of chromatography. A* **2004**, *1023*. 151-157.
(5) Shihabi, Z. K., *Electrophoresis* **2002**, *23*. 1612-1617.
(6) Xu, Z. Q., Hirokawa, T., Nishine, T., Arai, A., *Journal of chromatography. A* **2003**, *990*. 53-61.
(7) Burgi, D. S., Chien, R. L., *Analytical Chemistry* **1991**, *63*. 2042-2047.
(8) Sueyoshi, K., Kitagawa, F., Otsuka, K., *Analytical Chemistry* **2008**, *80*. 1255-1262.
(9) Lichtenberg, J., Verpoorte, E., de Rooij, N. F., *Electrophoresis* **2001**, *22*. 258-271.
(10) Li, J., Wang, C., Kelly, J. F., Harrison, D. J., Thibault, P., *Electrophoresis* **2000**, *21*. 198-210.
(11) Yang, H., Chien, R. L., *Journal of chromatography. A* **2001**, *924*. 155-163.
(12) Jung, B., Bharadwaj, R., Santiago, J. G., *Electrophoresis* **2003**, *24*. 3476-3483.
(13) Zhang, L., Yin, X. F., *Journal of chromatography. A* **2006**, *1137*. 243-248.
(14) Palmer, J., Burgi, D. S., Munro, N. J., Landers, J. P., *Analytical Chemistry* **2001**, *73*. 725-731.
(15) Kim, D. K., Kang, S. H., *Journal of chromatography. A* **2005**, *1064*. 121-127.
(16) Zhang, Y., Ping, G., Zhu, B., Kaji, N., Tokeshi, M., Baba, Y., *Electrophoresis* **2007**, *28*. 414-421.
(17) Shiddiky, M. J., Rahman, M. A., Shim, Y. B., *Analytical Chemistry* **2007**, *79*. 6886-6890.
(18) McDonald, J. C., Duffy, D. C., Anderson, J. R., Chiu, D. T., Wu, H., Schueller, O. J., Whitesides, G. M., *Electrophoresis* **2000**, *21*. 27-40.
(19) Vickers, J. A., Henry, C. S., *Electrophoresis* **2005**, *26*. 4641-4647.
(20) Jacobson, S. C., Hergenroder, R., Moore, A. W., Ramsey, J. M., *Analytical Chemistry* **1994**, *66*. 4127-4132.
(21) Gong, M., Wehmeyer, K. R., Stalcup, A. M., Limbach, P. A., Heineman, W. R., *Electrophoresis* **2007**, *28*. 1564-1571.
(22) Garcia, C. D., Liu, Y., Anderson, P., Henry, C. S., *Lab on a Chip* **2003**, *3*. 324-328.
(23) Chien, R. L., Helmer, J. C., *Analytical Chemistry* **1991**, *63*. 1354-1361.
(24) Wu, C. H., Chen, M. C., Su, A. K., Shu, P. Y., Chou, S. H., Lin, C. H., *Journal of chromatography. B, Analytical technologies in the biomedical and life sciences* **2003**, *785*. 317-325.
(25) Gong, M., Wehmeyer, K. R., Limbach, P. A., Arias, F., Heineman, W. R., *Analytical Chemistry* **2006**, *78*. 3730-3737.
(26) Fanguy, J. C., Henry, C. S., *Analyst* **2002**, *127*. 1021-1023.
(27) LaCourse, W. R., Owens, G. S., *Electrophoresis* **1996**, *17*. 310-318.
(28) Weber, P. L., Lunte, S. M., *Electrophoresis* **1996**, *17*. 302-309.
(29) Garcia, C. D., Henry, C. S., *Electroanalysis* **2005**, *17*. 223-230.

# CHAPTER 4. EOF MEASUREMANTS OF SINGLE AND MIXED SURFACTANT SYSTEMS USING BOTH CURRENT MONITORING AND $C^4D$ METHODS

## 4.1 INTRODUCTION

Surface chemistry is of great important in MCE, where surface effects play an increased role in comparison to classical CE due to the high surface area-to-volume ratio in miniaturized devices.[1, 2] Motivations for surface manipulation in MCE include control of EOF and reduction of analyte-wall interactions in order to obtain a reproducible sample plug during the injection process and improve the precision of migration times. The realization of internal surface coatings for EOF control in MCE has proven to be more challenging than in classical CE due to variety of materials used to make these devices. Glass and fused silica are popular chip materials for electrophoresis because of their well-understood surface chemistry, excellent optical properties, high insulating properties, and the inertness towards a variety of different solvents.[1] However, these materials suffer some manufacturing issues, making a growing interest in the use of alternative materials like different polymers due to the wide choice in microfabrication techniques. EOF within microfluidic devices made from polymers such as poly(dimethylsiloxane) (PDMS),[3] poly(methyl methacrylate) (PMMA),[4, 5] polycarbonate,[6] and polystyrene (PS)[6, 7] can vary widely due to the diversity of the surface-exposed functional groups. In addition, the zeta potential of these materials that gives rise to the EOF is often less than optimal for specific separations because of the lower surface charge density of polymeric chips as compared to glass-based fluidic chips.[2] To meet the requirement of microfluidic applications, chemical modification of microchannel surface is commonly used to minimize

unwanted analyte-wall interactions and manipulate EOF. Permanent,[8, 9] adsorbed,[10-12] and dynamic coatings,[1, 13] have been used for surface modification to control EOF in electrophoresis as discussed in several review papers.[1, 9, 13, 14]

As the easiest surface modification method, dynamic coatings have been employed in both conventional and microchip CE. Dynamic coatings rely on the equilibrium between the solution-phase modifier and the surface, changing the zeta potential,[15, 16] and therefore the EOF. Depending on the modifier's charges, the EOF can be suppressed, increased, or reversed. The most common dynamic coatings rely on ionic surfactants such as sodium dodecyl sulfate (SDS) to alter the surface charge of polymeric microchips.[17-19] The addition of SDS increases the EOF[17, 18] and even improve the electrochemical signal for molecules, such as carbohydrates,[20, 21] metabolites,[22] and catechols.[23] The improved electrochemical response for these species in the presence of surfactants can be attributed to increased solubility of the oxidation product of the electrochemical reaction.[23] In addition, cationic surfactants such as cetyltrimethylammonium bromide (CTAB),[24, 25] tetradecyltrimethylammonium bromide (TTAB),[26] and didodecyldimethylammonium bromide (DDAB)[27] have been added to reverse the EOF direction in microchip CE. Zwitterionic surfactants have also been used in both traditional and microchip CE. Lucy's group first investigated the use of low concentrations of zwitterionic surfactants to suppress the EOF and prevent adsorption of cationic proteins on the walls of fused silica capillaries for traditional CE.[28, 29] In particular, the separation of both cationic and anionic proteins with efficiencies as high as 1.4 million plates/m was achieved using a capillary coated with a double-chained zwitterionic phospholipid, 1, 2-dilauroyl-*sn*-phophatidylcholine (DLPC).[29] Another zwitterionic surfactant, dodecyldimethyl (2-hydroxy-3-sulfopropyl) ammonium (DSB) was also used to suppress EOF and prevent analyte absorption for the separation of basic

proteins and a mixture of eight inorganic anions. The later separations were achieved in 4.2 min with efficiencies of 24, 000 to 1 310, 000 plates/m.[30] Recently, our group reported the application of sulfobetaine zwitterionic surfactants in PDMS microchips for the determination of inorganic anions in atmospheric aerosols[31] and perchlorate in drinking water[32], in which these surfactants suppressed the EOF and influenced separation selectivity. Nonionic surfactants, such as polyoxyethylene ether (Brij 35), polyoxyethylene (20) sorbitan monolaurate (Tween 20), polyoxyethylene octyl phenyl ether (Triton X-100), have primarily been used for reducing analyte-wall interactions, since they create a hydrophilic, and nonionic coating that is highly effective at minimizing adsorption.[33, 34] Successful applications of these nonionic surfactants to suppress EOF and minimize surface adsorption of biomolecules in CE and microfluidic system have also been reported.[33-36]

Mixed surfactant systems represent an interesting alternative to single surfactant systems for both EOF control and separation chemistry. In Lucy's work, mixtures of zwitterionic (coco (amidopropyl)hydroxyldimethylsulfobetaine (CAS U)) and cationic (TTAB) surfactants were used to modify the EOF from nearly zero to $-5\times10^{-4}$ $cm^2\,V^{-1}\,s^{-1}$.[37] This ability to control EOF was employed to fine-tune the separation of inorganic anions[37] and to separate ammonium isotopes through EOF counterbalance.[38] Similar work has been done using a capillary semi-permanently coated with a cationic/zwitterionic mixture of DDAB/DLPC, which allowed the excess surfactant to be removed from the buffer prior to separation.[39] In another example, mixed CTAB/SDS cationic/anionic surfactants demonstrated enhanced EOF stability relative to CTAB alone for capillary electrophoretic separations of basic proteins.[40] Alternatively, the separation of proteins on PDMS-coated fused silica capillaries and glass microchips was achieved using a mixture of charged surfactants and nonionic Brij 35 to control EOF.[41] Furthermore, mixed

zwitterionic (N-tetradecylammonium-N,N-dimethyl-3-ammonio-1-propane sulfonate, TDAPS) and nonionic (Tween 20) surfactants were used for the direct determination of bromide and nitrate in undiluted seawater.[42] Despite these advances, the application of mixed surfactants systems for surface modification on polymeric microdevices has been limited. Here, we specifically address this gap in surface modification strategies.

In 1998, capacitively coupled contactless conductivity detection ($C^4D$) was reported for CE by two groups.[43, 44] Schematic drawing to demonstrate the principle of $C^4D$ system is shown in Figure 4.1. Briefly, two cylindrical electrodes are placed around a fused silica capillary a certain distance from each other. An AC voltage is applied to the actuator electrode passing current the capillary wall, the detection gap between the electrodes inside the capillary, and back to the pick-up electrode. By using suitable amplifier electronics, conductivity changes caused by electrolytes passing through the detection region can be monitored. $C^4D$ has some advantages over traditional conductivity, including the ability to isolate the detection electrodes from the

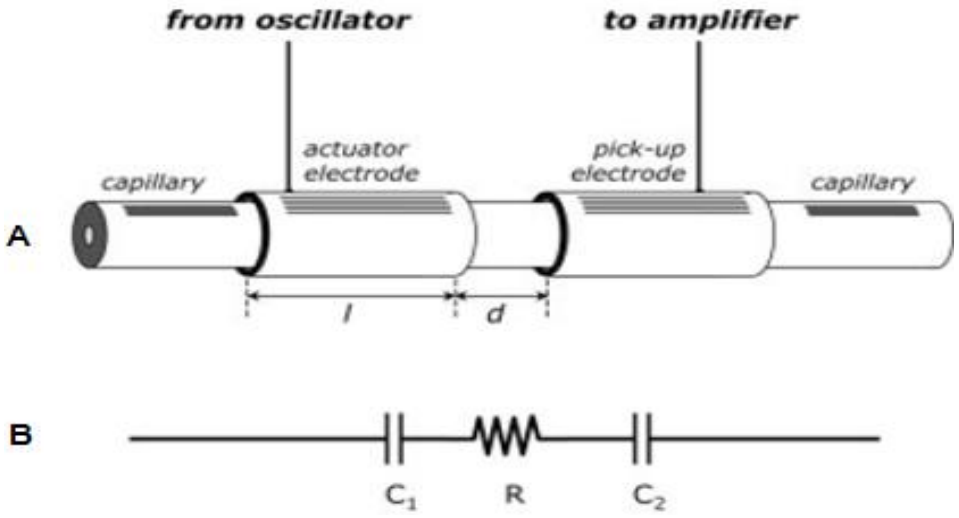


**Figure 4.1** Principle of a $C^4D$ system.[49] (A) Schematic drawing of the sensing electrodes. (B) Simplified equivalent circuitry for $C^4D$.

electric field and the ability to locate the electrodes anywhere along the separation capillary or channel. $C^4D$ has been used with microchip CE for a variety analytes.[45-48] $C^4D$ has not to the best of our knowledge, been used for EOF measurements but provides an excellent tool for these kinds of experiments as will be demonstrated here.

Here, representative single and mixed surfactant systems were chosen to study their EOF behavior with a poly(dimethylsiloxane) (PDMS) substrate. In this Chapter, the effect of surfactant concentration on EOF was first studied using the current monitoring method for a single anionic surfactant (SDS), a single zwitterionic surfactant (TDAPS), and a mixed ionic/zwitterionic surfactant system (SDS/TDAPS). After establishing the EOF behavior, the adsorption/desorption kinetics were measured using SDS and TDAPS as model analytes. Next, $C^4D$ was introduced for EOF measurements as an alternative to the current monitoring method. EOF measurements as a function of the surfactant concentration were performed simultaneously using both methods for three nonionic surfactants (Tween 20, Triton X-100, and polyethylene glycol, (PEG 400)), mixed ionic/nonionic surfactant systems (SDS/Tween 20, SDS/Triton X-100, and SDS/PEG 400) and mixed zwitterionic/nonionic surfactant systems (TDAPS/Tween 20, TDAPS/Triton X-100, and TDAPS/PEG 400).

## 4.2 EXPERIMENTAL

### 4.2.1 Chemicals

Reagents used for fabrication of microchips include SU-8 2035 photoresist (Microchem, Newton, MA), Sylgard 184 elastomer and curing agent (PDMS) (Dow Corning, Midland, MI), 4-in. silicon wafers (University Wafer, South Boston, MA), and microwires made of 99.99% Pd (25 μm) and 99.99% Au (25 μm) (Goodfellow, Huntingdon, England). Aqueous solutions were

prepared in 18.2 MΩ*cm water from a Millipore Milli-Q purification system (Milipore Corp., Billerica, MA). The BGEs were prepared by weighing the desired amount of N-tris[hydroxymethyl]methyl-2-aminoethanesulfonic acid (TES; Sigma-Aldrich, St. Louis, MO) or boric acid (Fisher, Pittsburgh, PA) and adjusting the pH with 2 M NaOH (Fisher). Sodium phosphate buffers at different pH values (4.0, 7.0, and 10.0) were prepared by mixing the appropriate amount of $Na_2HPO_4$ and $NaH_2PO_4$ (Fisher) and used as BGEs in the pH study of EOF measurements. Following pH adjustment, surfactant was added to the running BGE to the desired concentration. SDS (Aldrich, Milwaukee, WI, USA), TDAPS (Fluka, Buchs, Switzerland), N-dodecyl-N,N-dimethyl-3-ammonio-1-propansulfonate (DDAPS), Tween 20, PEG 400 (Sigma-Aldrich), and Triton X-100 (FisherBiotech, Fair Lawn, New Jersey) were selected as model surfactants for EOF measurements and their chemical structures are shown in Figure 4.2. All chemicals were used as received without further purification.

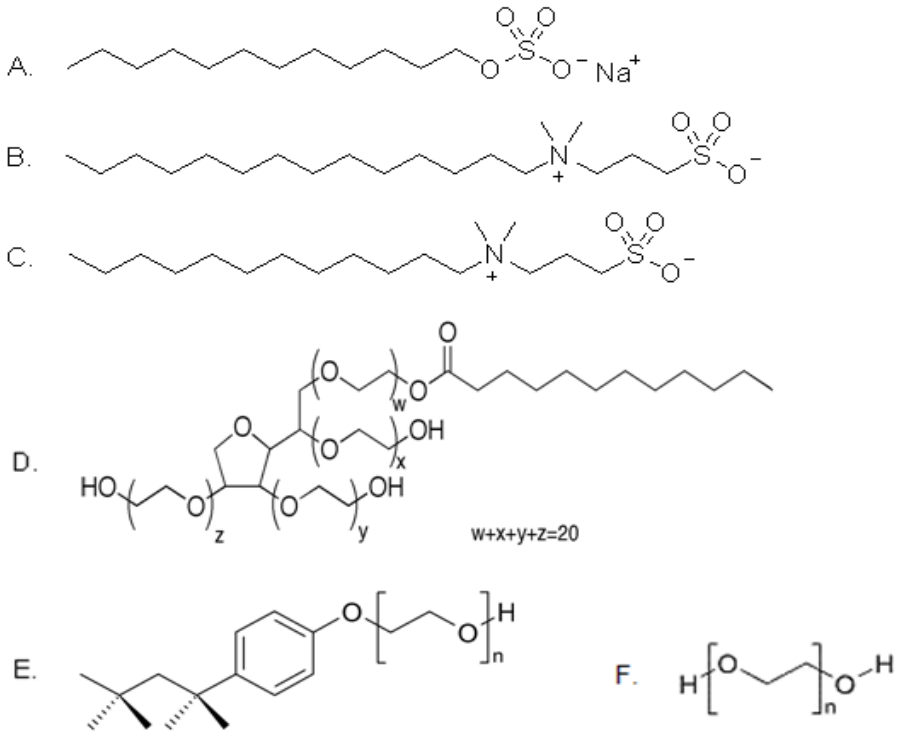


**Figure 4.2** Chemical structures of the selected surfactants. (A) SDS, (B) TDAPS, (C) DDAPS, (D) Tween 20, (E) Triton X-100, (F) PEG 400.

### 4.2.2 EOF measurements

PDMS microchips with single straight channels (50 μm × 50 μm × 4.75 cm) connected by two reservoirs (5 cm in diameter) were fabricated using previously described methods,[49, 50] and employed for all EOF measurements. EOF measurements were performed using only the current monitoring method for a single anionic surfactant (SDS), a single zwitterionic surfactant (TDAPS), and a mixed SDS/TDAPS system, while both current monitoring and $C^4D$ methods were used for three nonionic surfactants (Tween 20, Triton X-100, and PEG 400), mixed ionic/nonionic surfactant systems (SDS/Tween 20, SDS/Triton X-100, and SDS/PEG 400) and mixed zwitterionic/nonionic surfactant systems (TDAPS/Tween 20, TDAPS/Triton X-100, and TDAPS/PEG 400). The current monitoring method for EOF measurements was described

previously.[51] Briefly, the first reservoir and the channel were filled higher ionic strength BGE (typically 20 mM in BGE concentration) and the second reservoir was filled with lower ionic strength BGE (typically 18 mM in BGE concentration). The specific BGEs used in EOF measurements are discussed below. Upon application of a high positive voltage in the first reservoir, EOF caused the lower ionic strength BGE to displace the higher ionic strength BGE in the channel, resulting in an increase in the electrical resistance of the channel. The change in separation current under a constant applied voltage difference was monitored using a Fluke multimeter (Everett, WA). Once a constant current was obtained, the potential was reversed and the above procedure repeated. The time required to reach a current plateau was used to calculate EOF based on equation 4.1.

$$\mu_{eof} = \frac{L^2}{Vt} \tag{4.1}$$

Where, $L$ is the length of the separation channel, $V$ is the total applied voltage, and $t$ is the time in seconds required to reach the new current plateau.

For EOF measurements simultaneously using both current monitoring and $C^4D$ methods, the microchip was set up for a close contact with the $C^4D$ microfluidic platform by spring screws and the detection point was located at the center position between two detection electrodes on the platform (Figure 4.3). $C^4D$ detection was done in the microchip channel 2.0 cm from one BGE reservoir. The BGE loading and voltage control in this case is the same as that described in the current monitoring method. Separation current and the conductivity signal were measured simultaneously using an analog to digital convertor controlled by PowerChrom software (eDAQ, Australia). The time to the inflection point (mid-point between the maximum and minimum of the transition region) of the conductivity trace was used to calculate EOF for the $C^4D$ method based on 4.2.

$$\mu_{eof} = \frac{LL'}{Vt} \tag{4.2}$$

Where, $L'$ is the distance between the starting reservoir and the detection point, and the other parameters are the same as those in Equation 4.1. All values in this Chapter are reported as the average from four microchips, with six replicates performed on each microchip. Reported uncertainties are the standard deviations obtained from the total of 24 measurements.

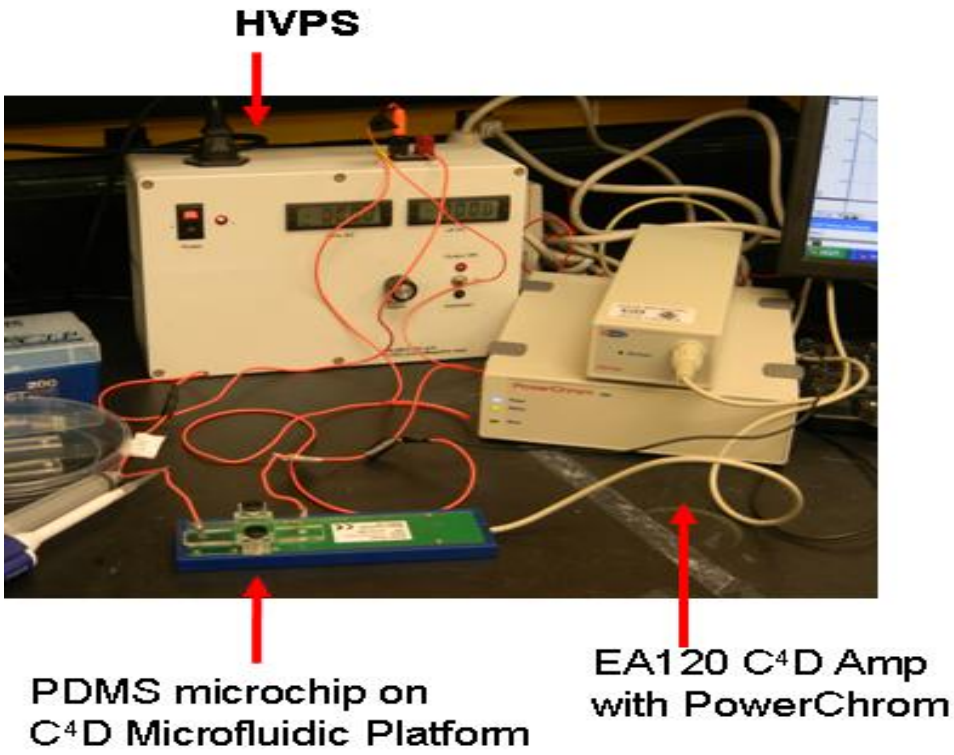


**Figure 4.3** Instrument setup for EOF measurements simultaneously using both current monitoring and $C^4D$ methods, which includes a PDMS microchip being placed on a ET121 $C^4D$ microfluidic platform, a laboratory built high-voltage power supply (HVPS) facilitating voltage control, and a EA120 $C^4D$ Amp. as well as a ER280 PowerChrom system for data collecting.

### 4.2.3 Adsorption/desorption rates study

Adsorption/desorption rates studies were performed in the following way. The initial EOF was measured using 20 and 18 mM sodium phosphate buffers at pH 7.0 as BGEs. After 30 min of consecutive runs, the solutions were replaced with 18 mM and 20 mM phosphate BGEs at pH 7.0 containing the corresponding surfactant and the analysis was repeated until a stable EOF was reached. Once a stable EOF was reached, the solutions were replaced with the initial BGEs without surfactant and the EOF was measured again until a stable value was observed.

## 4.3 RESULTS AND DISCUSSION

### 4.3.1 Single SDS surfactant system

Modification of PDMS surface chemistry to alter the EOF using a single surfactant has been reported by several research groups.[52, 53] In these studies, it was proposed that the surfactant molecules interact with the PDMS surface by their hydrophobic tails, while exposing negatively charged head groups to the solution, leading to an increase in the zeta potential and a higher EOF.[54] In order to systematically study the effect of mixed surfactants on EOF in PDMS microchips, we initially measured the concentration dependent effect of SDS on EOF. EOF measurements were performed using the TES BGE at pH 7.0 as shown in Figure 4.4 (inverted triangles). As the SDS concentration increased, EOF increased, reaching a plateau above 3.0 mM, with its value changing from $3.56 \pm 0.10$ to $7.13 \pm 0.13 \times 10^{-4}$ $cm^2$ $V^{-1}$ $s^{-1}$ in the range of 0 to 6 mM SDS (CMC: 8.1 to 8.4 mM in pure water[55] and 2.9 to 3.7 mM in 30 mM NaCl[55, 56] at 25 °C). The plateau in EOF at SDS concentrations above 3.0 mM suggests the surface of PDMS microchip was fully coated. EOF was also measured in phosphate BGEs at pH 4.0, 7.0, and 10.0 for SDS concentrations of 0 to 20 mM to explore pH effects. As depicted in Figure 4.4, the EOF shows a

similar trend as a function of SDS concentration as that measured for the pH 7.0 TES BGE. Furthermore, the EOF increases as pH increases, consistent with an increased negative charge density on the PDMS surface at the higher pH.[17] It should be noted, however, that the differences in EOF as a function of pH might be affected by differences in the ionic strength of the BGEs because nothing was done to keep these constant between pHs. The results are also in agreement with previous work presented by Harrison's and Culbertson's groups.[17, 18]

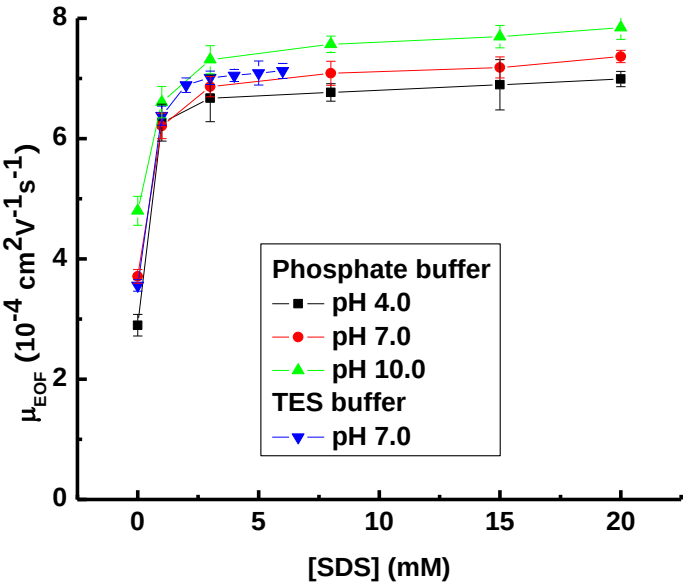


**Figure 4.4** EOF as a function of concentration in TES buffer (20 mM) at pH 7.0 and phosphate buffer (20 mM) at pH 4.0, 7.0 and 10.0 for an anionic surfactant SDS.

### 4.3.2 Single TDAPS surfactant system

Zwitterionic surfactants represent an interesting alternative for surface modification in polymeric microchips as well as for alternative agents for micellar electrokinetic chromatography (MEKC). The impact of these surfactants on EOF in fused silica capillaries has

been studied by Lucy's group,[28, 29] but their impact on EOF in polymeric microchips has not been studied. Here, we measured the impact of 0 to 2 mM TDAPS (CMC: 0.1 to 0.4 mM at 20 to 25 ℃[53]) on EOF for pH 7.0 TES and pH 4.0, 7.0, and 10.0 phosphate BGEs. Figure 4.5A shows a similar EOF trend for all four BGEs, in which EOF rapidly increases at low concentrations, and after reaching a highest EOF value at 0.1 mM TDAPS, gradually decreases to a nearly constant value. Differences in the starting EOF values are the result of differences in the ionic strength of the BGEs, the pH effects on surface charge, and the inherent variability of the EOF of PDMS. The unique behavior of TDAPS on PDMS can be explained by considering existing models for the interaction of surfactants with surfaces. Lucy's group showed a decreasing EOF trend for three sulfobetaine zwitterionic surfactants, N-dodecyl-N,N-dimethyl-3-ammonio-1-propansulfonate (DDAPS) (Figure 4.6A), N-hexadecyl-N,N-dimethyl-3-ammonio-1-propansulfonate (HDAPS), and coco (amidopropyl)hydroxyldimethyl sulfobetaine (CAS U) in fused silica capillaries, and a hemimicelle model (Figure 4.6B) was proposed for this behavior.[28] It was believed that the EOF results from the migration of the cations associated with the silanols on the surface of fused silica capillary, and the decrease of EOF can be attributed to the shielding of the silanols layer from the bulk solution by the adsorbed zwitterionic surfactants, leading to the decrease in zeta potential. This model can explain the decrease in EOF at higher TDAPS concentrations but does not explain the initial increase observed with a PDMS substrate. To verify that the behavior was not unique to TDAPS, DDAPS (CMC: 2.2 mM[28]), which has two less carbon chains than TDAPS, was tested as well. A similar EOF trend was obtained for DDAPS in PDMS microchips as compared to TDAPS, while the highest EOF value was obtained at 2 mM DDAPS (Figure 4.5B). The mechanism for the EOF decrease could be from one of several possible behaviors, including bilayer, hemimicelle or

full micelle formation. As hypothesized in the inserted panel in Figure 4.5A, the molecules of zwitterionic surfactants at their low concentrations may preferentially interact with the PDMS surface by their hydrophobic tails rather than their charged headgroups. Two potential results could cause an increase in EOF. First, the outermost exposed group of the surfactant is the anionic sulfonate functionality which would cause formation of the cationic double layer. Second, the larger head group of the zwitterionic surfactant will extend further from the surface resulting in a thicker double layer, a larger zeta potential and thus higher EOF. As the TDAPS concentration increases, a variety of mechanisms are again possible, ranging from bilayer formation to hemimicelle layer formation. The gradual decrease in EOF could also be attributed to charge neutralization of adsorbed surfactant molecules in the diffuse part of the double layer. The highest EOF was achieved at 0.1 mM of TDAPS which might be evidence of micelle formation of TDAPS at this BGE condition. More experiments using zwitterionic surfactants with different headgroup functionalities are needed to validate this hypothesis. However, some of necessary surfactants are currently not commercially available and synthesis of these molecules was outside the scope of the present work.

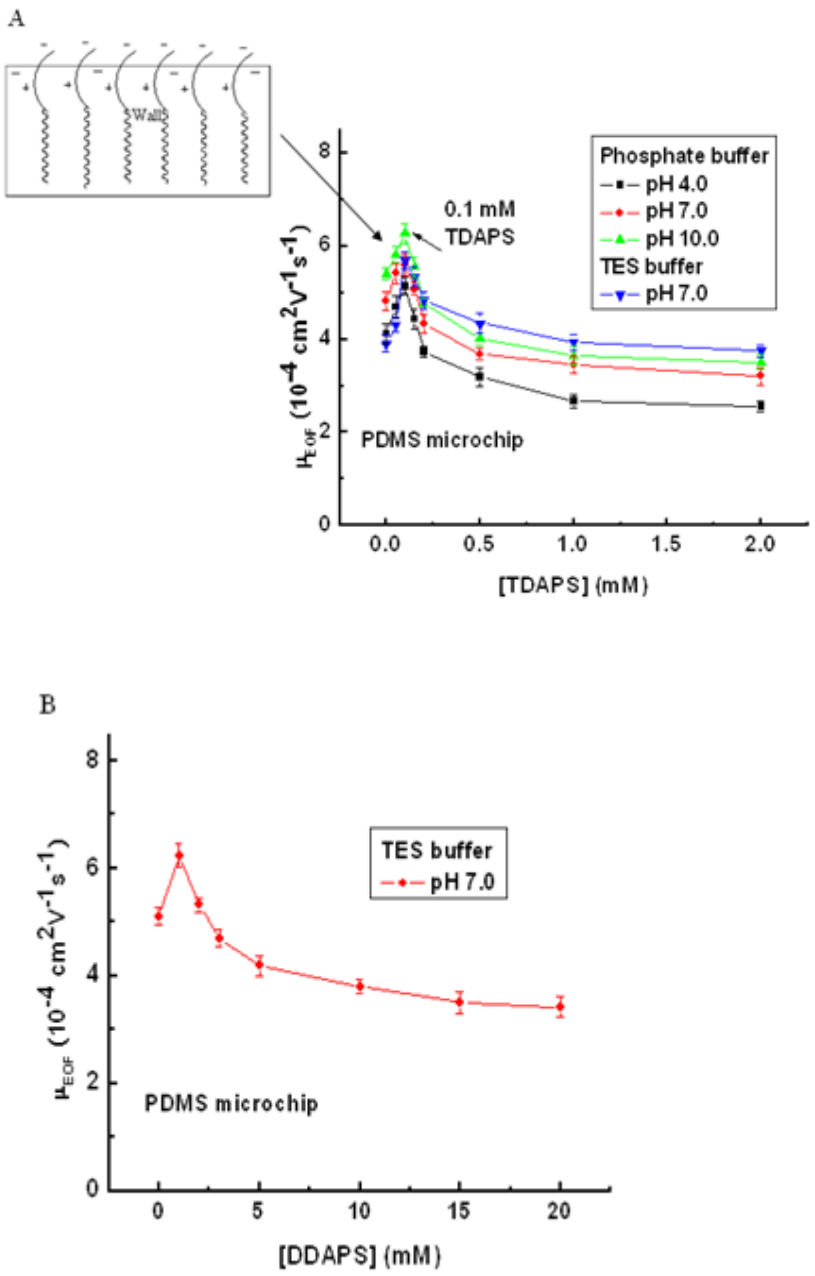


**Figure 4.5** (A) EOF as a function of concentration in TES buffer (20 mM) at pH 7.0 and phosphate buffer (20 mM) at pH 4.0, 7.0 and 10.0 for a zwitterionic surfactant TDAPS. The inserted panel describes the hypothesized surfactant molecule interaction with the PDMS surface. (B) EOF as a function of concentration in TES buffer (20 mM) at pH 7.0 for a zwitterionic surfactant DDAPS.

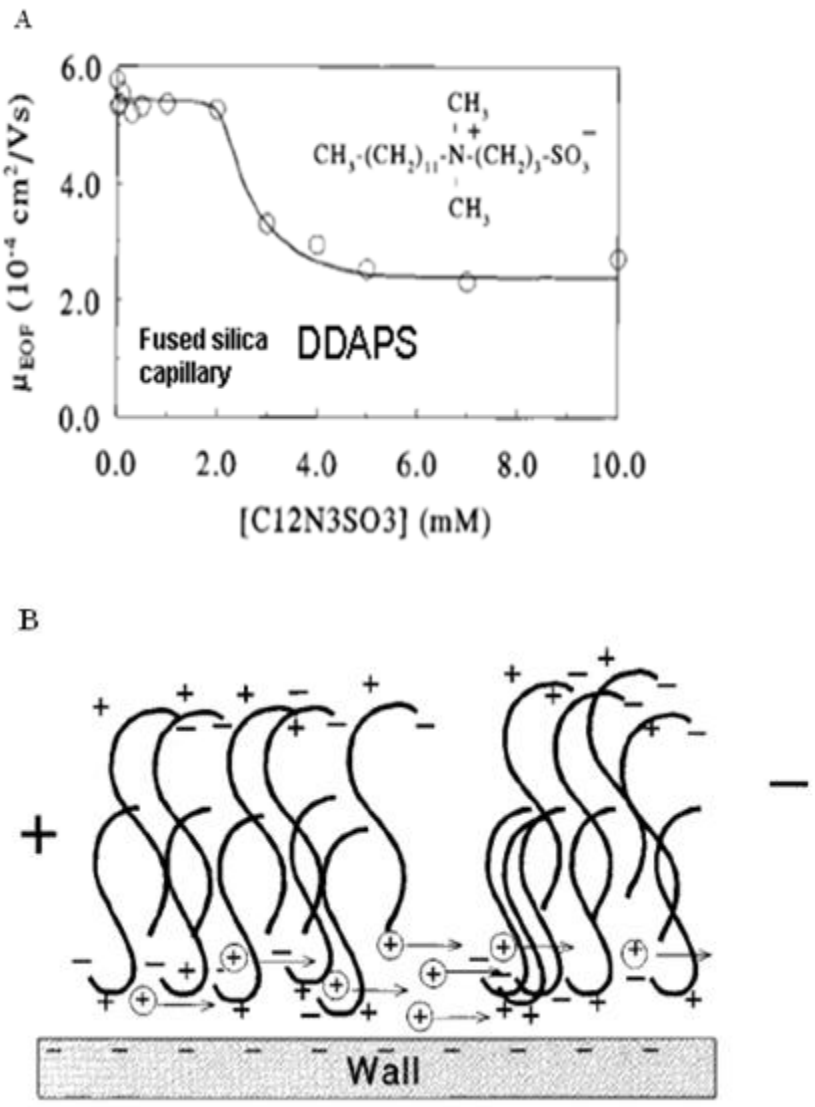


**Figure 4.6** (A) EOF as a function of concentration for a zwitterionic surfactant DDAPS in fused silica capillary. (B) Proposed hemimicelle model.

### 4.3.3 Mixed SDS/TDAPS surfactant system

Mixtures of anionic (SDS) and zwitterionic surfactants (TDAPS) were investigated next. EOF was measured at 0 to 20 mM SDS concentrations from while the concentration of TDAPS was fixed at 0.1 mM, 0.5 mM, 1.0 mM, or 2.0 mM (Figure 4.7A). In the absence of SDS, the EOF values measured for varying concentrations of TDAPS matched the values shown in Figure

4.5A. The addition of SDS caused an increase in EOF for all four TDAPS concentrations with a trend similar to that seen with SDS alone. However, the overall magnitude of the EOF was dependent on the TDAPS concentration with 0.1 mM TDAPS giving the highest average EOF and 2.0 mM giving the lowest. EOF values were similar to or higher than values measured for SDS alone. For example, an EOF value of $8.37 \pm 0.15 \cdot 10^{-4}$ $cm^2$ $V^{-1}$ $s^{-1}$ was produced using a mixture of 3.0 mM SDS and 0.1 mM TDAPS, which is 19% higher than that using 3.0 mM SDS alone. Hence, it would be advantageous to use these mixed surfactants for separations that require high EOF. The SDS/TDAPS ratio was also plotted to show the relative effect (Figure 4.7B). Except for data obtained at 0.1 mM TDAPS, the observed EOF closely correlates with the SDS/TDAPS ratio, irrespective of absolute surfactant concentrations. Monomeric SDS adsorbs to the PDMS surface and increases the EOF, whereas TDAPS suppresses the EOF above the critical micelle concentration. These results suggest that a desired EOF can be achieved through the range presented by simply varying the ratio of anionic and zwitterionic surfactants. Additionally, pH effects on the EOF for mixed surfactants in phosphate buffer at pH 4.0, 7.0, and 10.0 were studied, and the results are shown in Figure 4.8 and 4.9. Similar EOF behaviors as those in TES BGE at pH 7.0 can be observed for all three phosphate BGEs with different pH values.

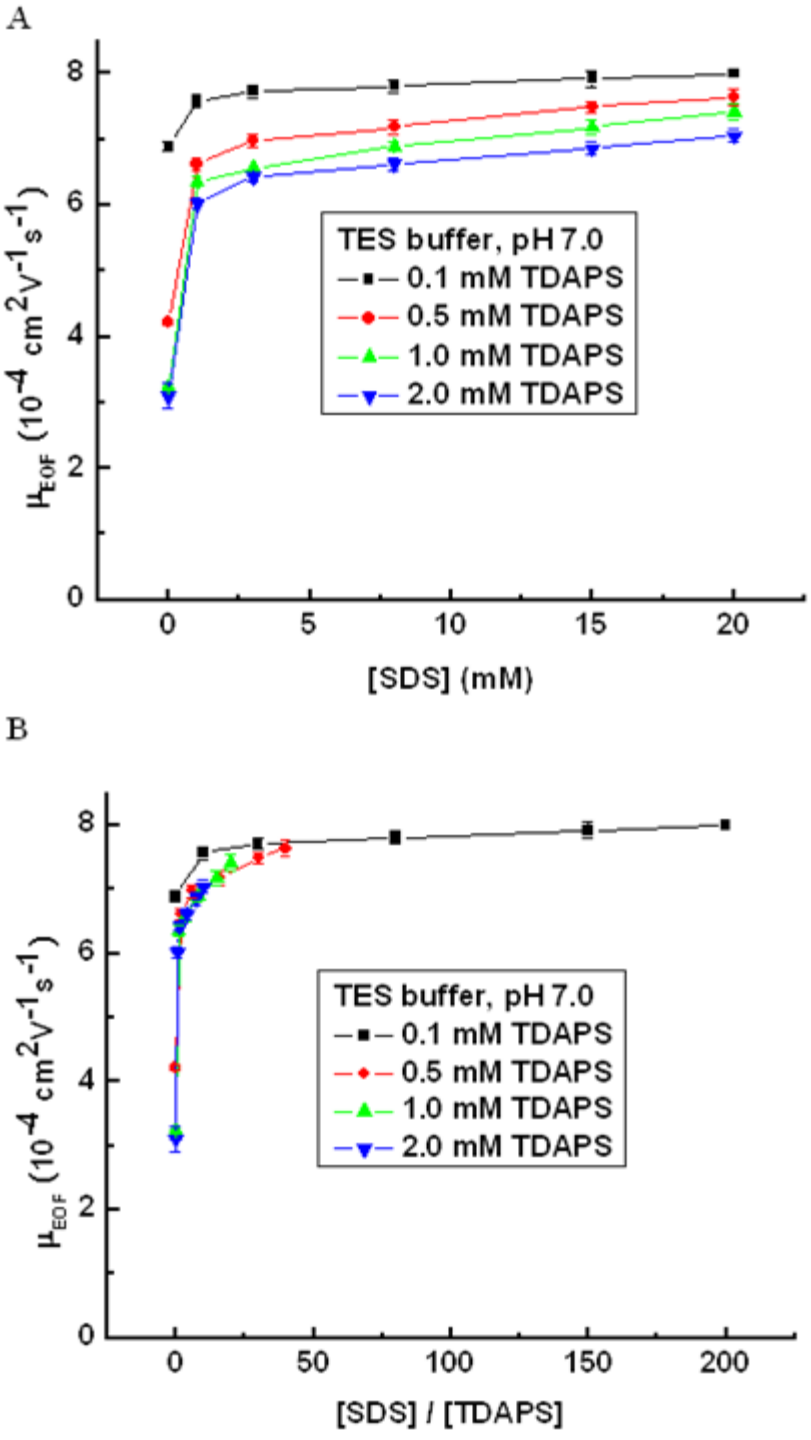


**Figure 4.7** (A) EOF as a function of SDS concentration using TDAPS in TES buffer (20 mM) at pH 7.0. (B) EOF as a function of the ratio of SDS/TDAPS concentration in TES buffer (20 mM) at pH 7.0.

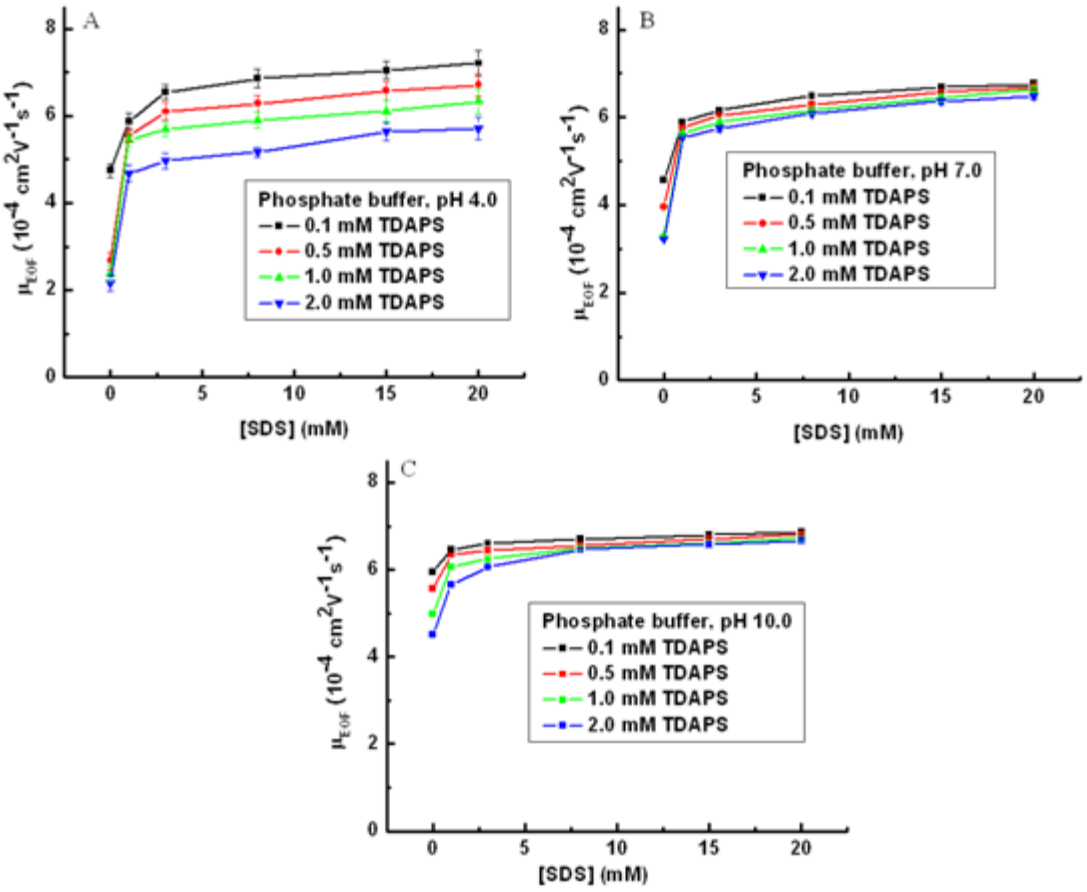


**Figure 4.8** EOF as a function of SDS concentration using TDAPS in phosphate buffer (20 mM) at (A) pH 4.0, (B) pH 7.0, and (C) pH 10.0.

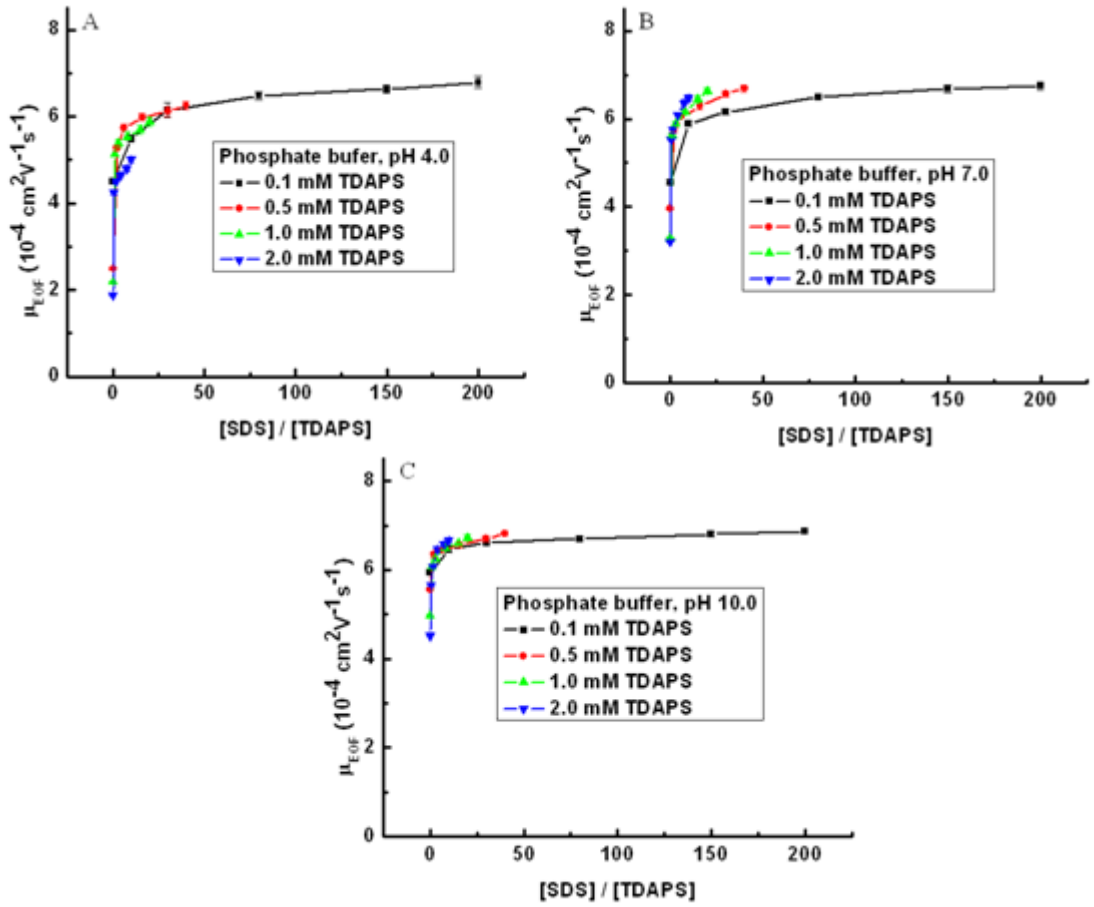


**Figure 4.9** EOF as a function of the ratio of SDS/TDAPS concentration in phosphate buffer (20 mM) at (A) pH 4.0, (B) pH 7.0, and (C) pH 10.0.

### 4.3.4 Adsorption/desorption rates of surfactants

After establishing EOF behavior, measurements were performed using the current monitoring method to evaluate the adsorption and desorption kinetics of SDS and TDAPS. Similar studies have been made on PDMS using the separation of a neutral marker for EOF measurements.[57] Figure 4.10 shows the experimental results of adsorption/desorption kinetics of SDS (0.8 mM) and TDAPS at concentrations of 0.1 mM, 0.5 mM, and 2.0 mM. The differences observed in the initial EOF values likely arise from variability in the native surface charge of

PDMS and/or variations in ionic strength. As can be observed in Figure 4.10, a significant increase in the EOF was observed once SDS was added to the BGE, with EOF changing from the initial value of 3.5 $\times 10^4$ $cm^2$ $V^{-1}$ $s^{-1}$ for native PDMS to 5.0 $\times 10^4$ $cm^2$ $V^{-1}$ $s^{-1}$ with 0.8 mM SDS. The equilibrium was reached in less than 10 min. When BGEs without SDS were reloaded, the EOF rapidly decreased to a value of 4.0 $\times 10^4$ $cm^2$ $V^{-1}$ $s^{-1}$, resulting from the desorption of SDS from the surface. However, the initial EOF value was never reached even after 40 min, suggesting a significant amount of SDS was retained on the surface. Similar behavior was observed when 0.1 mM TDAPS was added to the BGE. As can be observed in Figure 4.10, the initial EOF increased from 3.2 $\times 10^4$ $cm^2$ $V^{-1}$ $s^{-1}$ to 3.9 $\times 10^4$ $cm^2$ $V^{-1}$ $s^{-1}$, and decreased to a final EOF value of 3.7 $\times 10^4$ $cm^2$ $V^{-1}$ $s^{-1}$, showing slower adsorption and desorption kinetics than those in 0.8 mM SDS. After 40 min, ~69% of the total EOF change due to TDAPS remained due to semi-permanently attached TDAPS on the PDMS surface. When 0.5 mM TDAPS was added to the BGE, EOF decreased from 2.9 $\times 10^4$ $cm^2$ $V^{-1}$ $s^{-1}$ to 2.3 $\times 10^4$ $cm^2$ $V^{-1}$ $s^{-1}$, while in the case of 2.0 mM TDAPS, EOF changed from 3.4 $\times 10^4$ $cm^2$ $V^{-1}$ $s^{-1}$ to 2.6 $\times 10^4$ $cm^2$ $V^{-1}$ $s^{-1}$. Likewise, after removing TDAPS from the BGE, EOF did not recover to its initial value. Hence, the PDMS channels should be in contact with each solution prior to EOF measurements for at least 40 min to minimize kinetic contributions in the adsorption stage.

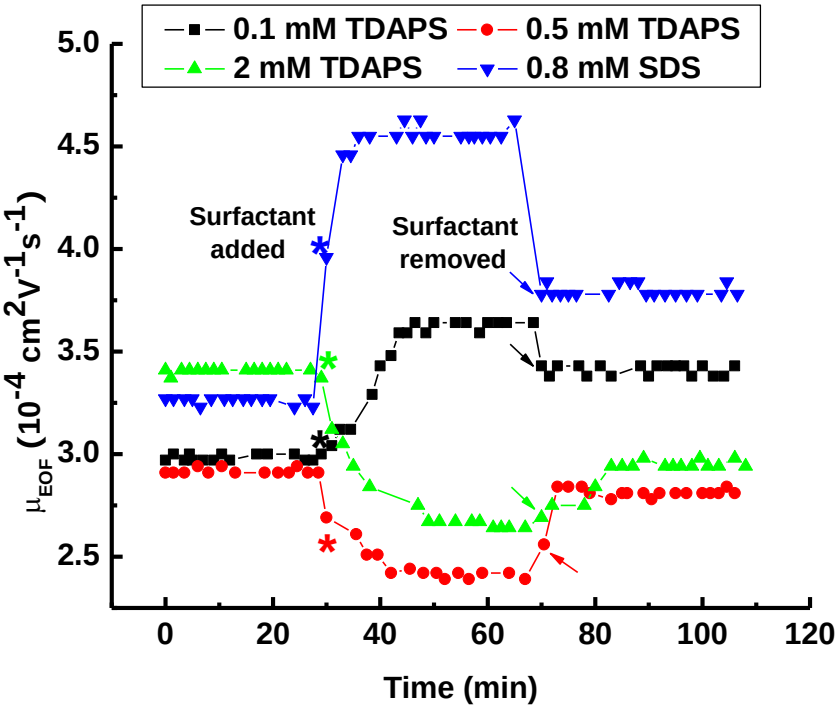


**Figure 4.10** Adsorption/desorption experiments of surfactants. The mark* denotes the point when the surfactant was added and the arrow denotes the point when the surfactant was removed from the solution reservoirs.

### 4.3.5 EOF measurements by $C^4D$ and current monitoring methods

Next, EOF measurements were performed simultaneously using current monitoring and $C^4D$ methods for three nonionic surfactants (Tween 20, Triton X-100, and PEG 400), and mixed ionic/nonionic surfactant systems (SDS/Tween 20, SDS/Triton X-100, and SDS/PEG 400) as well as mixed zwitterionic/nonionic surfactant systems (TDAPS/Tween 20, TDAPS/Triton X-100, and TDAPS/PEG 400). Example traces for current/conductivity signals for EOF measurements obtained simultaneously from these two methods are shown in Figure 4.11A. The current monitoring method measures the average conductivity along the channel and gives a

gradual decrease in the current until a current plateau is reached, indicating total replacement of BGE in the channel. The $C^4D$ measures conductivity at a point along the channel, and thus there is a sudden decrease in conductivity when the lower ionic strength BGE reaches detection electrodes. To compare the two methods, the EOF reproducibility using 20 mM TES buffer (pH 7.0) combined with 5, 10, and 18 mM TES buffer (pH 7.0) as the high and low ionic strength BGEs, respectively, was established. As shown in Figure 4.11B, while the two methods give statistically indistinguishable EOF values, the reproducibility of the $C^4D$ method is superior to that of the current monitoring method as evidenced by the relative standard deviations. The current monitoring method gave a relative standard deviation of 1.89%, while the $C^4D$ detector had a relative standard deviation of 1.41%, when using 20 and 18 mM TES BGEs. As the difference in ionic strength between the BGEs increased (resulting in the net ionic strength decreasing), the EOF increased slightly (from $4.52 \pm 0.09 \ 10^4$ $cm^2\ V^{-1}s^{-1}$ (current monitoring) and $4.51 \pm 0.06 \ 10^4$ $cm^2\ V^{-1}s^{-1}$ ($C^4D$) when using 20 and 18 mM TES BGEs to $4.65 \pm 0.31\ 10^4$ $cm^2\ V^{-1}s^{-1}$ (current monitoring) and $4.65 \pm 0.24\ 10^4$ $cm^2\ V^{-1}s^{-1}$ ($C^4D$) when using 20 and 5 mM TES BGEs), while the standard deviation increased significantly (6.69% (current monitoring) and 5.18% ($C^4D$) when using 20 and 5 mM TES BGEs). These results indicate that more precise EOF measurements can be made using BGEs with smaller differences in ionic strength in accordance with previous reports and with the use of $C^4D$.[58] Based on these results, 20 mM and 18 mM BGEs (TES buffer at pH 7.0 or boric acid buffer at pH 9.2) were used for all remaining EOF measurements.

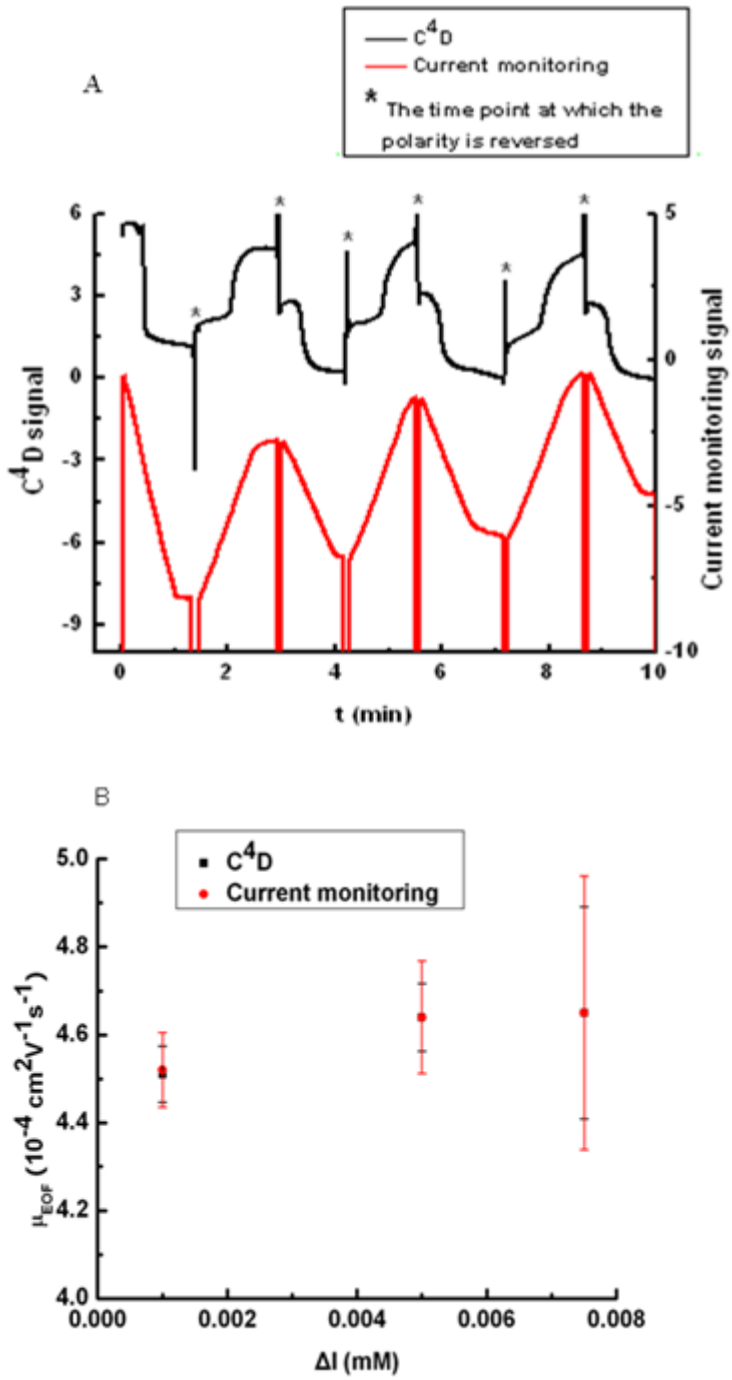


**Figure 4.11** (A) EOF measurements using both current monitoring and $C^4D$ methods. The mark* denotes the time point at which the polarity is reversed. Field strength: 200 V/cm; BGE: TES buffer (20 mM) at pH 7.0. (B) EOF as a function of difference in ionic strength between the BGEs used in both current monitoring and $C^4D$ methods.

### 4.3.6 Single nonionic surfactant system

Modification of PDMS surface chemistry using nonionic surfactants has been reported by several groups who have suggested that this class of surfactants interacts with the surface through their hydrophobic tails, creating an uncharged hydrophilic surface that minimizes protein adsorption and reduces EOF.[34, 35] Here, two molecular nonionic surfactants, Tween 20 (CMC: 0.08 mM [33]) and Triton X-100 (CMC: 0.24 mM [59]), were studied. Measurement of EOF in boric acid buffer (pH 9.2) was performed using both $C^4D$ and current monitoring methods and the results are shown in Figure 4.12A. The EOF decreased with increasing surfactant concentration most likely as the result of the hydrophobic tail of the nonionic surfactant interacting with the PDMS to shield surface charges. As an example, Figure 4.12A shows EOF deceasing for Tween 20, from $4.30 \pm 0.08 \times 10^{-4}$ $cm^2 V^{-1}s^{-1}$ at 0 mM to $1.34 \pm 0.04 \times 10^{-4}$ $cm^2 V^{-1}s^{-1}$ at 5 mM. The results are also in agreement with previous work presented by Chen's group.[34] The increasing buffer viscosity in the presence of nonionic surfactants will also play a role in this behavior but is expected to be minimal relative to changes in surface charge. Similar results were found for Triton X-100 although the net change in EOF was smaller ($4.22 \pm 0.13$ to $2.05 \pm 0.16 \times 10^{-4}$ $cm^2 V^{-1} s^{-1}$) than Tween 20. The reason for the difference in final EOF values is not known at this time but is most likely the result of differences in surfactant packing density on the PDMS surface.

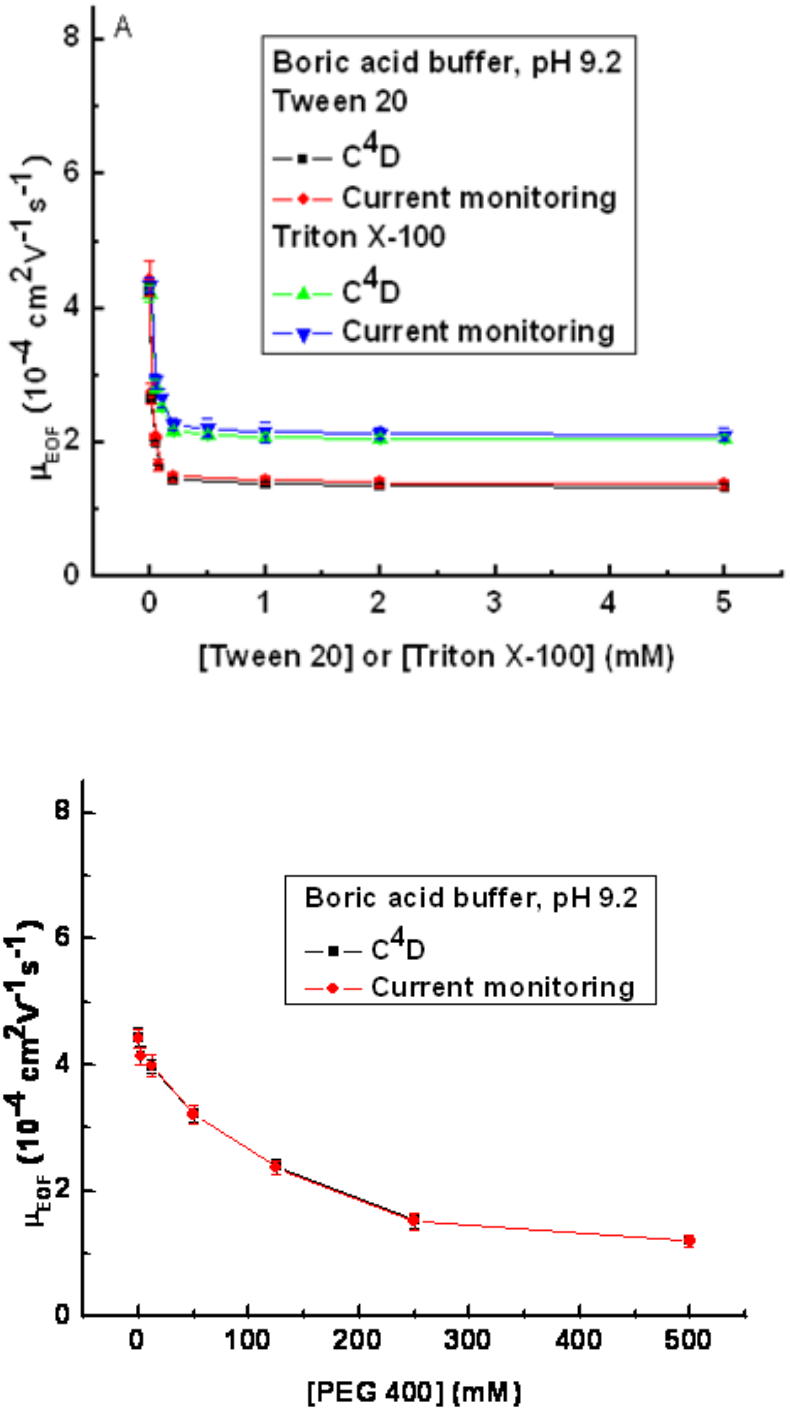


**Figure 4.12** EOF as a function of concentration in boric acid buffer (20 mM) at pH 9.2 for nonionic surfactants (A) Tween 20 and Triton X-100, and (B) PEG 400.

The use of hydrophilic neutral polymers, such as polyethylene glycol (PEG), poly(vinyl pyrrolidone) (PVP), hydroxyethylcellulose (HEC), has been applied for surface modification in chip electrophoresis.[1,13] Successful permanent[60-62] and dynamic coatings[63, 64] using PEG to suppress EOF have been reported on various materials, including glass and plastic chips. It has been reported that the adsorption of PEG on the surface of fused silica capillary via hydrogen bonds prevent the dissociation of silanol groups under higher pH.[64] Here, PEG (with its average molecular weight of approximately 400 daltons) was chosen as a starting point to study the EOF behavior of this type of polymeric surfactant with PDMS substrate. Measurement of EOF in boric acid buffer (pH 9.2) was performed using both $C^4D$ and current monitoring methods. As shown in Figure 4.12B, the presence of PEG 400 in BGE also decreased the EOF with increasing concentration, with its value changing from $4.42 \pm 0.14 \times 10^4$ $cm^2$ $V^{-1}s^{-1}$ to $1.20 \pm 0.09 \times 10^4$ $cm^2$ $V^{-1}s^{-1}$ in the range of 0 to 500 mM PEG 400 (corresponding to 0 to 18% w/v). However, the overall behavior was very different from Tween or Triton surfactants. Instead of causing a rapid decrease at the beginning phase and then reaching a plateau in EOF as concentration increased, the EOF decreased slowly with PEG, which is desirable for tuning the EOF over a wider range of operating conditions. Here, the decrease in EOF might be attributed to two factors. One is the noncovalent coating of PEG 400 on the PDMS surface via hydrogen bonds to shield surface charges, the other is the significant increase in BGE viscosity as the PEG 400 concentration increases.[65]

### 4.3.7 Mixed anionic/nonionic surfactant systems

Several groups have reported surface modification using mixed surfactant systems for CE. The combination of neutral and charged surfactants together provides a better means to fine tune

the EOF on bare silica than individual surfactants, resulting in a larger functional mobility window.[66, 67] Additionally, by employing a mixture of charged surfactants and the nonionic surfactant, polyoxyethylene ether (Brij 35), on PDMS-coated fused silica capillaries and glass microchips, improved control of the EOF across a larger functional mobility window was achieved for protein separations.[41] Here, mixtures of ionic (SDS) and nonionic surfactants (Tween 20, Triton X-100 and PEG 400) were investigated. EOF was measured using both $C^4D$ and current monitoring methods (only $C^4D$ data is shown for figure clarity) at 0 to 20 mM SDS concentrations while the concentration of Tween 20 was fixed at 0.1 mM, 0.5 mM, 1.0 mM, or 5.0 mM in 20 mM boric acid buffer (pH 9.2) (Figure 4.13A). In the absence of SDS, the EOF values measured for varying concentrations of Tween 20 matched the values shown in Figure 4.12A. The addition of SDS dominated the EOF behavior for all Tween 20 concentrations with only small differences in EOF obtained as a function of Tween 20 concentration. For example, an EOF value of $5.79 \pm 0.16 \times 10^4$ $cm^2\ V^{-1}s^{-1}$ was measured using a mixture of 3.0 mM SDS and 1.0 mM Tween 20, which is almost 3.5-fold higher than that using 1.0 mM Tween 20 alone ($1.39 \pm 0.03 \times 10^4$ $cm^2\ V^{-1}s^{-1}$). The SDS/Tween 20 ratio was also plotted to show the relative effect (Figure 4.14A). A similar EOF trend but a smaller net change in EOF was observed for mixed SDS/Triton X-100 system ($2.12 \pm 0.07$ to $6.49 \pm 0.23 \times 10^4$ $cm^2\ V^{-1}s^{-1}$) than mixed SDS/Tween 20 systems ($1.38 \pm 0.06$ to $6.51 \pm 0.22 \times 10^4$ $cm^2\ V^{-1}s^{-1}$) as shown in Figure 4.13B and 4.14B. The fact that the final EOF in both mixtures was statistically identical shows the dominant role of SDS in this system. Although the polymeric nonionic surfactant PEG 400 modifies EOF with a different mechanism as compared to two molecular nonionic surfactants (Tween 20 and Triton X-100), the mixed SDS/PEG 400 surfactant system still exhibited a similar EOF behavior as the above two mixed surfactant systems, showing an EOF change from $1.66 \pm 0.08$ to $6.75 \pm$

0.16 ×10$^{4}$ cm$^{2}$ V$^{-1}$s$^{-1}$ for increased SDS concentration (Figure 4.13C and 4.14C). These results are in agreement with the EOF behavior shown in the mixed SDS/Brij 35 surfactant system in previous work presented by Harrison's groups.[41] For all three mixed ionic/nonionic surfactant systems, the significant increase in EOF as a result of SDS concentration is most likely the result of its higher packing density on the surface coupled with a higher affinity for the surfaces.

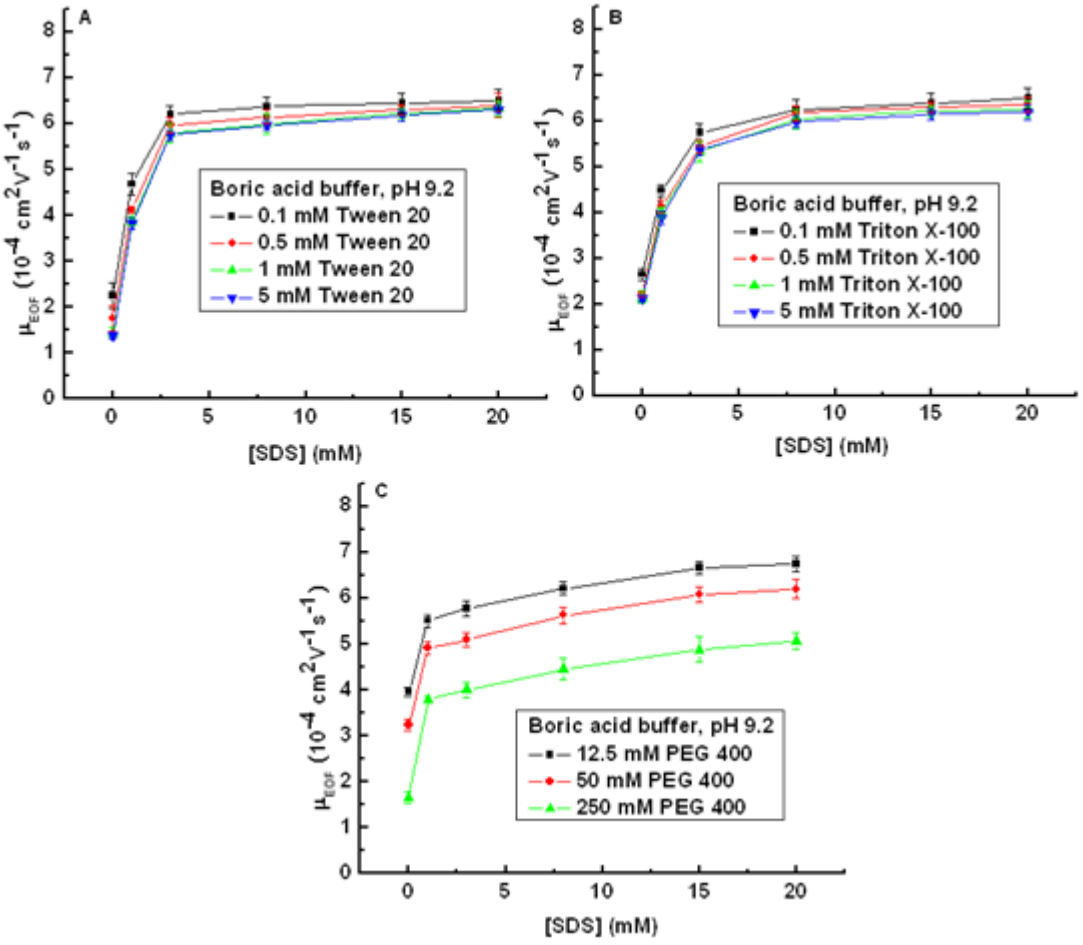


**Figure 4.13** EOF as a function of SDS concentration using (A) Tween 20, (B) Triton X-100, and (C) PEG 400 in boric acid buffer (20 mM) at pH 9.2.

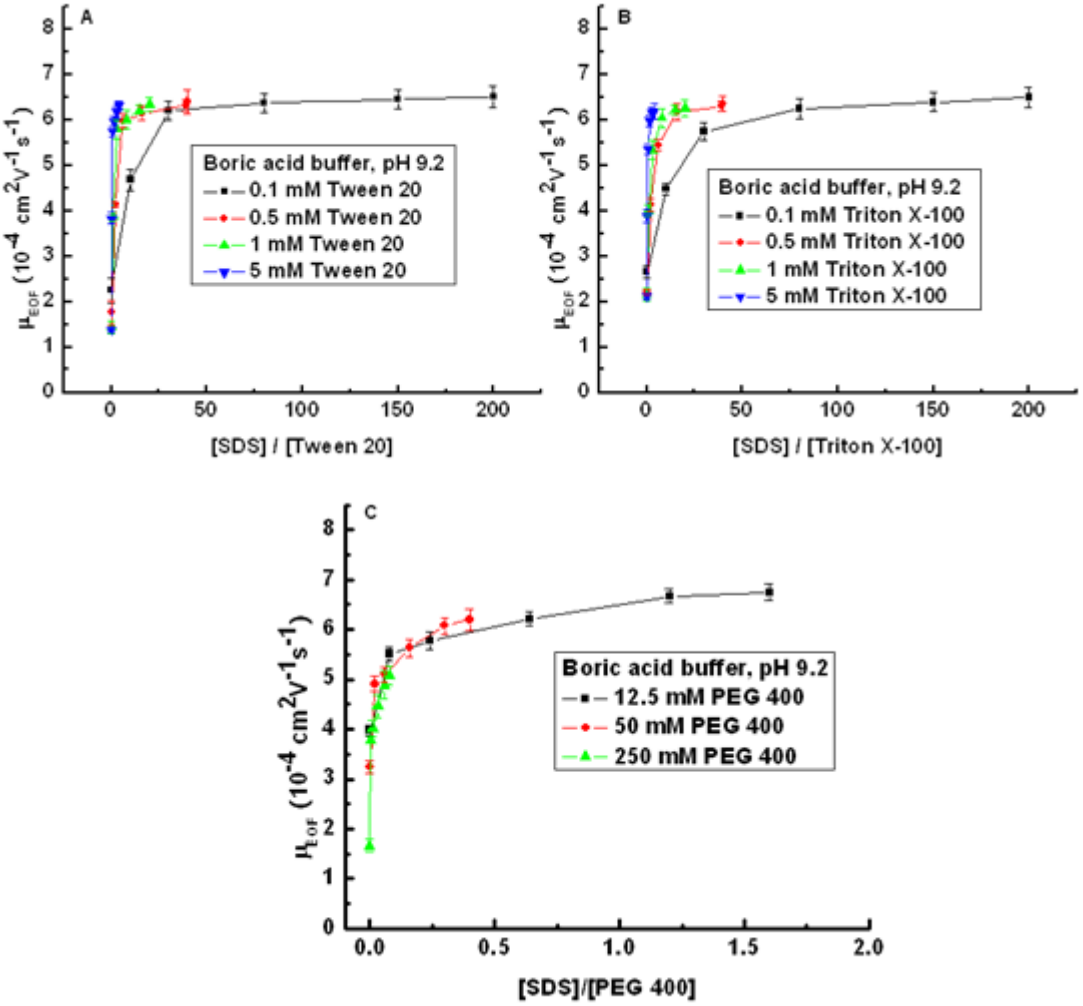


**Figure 4.14** EOF as a function of the ratio of (A) SDS/Tween 20, (B) SDS/Triton X-100, and (C) SDS/PEG 400 concentration in boric acid buffer (20 mM) at pH 9.2.

### 4.3.8 Mixed zwitterionic/nonionic surfactant systems

Next, the concentration dependent effect of mixtures of zwitterionic (TDAPS) and nonionic surfactants (Tween 20, Triton X-100 and PEG 400) on EOF was studied. EOF measurements were performed using both $C^4D$ and current monitoring methods (only $C^4D$ data is shown for figure clarity) at 0 to 4 mM TDAPS concentrations while the concentration of

Tween 20 was fixed at 0.1 mM, 0.5 mM, 1 mM, or 5 mM in 20 mM boric acid buffer (pH 9.2) (Figure 4.15A). In the absence of TDAPS, the EOF values measured for varying concentrations of Tween 20 were consistent with those obtained in pure Tween 20 system. The addition of TDAPS caused an increase in EOF for all four Tween 20 concentrations. For example, EOF values in the mixture of 0.5 mM TDAPS/2 mM Tween 20 and 4 mM TDAPS/2 mM Tween 20 are $3.85 \pm 0.12$ and $4.05 \pm 0.13$ $\times 10^4$ $cm^2$ $V^{-1}s^{-1}$, respectively, which are approximately two-fold higher than the $1.36 \pm 0.04$ $\times 10^4$ $cm^2$ $V^{-1}s^{-1}$ obtained using 2.0 mM Tween 20 alone. The overall EOF magnitude was dependent on the Tween 20 concentration with 0.1 mM Tween 20 giving the highest average EOF and 5 mM giving the lowest. Here, nonionic surfactant Tween 20 would more likely adsorb on the hydrophobic PDMS surface than the less hydrophobic zwitterionic surfactant TDAPS due to the presence of both cationic and anionic groups in molecules of zwitterionic surfactant.[68] One possible hypothesis to explain the EOF behavior of mixed Tween 20/TDAPS system is that Tween 20 shields the PDMS surface charge decreasing the EOF, whereas the adsorption of TDAPS onto the surface exposed the outermost anionic sulfonate group to form a thicker cationic double layer, a larger zeta potential and thus higher EOF. The same experiments were performed for the mixed TDAPS/Triton X-100 system, and similar EOF behavior with a smaller EOF change ($2.03 \pm 0.08$ to $4.30 \pm 0.13$ $\times 10^4$ $cm^2$ $V^{-1}s^{-1}$) (Figure 4.15B) was observed when compared to mixed TDAPS/Tween 20 system ($1.37 \pm 0.07$ to $4.66 \pm 0.15$ $\times 10^4$ $cm^2$ $V^{-1}s^{-1}$). The TDAPS/(Tween 20 or Triton X-100) ratios were also plotted to show the relative effect (Figure 4.16A and 4.16B). These results show that mixtures of zwitterionic (TDAPS)/nonionic (Tween 20 or Triton X-100) surfactants give a higher EOF than nonionic surfactant alone and thus provide a larger EOF working range relative to single surfactant systems. However, as depicted in Figure 4.15C and 4.16C for the mixed TDAPS/PEG 400

surfactant system, the addition of TDAPS caused an initial decrease, followed an increase in EOF at the lower concentration of PEG 400 (12.5 mM), and then an overall increase at the medium or higher concentration of PEG 400 (50 mM and 250 mM). The reason for this behavior is not clear at this time but is probably caused by the difference in the interaction mechanism of PEG 400 with PDMS substrate as compared to the other two molecular nonionic surfactants and the fact that TDAPS is not as strong a surfactant as SDS. Finally, EOF measurements were made for the same mixtures using pH 7.0 TES (20 mM) as the BGE since these conditions are common for separation of catecholamines (Figure 4.17 and 4.18). The resulting EOF values align very closely with the values measured at pH 9.2. The combined results show that a desired EOF can be achieved in the operating range provided by the surfactants by adjusting the surfactant ratio. This should provide a better control of EOF than is presently possible with single surfactant systems.

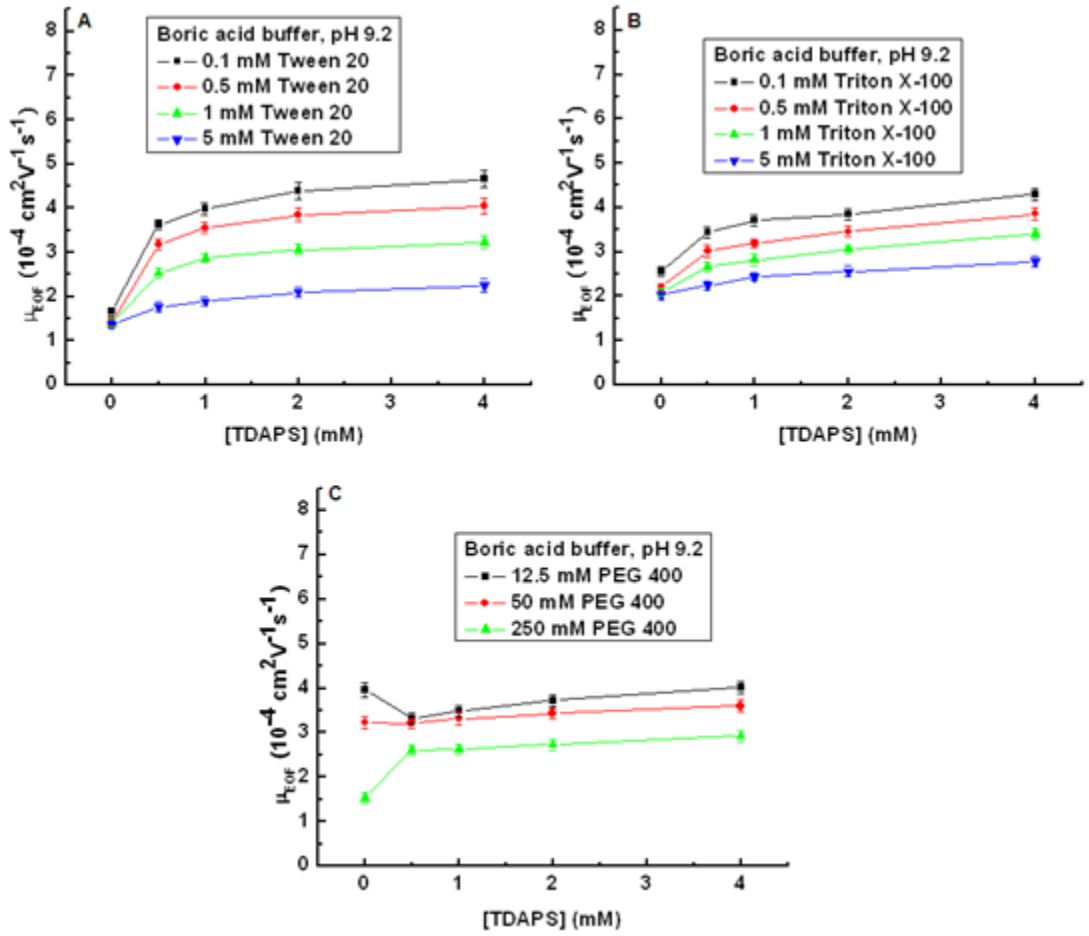


**Figure 4.15** EOF as a function of TDAPS concentration using (A) Tween 20, (B) Triton X-100, and (C) PEG 400 in boric acid buffer (20 mM) at pH 9.2.

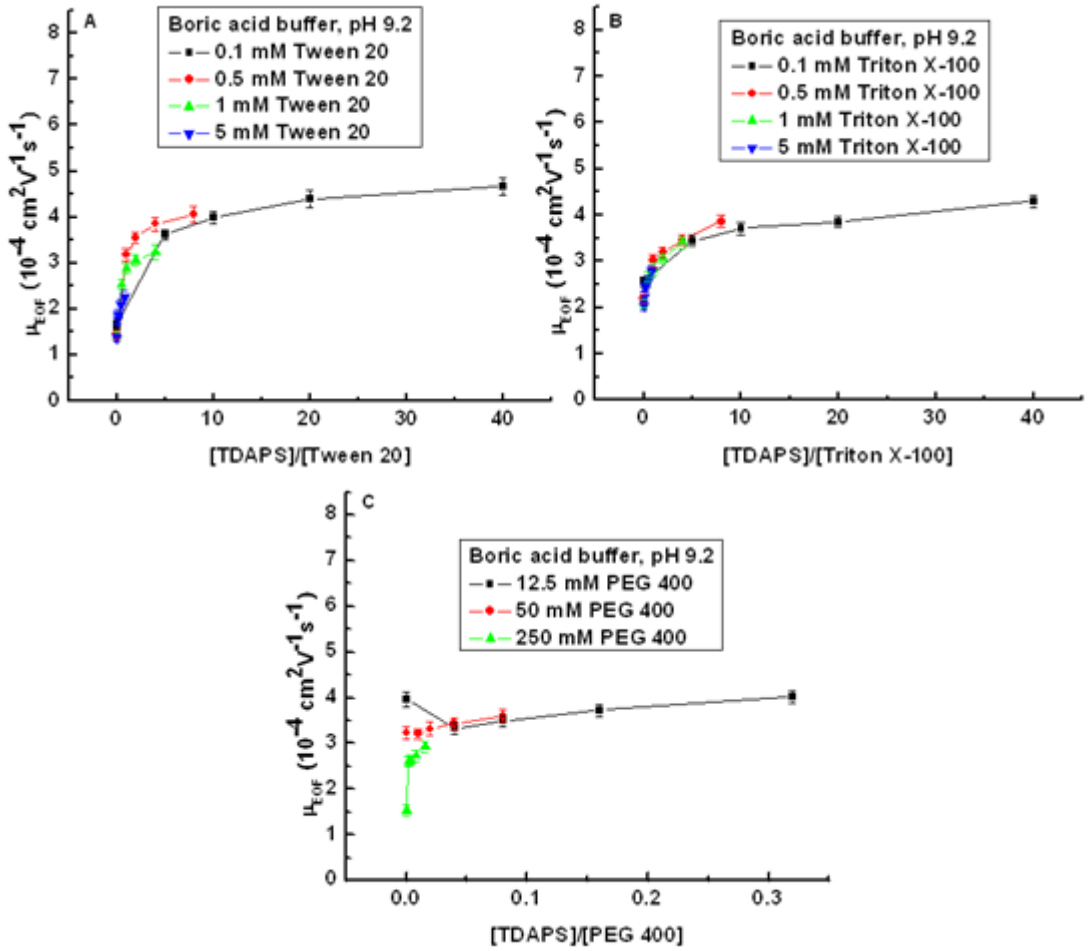


**Figure 4.16** EOF as a function of the ratio of (A) TDAPS/Tween 20, (B) TDAPS/Triton X-100, and (C) TDAPS/PEG 400 concentration in boric acid buffer (20 mM) at pH 9.2.

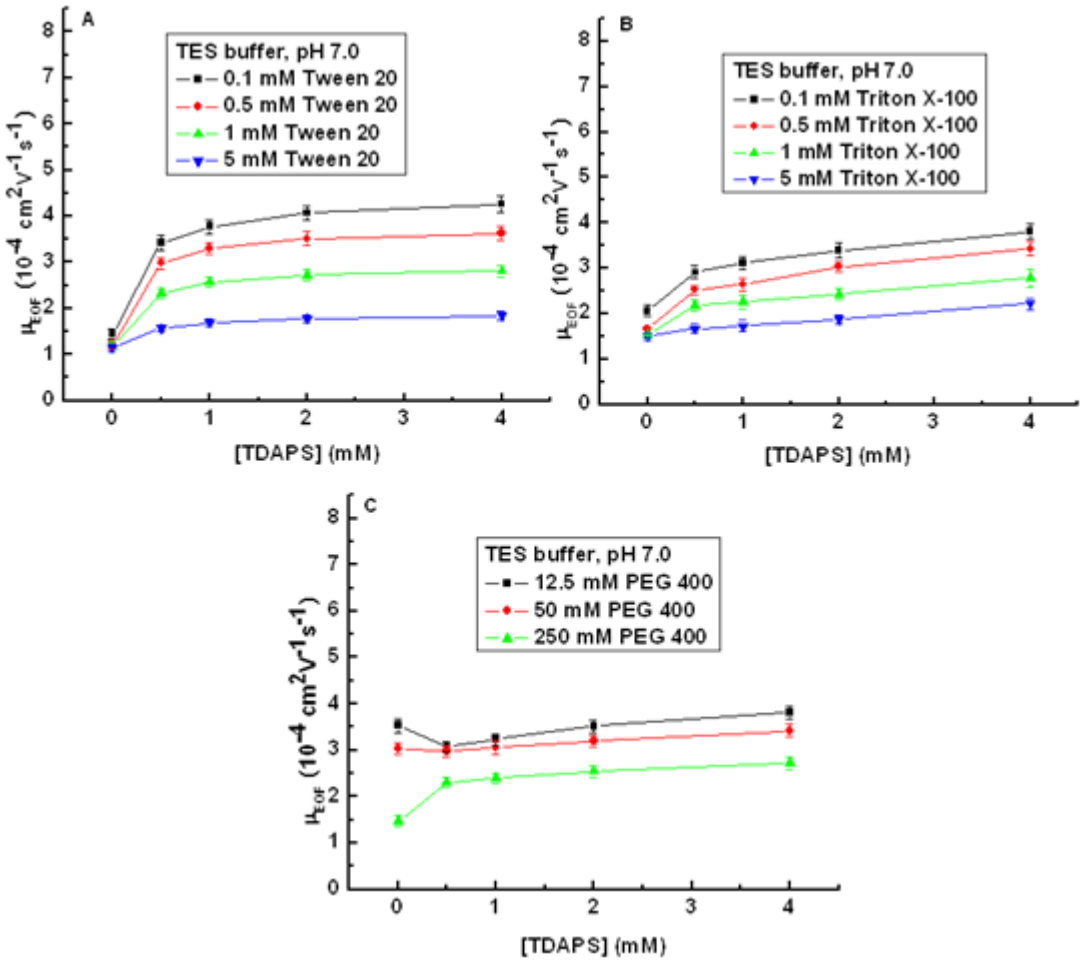


**Figure 4.17** EOF as a function of TDAPS concentration using (A) Tween 20, (B) Triton X-100, and (C) PEG 400 in TES buffer (20 mM) at pH 7.0.

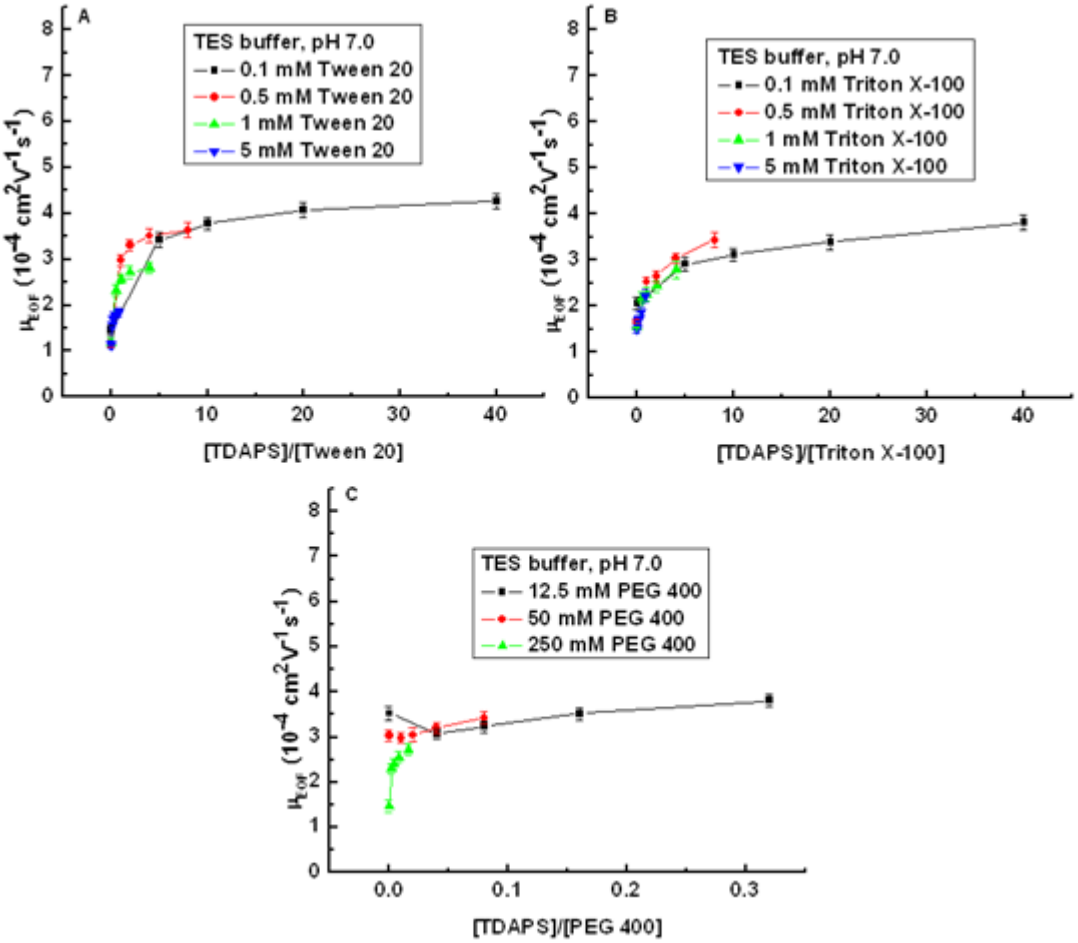


**Figure 4.18** EOF as a function of the ratio of (A) TDAPS/Tween 20, (B) TDAPS/Triton X-100, and (C) TDAPS/PEG 400 concentration in TES buffer (20 mM) at pH 7.0.

## 4.4 CONCLUSIONS

Here, the use of mixed ionic/zwitterionic, ionic/nonionic or zwitterionic/nonionic surfactants on PDMS microchips to control EOF was reported. EOF measurements as a function of the surfactant concentration were first performed using the current monitoring method with SDS, TDAPS, and a mixed SDS/TDAPS surfactant system. SDS increased the EOF as reported previously while TDAPS showed an initial increase in EOF followed by a reduction above the

CMC. pH effects were also studied in these single and mixed surfactant systems, exhibiting the expected pH dependence of EOF. With use of these mixed surfactants, higher EOF values and expanded EOF working windows were obtained as compared to single surfactants. Also, the correlation between EOF and surfactant concentration demonstrated that EOF could be tuned over a range of values based on the surfactant ratio. SDS exhibited faster adsorption/desorption rate than TDAPS. In all cases, the initial EOF was not fully recovered after removal of the surfactant, showing a residual amount of surfactant remaining on the PDMS surface. Next, $C^4D$ was introduced for EOF measurements and provided improved measurement reproducibility relative to the current monitoring method. EOF measurements as a function of the surfactant concentration were performed simultaneously using both methods for three nonionic surfactants (Tween 20, Triton X-100, and PEG 400), mixed ionic/nonionic surfactant systems (SDS/Tween 20, SDS/Triton X-100, and SDS/PEG 400), and mixed zwitterionic/nonionic surfactant systems (TDAPS/Tween 20, TDAPS/Triton X-100, and TDAPS/PEG 400), respectively. EOF for the nonionic surfactants decreased with increasing surfactant concentration. Using mixed surfactants, higher EOF values and a wider tunable EOF range was obtained as compared to BGEs containing a single nonionic surfactant.

## 4.5 REFERENCES


(1) Belder, D., Ludwig, M., *Electrophoresis* **2003**, *24*. 3595-3606.
(2) Muck, A., Svatos, A., *Talanta* **2007**, *74*. 333-341.
(3) Duffy, D. C., McDonald, J. C., Schueller, O. J. A., Whitesides, G. M., *Analytical Chemistry* **1998**, *70*. 4974-4984.
(4) Henry, A. C., Tutt, T. J., Galloway, M., Davidson, Y. Y., McWhorter, C. S., Soper, S. A., McCarley, R. L., *Analytical Chemistry* **2000**, *72*. 5331-5337.
(5) Johnson, T. J., Waddell, E. A., Kramer, G. W., Locascio, L. E., *Applied Surface Science* **2001**, *181*. 149-159.
(6) Roberts, M. A., Rossier, J. S., Bercier, P., Girault, H., *Analytical Chemistry* **1997**, *69*. 2035-2042.
(7) Barker, S. L. R., Tarlov, M. J., Canavan, H., Hickman, J. J., Locascio, L. E., *Analytical Chemistry* **2000**, *72*. 4899-4903.
(8) Schmalzing, D., Piggee, C. A., Foret, F., Carrilho, E., Karger, B. L., *Journal of chromatography. A* **1993**, *652*. 149-159.
(9) Dolnik, V., *Electrophoresis* **2004**, *25*. 3589-3601.
(10) Decher, G., *Science* **1997**, *277*. 1232-1237.
(11) Katayama, H., Ishihama, Y., Asakawa, N., *Analytical Chemistry* **1998**, *70*. 5272-5277.
(12) Katayama, H., Ishihama, Y., Asakawa, N., *Analytical Chemistry* **1998**, *70*. 2254-2260.
(13) Pallandre, A., de Lambert, B., Attia, R., Jonas, A. M., Viovy, J. L., *Electrophoresis* **2006**, *27*. 584-610.
(14) Ludwig, M., Belder, D., *Electrophoresis* **2003**, *24*. 2481-2486.
(15) Kirby, B. J., Hasselbrink, E. F., *Electrophoresis* **2004**, *25*. 187-202.
(16) Kirby, B. J., Hasselbrink, E. F., *Electrophoresis* **2004**, *25*. 203-213.
(17) Ocvirk, G., Munroe, M., Tang, T., Oleschuk, R., Westra, K., Harrison, D. J., *Electrophoresis* **2000**, *21*. 107-115.
(18) Roman, G. T., Carroll, S., McDaniel, K., Culbertson, C. T., *Electrophoresis* **2006**, *27*. 2933-2939.
(19) Effenhauser, C. S., Bruin, G. J. M., Paulus, A., *Electrophoresis* **1997**, *18*. 2203-2213.
(20) Garcia, C. D., Henry, C. S., *Analytica Chimica Acta* **2004**, *508*. 1-9.
(21) Garcia, C. D., Henry, C. S., *Analytical Chemistry* **2003**, *75*. 4778-4783.
(22) Garcia, C. D., Henry, C. S., *Analyst* **2004**, *129*. 579-584.
(23) Wallingford, R. A., Ewing, A. G., *Analytical Chemistry* **1988**, *60*. 258-263.
(24) Vrouwe, E. X., Luttge, R., Olthuis, W., van den Berg, A., *Journal of chromatography. A* **2006**, *1102*. 287-293.
(25) Wang, W., Zhao, L., Zhang, J. R., Zhu, J. J., *Journal of chromatography. A* **2007**, *1142*. 209-213.
(26) Gong, M., Wehmeyer, K. R., Limbach, P. A., Heineman, W. R., *Journal of chromatography. A* **2007**, *1167*. 217-224.
(27) Han, B., Xu, Y., Zhang, L., Yang, X., Wang, E., *Talanta* **2009**, *79*. 959-962.
(28) Yeung, K. K., Lucy, C. A., *Analytical Chemistry* **1997**, *69*. 3435-3441.
(29) Cunliffe, J. M., Baryla, N. E., Lucy, C. A., *Analytical Chemistry* **2002**, *74*. 776-783.
(30) Wei, W., Ju, H., *Electrophoresis* **2005**, *26*. 586-592.
(31) Noblitt, S. D., Schwandner, F. M., Hering, S. V., Collett, J. L., Jr., Henry, C. S., *Journal of chromatography. A* **2009**, *1216*. 1503-1510.

(32) Gertsch, J. C., Noblitt, S. D., Cropek, D. M., Henry, C. S., *Analytical Chemistry* **2010**, *82*. 3426-3429.
(33) Towns, J. K., Regnier, F. E., *Analytical Chemistry* **1991**, *63*. 1126-1132.
(34) Wang, A. J., Xu, J. J., Chen, H. Y., *Analytica Chimica Acta* **2006**, *569*. 188-194.
(35) Xu, Y., Jiang, H., Wang, E., *Electrophoresis* **2007**, *28*. 4597-4605.
(36) Dou, Y. H., Bao, N., Xu, J. J., Meng, F., Chen, H. Y., *Electrophoresis* **2004**, *25*. 3024-3031.
(37) Yeung, K. K., Lucy, C. A., *Analytical Chemistry* **1998**, *70*. 3286-3290.
(38) Yeung, K. K., Lucy, C. A., *Electrophoresis* **1999**, *20*. 2554-2559.
(39) Baryla, N. E., Lucy, C. A., *Journal of chromatography. A* **2002**, *956*. 271-277.
(40) Wang, C., Lucy, C. A., *Electrophoresis* **2004**, *25*. 825-832.
(41) Badal, M. Y., Wong, M., Chiem, N., Salimi-Moosavi, H., Harrison, D. J., *Journal of chromatography. A* **2002**, *947*. 277-286.
(42) Mori, M., Hu, W. Z., Haddad, P. R., Fritz, J. S., Tanaka, K., Tsue, H., Tanaka, S., *Analytical and Bioanalytical Chemistry* **2002**, *372*. 181-186.
(43) Zemann, A. J., Schnell, E., Volgger, D., Bonn, G. K., *Analytical Chemistry* **1998**, *70*. 563-567.
(44) da Silva, J. A. F., do Lago, C. L., *Analytical Chemistry* **1998**, *70*. 4339-4343.
(45) Pumera, M., Wang, J., Opekar, F., Jelinek, I., Feldman, J., Lowe, H., Hardt, S., *Analytical Chemistry* **2002**, *74*. 1968-1971.
(46) Wang, J., Pumera, M., *Analytical Chemistry* **2002**, *74*. 5919-5923.
(47) Wang, J., Pumera, M., Collins, G. E., Mulchandani, A., *Analytical Chemistry* **2002**, *74*. 6121-6125.
(48) Lichtenberg, J., de Rooij, N. F., Verpoorte, E., *Electrophoresis* **2002**, *23*. 3769-3780.
(49) McDonald, J. C., Duffy, D. C., Anderson, J. R., Chiu, D. T., Wu, H., Schueller, O. J., Whitesides, G. M., *Electrophoresis* **2000**, *21*. 27-40.
(50) Vickers, J. A., Henry, C. S., *Electrophoresis* **2005**, *26*. 4641-4647.
(51) Huang, X. H., Gordon, M. J., Zare, R. N., *Analytical Chemistry* **1988**, *60*. 1837-1838.
(52) Zhou, J., Ellis, A. V., Voelcker, N. H., *Electrophoresis* **2010**, *31*. 2-16.
(53) Makamba, H., Kim, J. H., Lim, K., Park, N., Hahn, J. H., *Electrophoresis* **2003**, *24*. 3607-3619.
(54) Ro, K. W., Lim, K., Kim, H., Hahn, J. H., *Electrophoresis* **2002**, *23*. 1129-1137.
(55) Mukerjee, P. M., K. J. Washington, DC, 1970.
(56) Jacquier, J. C., Desbene, P. L., *Journal of Chromatography A* **1996**, *743*. 307-314.
(57) Garcia, C. D., Dressen, B. M., Henderson, A., Henry, C. S., *Electrophoresis* **2005**, *26*. 703-709.
(58) Pittman, J. L., Henry, C. S., Gilman, S. D., *Analytical Chemistry* **2003**, *75*. 361-370.
(59) Morandat, S., El Kirat, K., *Langmuir : the ACS journal of surfaces and colloids* **2006**, *22*. 5786-5791.
(60) Razunguzwa, T. T., Warrier, M., Timperman, A. T., *Analytical Chemistry* **2006**, *78*. 4326-4333.
(61) Schmolke, H., Demming, S., Edlich, A., Magdanz, V., Buttgenbach, S., Franco-Lara, E., Krull, R., Klages, C. P., *Biomicrofluidics* **2010**, *4*. 44113.
(62) Kitagawa, F., Kubota, K., Sueyoshi, K., Otsuka, K., *Journal of Pharmaceutical and Biomedical Analysis* **2010**, *53*. 1272-1277.
(63) Vayaboury, W., Kirby, D., Giani, O., Cottet, H., *Electrophoresis* **2005**, *26*. 2187-2197.

(64) Iki, N., Yeung, E. S., *Journal of Chromatography A* **1996**, *731*. 273-282.
(65) Han, F., Zhang, J. B., Chen, G. H., Wei, X. H., *Journal of Chemical and Engineering Data* **2008**, *53*. 2598-2601.
(66) Yeung, K. K. C., Lucy, C. A., *Journal of Chromatography A* **1998**, *804*. 319-325.
(67) Lucy, C. A., Underhill, R. S., *Analytical Chemistry* **1998**, *70*. 1045.
(68) Wydro, P., *Journal of colloid and interface science* **2007**, *316*. 107-113.

# CHAPTER 5. ELECTROPHORETIC SEPARATIONS IN POLY(DIMETHYLSILOXANE) MICROCHIPS USING MIXTED SURFACTANT SYSTEMS

## 5.1 EXPERIMENTAL

### 5.1.1 Chemicals

Reagents used for fabrication of microchips include SU-8 2035 photoresist (Microchem, Newton, MA), Sylgard 184 elastomer and curing agent (PDMS) (Dow Corning, Midland, MI), 4-in. silicon wafers (University Wafer, South Boston, MA), and microwires made of 99.99% Pd (25 μm) and 99.99% Au (25 μm) (Goodfellow, Huntingdon, England). Aqueous solutions were prepared in 18.2 MΩ*cm water from a Millipore Milli-Q purification system (Milipore Corp., Billerica, MA). The BGEs were prepared by weighing the desired amount of N-tris[hydroxymethyl]methyl-2-aminoethanesulfonic acid (TES; Sigma-Aldrich, St. Louis, MO) or boric acid (Fisher, Pittsburgh, PA) and adjusting the pH with 2 M NaOH (Fisher). Following pH adjustment, surfactant was added to the running BGE to the desired concentration. SDS (Aldrich, Milwaukee, WI, USA), TDAPS (Fluka, Buchs, Switzerland), Tween 20, PEG 400 (Sigma-Aldrich), and Triton X-100 (FisherBiotech, Fair Lawn, New Jersey) were selected for the present study. 10-mM stock solutions of dopamine (DA), Norepinephrine (NE), Epinephrine (E), 3,4-dihydroxy-L-phenylalanine (L-DOPA), catechol (CA), ascorbic acid (AA), DL-homocysteine (Hcy), reduced glutathione (GSH) (Sigma-Aldrich), and L-cysteine (Cys) (Fluka) were prepared daily in 10 mM HCl, while L-tyrosine (Tyr) (Sigma-Aldrich) was prepared daily in 10 mM NaOH. Samples were prepared by dilution of the stock with BGE. All chemicals were used as

received without further purification. An industrial incineration ash sample (RTC-CRM012) certified for metals was purchased for real sample analysis (LGC Standards, Teddington, UK).

### 5.1.2 Sample preparation and analysis

Rat pheochromocytoma (PC12) cells obtained from American Type Culture Collection (ATCC, Manassas, VA) were cultured on poly-D-lysine-coated T-25 culture flasks (VWR International, Radnor, PA) with F-12 K medium supplemented with 10% fetal bovine serum. Cell medium was replaced every 3 days and subcultured as needed. After centrifugation, the supernatant was discarded and the cells in the pellet were resuspended in 4 mL phosphate buffered saline (PBS) (0.2 M, NaCl (Mallinckrodt, Phillipsburg, NJ) 0.9%, pH 7.4). Cells were washed 3× with PBS to remove any residual media prior to analysis. Stimulation of the PC12 cells was carried out by exposing approximately $1.5 \times 10^5$ cells (300 μL) to 80 mM $K^+$ (as KCl) (300 μL) in PBS at room temperature for 3 min.[1] The cells were centrifuged at 1000 × g for 5 min, and 500 μL of supernatant was removed and placed in a fresh microcentrifuge tube for analysis. Samples were kept on ice until analysis to prevent analyte degradation.

The red blood cell (RBC) sample for the detection of reduced GSH was treated according to the literature.[2] Briefly, 10 mL of whole blood was collected from a healthy volunteer in heparinized tubes. The sample was centrifuged 1,000 × g for 15 min at 4 ℃, and the plasma discarded. The remaining erythrocytes were washed 3× with PBS. Aliquots of the erythrocyte were then hemolysed (1:1 v/v) in 1 mM $Na_2H_2EDTA$ (Mallinckrodt) solution with 10% (w/v) 5-sulfosalicylic acid (Sigma). The mixed solution was centrifuged at 1,000 × g for 10 min at 4 ℃. The supernatant was collected as hemolysate sample and was 4× diluted in 20 mM boric acid buffer (pH 9.2) with an appropriate composition of mixed SDS/TDAPS surfactants. The solution

containing GSH was analyzed by MCE-ECD immediately after removing the precipitated protein with a 3K microcentrifuge filter. For time studies of GSH in RBCs exposed to fly ash with or without $H_2O_2$, erythrocytes ($6 \times 10^6$ cells/mL) collected in the above procedure were cultured in six-well plates in an incubator at 37 ℃, 5% CO, and 99% humidity. RBC suspension (10% cells in RPMI1640 media (Sigma-Aldrich) with 1% antibiotic-antimycotic solution (APS) (Mediatech, Manassas, VA)) was supplemented with $H_2O_2$ (0.5 mM final concentration), fly ash (25 μg/mL final concentration) or both, respectively, at 2, 4 and 6 h. After hemolyzation using the same protocols, the supernatant was collected and 2× diluted in 20 mM boric acid buffer (pH 9.2) with an appropriate composition of mixed SDS/PEG 400 surfactants. The solution containing GSH was analyzed by MCE-ECD immediately after removing the precipitated protein with a 3K microcentrifuge.

### 5.1.3 PDMS microchip fabrication

The method used to fabricate PDMS microchips using incorporated microwires for detection has been published previously.[3, 4] A previously reported design consisting of a straight T injector and a bubble cell with its width 4× that of the separation channel width in the detection zone[5] was used and had channel width and depth of 50 μm, respectively (Figure 3.1). The microchip used for the detection of DA, NE, E, CA, and L-DOPA had sample and buffer channel lengths of 2.0 cm, a sample waste channel length of 4.0 cm, and a separation channel length of 10.0 cm, while the microchip used for the detection of another two groups of analytes (Group 1: DA, CA and AA; Group 2: Tyr, Hcy, Cys and GSH) has sample, sample waste, and buffer channel lengths of 0.8 cm, and the separation channel length of 5.0 cm. A Pd decoupler and Au

working electrode (WE) were placed in the bubble cell using electrode alignment channels.[4] Each electrode channel was 50 μm wide and separated by 125 μm.

### 5.1.4 MCE-ECD

A 3-channel (two positives and one negative) laboratory built high-voltage power supply was used for all the experiments involving an injection/separation step.[6] A 10-s hydrodynamic injection[7] was used for the separation of DA, NE, E, CA, and L-DOPA, while a 1-s and 3-s gated injections[8] were employed for the separation of another two groups of analytes (Group 1: DA, CA and AA; Group 2: Tyr, Hcy, Cys and GSH), respectively. The Pd decoupler and the sample waste reservoir were always held at ground to isolate the potentiostat from high voltage. During the hydrodynamic injection, both sample and buffer reservoirs were grounded. Sample introduction was achieved by filling the sample reservoir with 80 μL of sample solution and the remaining reservoir were filled with 50 μL of buffer solution. The separation was performed by applying the high positive potentials of 2,220 V and 1,850 V in sample and buffer reservoirs, respectively, resulting in a field strength of 150 V $cm^{-1}$ in 10.0 cm long separation channel. For gated injection, equal solution volumes were loaded in all reservoirs, and sample introduction was achieved by applying a positive potential of 1,050 V to the sample reservoir while floating the buffer reservoir. The separation was performed by applying 900 V to the buffer reservoir while keeping voltage settings in all other reservoirs the same as its injection phase, resulting in a field strength of 123 V $cm^{-1}$ in 5.0 cm long separation channel. DC amperometric detection and pulsed amperometric detection (PAD) were employed (CHI 1010A Electrochemical Analyzer, CH Instruments, Austin, TX) in a two-electrode configuration.[4] The former was used for the detection of catecholamines and their related analytes, including DA, NE, E, CA, L-DOPA, and ascorbic acid, while the latter was used for the detection of Tyr, Hcy, Cys and GSH. A Pt wire (1

mm diameter) in the waste reservoir was acted as both auxiliary and psuedo-reference electrode.[4] Cleaning of Pd decoupler was done initially by running cyclic voltammetry (CV) from -1.0 V to 1.0 V at 0.1 V/s for 50 cycles. Two gold working electrodes were cleaned using CV by scanning from -0.5 V to 1.8 V at 0.5 V/s for 100 cycles while buffer was flowed over the electrodes.

## 5.2 RESULTS AND DISCUSSION

### 5.2.1 Separation applications using mixed SDS/TDAPS surfactant system

The use of the mixed SDS/TDAPS surfactant system was demonstrated with the separation of dopamine (DA), catechol (CA) and ascorbic acid (AA). Separations were performed with different mixtures of SDS and TDAPS and compared to the individual surfactant systems. Electropherograms for 50 μM analytes under these buffer conditions are shown in Figure 5.1, with calculated EOF values of 7.22 ± 0.31, 8.20 ± 0.32, 6.17 ± 0.26, 8.75 ± 0.37, 8.00 ± 0.31, 7.74 ± 0.32 and 7.17 ± 0.33 $\cdot 10^{-4}$ $cm^2$ $V^{-1}$ $s^{-1}$ (n = 3) corresponding to the electropherograms from bottom to top, respectively. Shorter migration times (37.4 ± 1.3 to 39.7 ± 1.4, 46.9 ± 2.0 to 58.2 ± 2.1, and 60.5 ± 2.4 to 77.2 ± 3.5 s, n = 3) and higher peak heights (8.6 ± 0.8 to 12.0 ± 0.8, 4.6 ± 0.4 to 5.0 ± 0.5, and 1.1 ± 0.2 to 1.3 ± 0.3 nA, n = 3) were obtained for DA, CA, and AA, respectively, in the four mixed SDS/TDAPS surfactant systems as compared to the TES buffer with 0.1 mM TDAPS (Migration time of 46.9 ± 1.8, 62.3 ± 2.6, and 88.1 ± 2.6 s and peak heights of 8.0 ± 0.7, 2.5 ± 0.3, and 0.6 ± 0.1 nA (n = 3) for three analytes, respectively). Differences in the relative migration times here with respect to the EOF results discussed above are likely due to differences in the interaction of the analytes with the surfactant. Furthermore, differences in peak height may be the result of variation in injection volume in addition to improvements due to the increased solubility of the oxidized products of the

electrochemical reaction.[9] A significant improvement in the resolution (R = 4.16 ± 0.08, 4.32 ± 0.09, 5.88 ± 0.11, and 9.39 ± 0.15 (n = 3) for 0.5 mM SDS mixed with 0.1, 0.5, 1.0, and 2.0 mM TDAPS, respectively) between DA and CA was also achieved by using mixed surfactants as compared to the resolution (R = 1.37 ± 0.05, n = 3) of these two analytes in TES buffer with 1.0 mM SDS. However, the resolution for all analytes obtained using 0.1 mM TDAPS were still higher than those in mixed surfactant systems due to the much slower EOF with the TDAPS surfactant as compared to the mixed surfactant systems. Although clear separation can be obtained using TES buffer with SDS concentrations lower than 1.0 mM, mixed SDS/TDAPS surfactant system may provide a faster analysis time than single surfactant system with the same SDS concentration, while still keeping comparable or even better analyte resolution. As the TDAPS concentration increased in the surfactant mixtures, analytes resolution was enhanced, and the best results were achieved using a mixture of 0.5 mM SDS and 2.0 mM TDAPS among four tested mixed surfactant systems. In addition, the highest separation efficiencies of 150,000 ± 8,100, 200,000 ± 12,000, and 170,000 ± 20,000 plates/m (n = 3) (corresponding to 7,300 ± 380, 9,700 ± 550, and 8,000 ± 950 plates) were also obtained for dopamine, catechol and ascorbic acid, respectively, using the same SDS and TDAPS ratio. Comparisons of resolution and separation efficiency calculated form peak information in electropherograms under different conditions is shown in Figure 5.2 and Table 5.1. Furthermore, comparable or lower LODs were observed in mixed surfactant systems relative to individual surfactants, with an example LODs of dopamine, catechol and ascorbic acid at 60 ± 15 nM, 150 ± 42 nM, and 600 ± 180 nM, using a mixture of 0.5 mM SDS and 2.0 mM TDAPS, as compared to LODs of these analytes at 80 ± 19 nM, 150 ± 30 nM, and 550 ± 150 nM using 0.5 mM SDS or 120 ± 25 nM, 250 ± 50 nM, and 1,000 ± 360 nM (n = 3, S/N = 3) using 2.0 mM TDAPS, respectively.

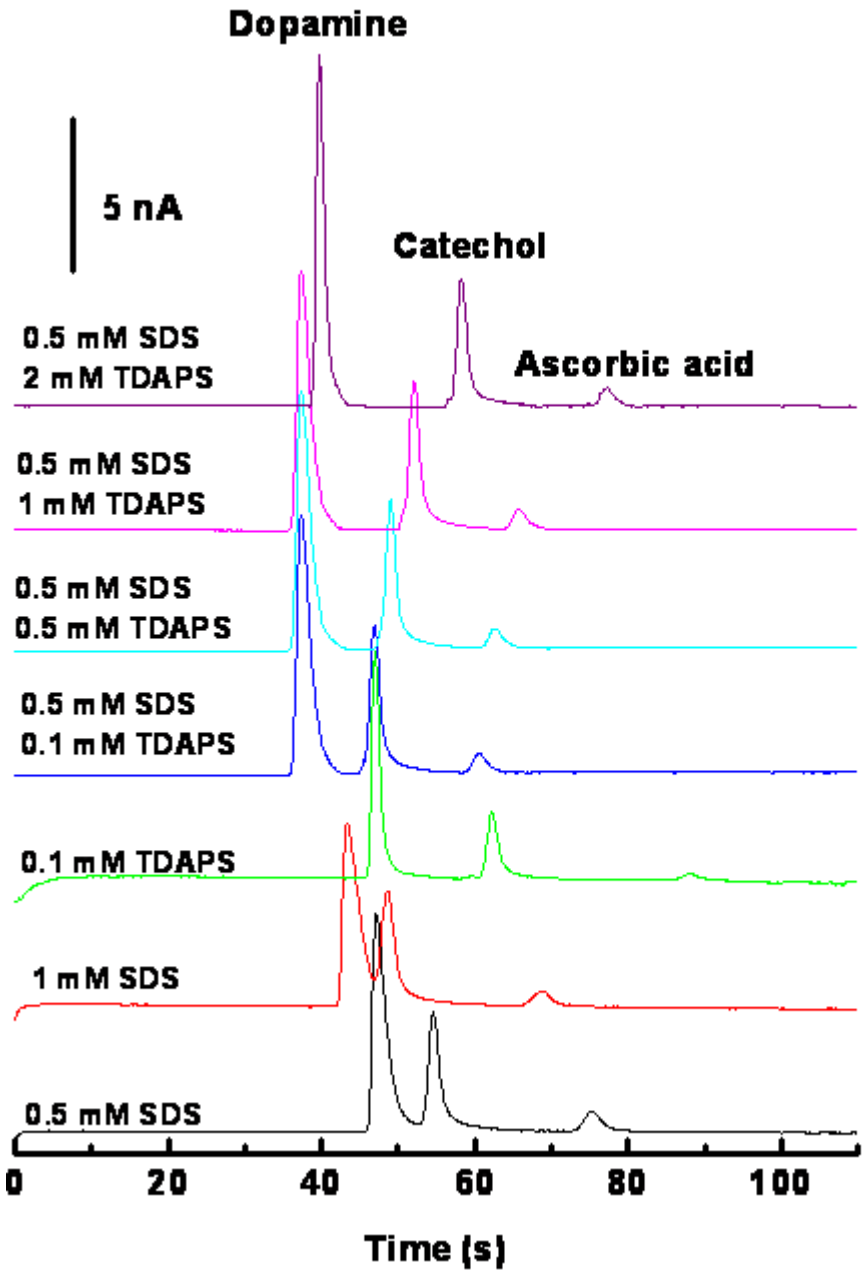


**Figure 5.1** Example electropherograms for 50 μM dopamine, catechol, and ascorbic acid in 20 mM TES buffer at pH 7.0 with various surfactant conditions. Field strength: 123 V/cm, 1-s gated injection; detection: DC Amp., $E_{det}$ = 1.2 V.

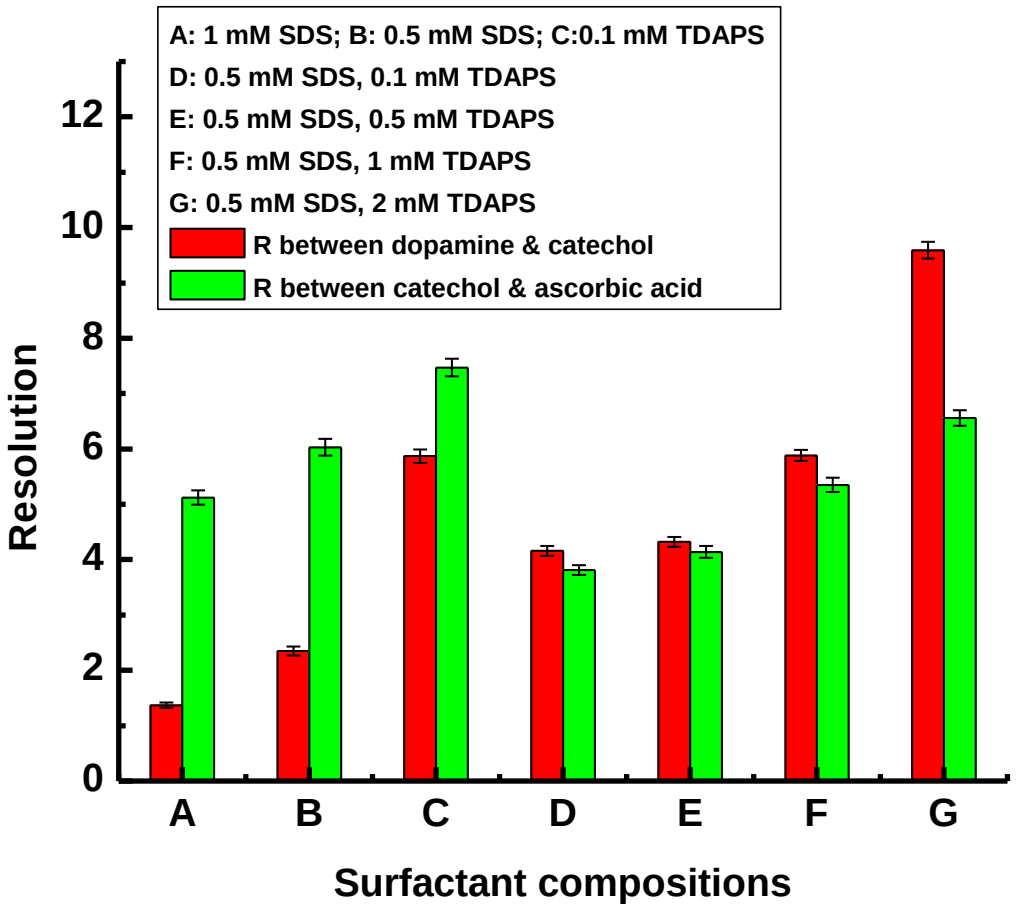


**Figure 5.2** Comparisons of resolution results of dopamine, catechol and ascorbic acid calculated form peak information in electropherograms under different conditions. Resolution ($R$) is calculated based on the following equation where $t_1$, $t_2$ are the migration time of two analytes, respectively, and $W_{h1}$, $W_{h2}$ are the half peak widths of two analytes in seconds, respectively. $R = [2\ln(2)]^{0.5}(t_2—t_1)/(W_{h1}+W_{h2})$, which will be used for all resolution calculations in this thesis.

**Table 5.1** Comparisons of separation efficiency results of dopamine, catechol and ascorbic acid under different surfactant conditions.

| | Separation efficiency (plates/m) (number in plates) | | |
|---|---|---|---|
| | Dopamine | Catechol | Ascorbic acid |
| 0.5 mM SDS | 70,720 ± 4,000 (3,360 ± 190) | 130,930 ± 8,400 (6,220 ± 400) | 102,400 ± 9,100 (4,860 ± 430) |
| 1 mM SDS | 42,320 ± 3,200 (2,010 ± 150) | 69,250 ± 7,000 (3,290 ± 330) | 80,210 ± 6,400 (3,810 ± 300) |
| 1 mM TDAPS | 215,400 ± 9,100 (10,230 ± 430) | 195,370 ± 8,000 (9,280 ± 380) | 132,630 ± 15,000 (6,300 ± 710) |
| 0.5 mM SDS 0.1 mM TDAPS | 42,130 ± 3,000 (2,000 ± 140) | 133,050 ± 5,900 (6,320 ± 280) | 106,480 ± 6,800 (5,060 ± 320) |
| 0.5 mM SDS 0.5 mM TDAPS | 46,740 ± 3,000 (2,220 ± 140) | 123,160 ± 7,200 (5,850 ± 340) | 99770 ± 6,100 (4,740 ± 290) |
| 0.5 mM SDS 1 mM TDAPS | 59,790 ± 5,890 (2,840 ± 280) | 133,260 ± 9890 (6,330 ± 470) | 122,530 ± 9,050 (5,820 ± 430) |
| 0.5 mM SDS 2 mM TDAPS | 153,900 ± 8,000 (7,310 ± 380) | 203,510 ± 11,600 (9,670 ± 550) | 168,420 ± 20,000 (8,000 ± 950) |

Next, the mixed SDS/TDAPS surfactant system was employed for the separation of Tyrosine (Tyr) and three aminothiols (Homocysteine (Hcy), Cysteine (Cys) and reduced glutathione (GSH)). Electropherograms for 200 μM Tyr, Hcy, and Cys as well as 600 μM GSH as a function of SDS/TDAPS ratio are shown in Figure 5.3. The calculated EOF values for the electropherograms from bottom to top under different buffer conditions are 7.87 ± 0.32, 6.73 ± 0.27, 6.27 ± 0.28, 5.72 ± 0.23, 4.86 ± 0.19, and 3.95 ± 0.20 $\cdot 10^{-4}$ $cm^2$ $V^{-1}$ $s^{-1}$ (n = 3), respectively. Longer migration times (79.3 ± 2.8 to 124.5 ± 4.1, 88.5 ± 2.9 to 149.5 ± 7.2, 107.8 ± 3.3 to 226.8 ± 10.2, and 116.3 ± 4.1 to 268.8 ± 11.5 s, n = 3) were obtained for Tyr, Hcy, and Cys and GSH, respectively, using mixed SDS/TDAPS surfactant system than single SDS surfactant (0.1 mM) system (75.3 ± 2.4, 86.3 ± 2.6, 100.3 ± 3.4, and 108.0 ± 3.9 s (n = 3) for four analytes, respectively) due to the decreased EOF. The separation of four analytes using a single TDAPS surfactant (2 mM) was also performed but produced much longer migration times (160.3 ± 7.7,

210.6 ± 9.1, 280.3 ± 13.7, and 340.8 ± 18.1 s (n = 3) for four analytes, respectively) and broader analyte peaks relative to the mixed surfactant system. A clear baseline resolution was achieved for four analytes using the same BGE with 0.1 mM SDS and 0.5 mM TDAPS, with separation efficiencies of Tyr, Hcy, Cys, and GSH of 56,000 ± 2,600, 82,000 ± 4,400, 120,000 ± 7,100, and 92,000 ± 6,500 plates/m (n = 3) (corresponding to 2,700 ± 120, 4,000 ± 210, 5,800 ± 340, 4,400 ± 310 plates), respectively, while separations using only SDS resulted in co-migration. Under this surfactant condition, LODs of Tyr, Hcy, Cys, and GSH are 4.5 ± 1.2 μM, 4.3 ± 1.4 μM, 5.6 ± 1.9 μM, and 15.8 ± 4.8 μM, (n = 3 and S/N = 3), respectively. Additionally, analyte resolution improved with the increase of relative TDAPS concentration. Comparisons of resolution and separation efficiency for these four analytes under different conditions are shown in Figure 5.4 and Table 5.2.

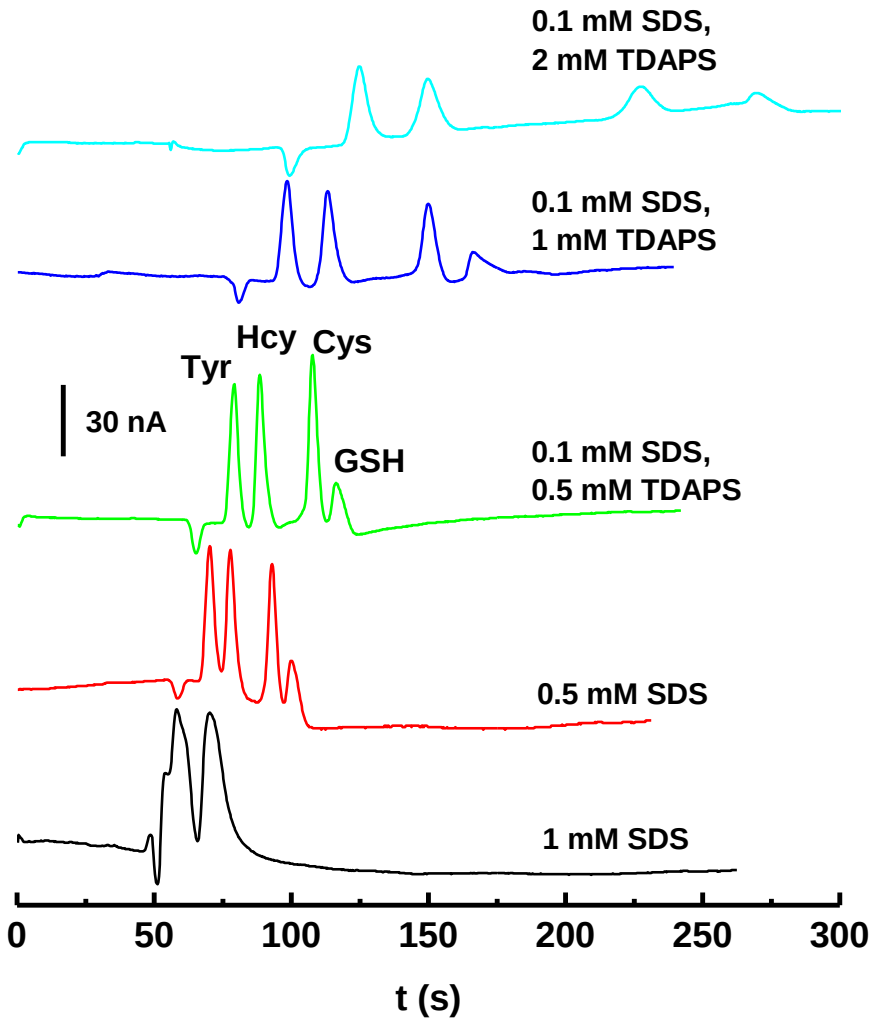


**Figure 5.3** Example electropherograms for 200 µM Tyr, Hcy, Cys and 600 µM GSH in 20 mM boric acid buffer at pH 9.2 with various surfactant conditions (mixed SDS/TDAPS system). Experimental conditions: separation field strength: 123 V/cm, 3-s gated injection; detection: PAD, $E_{det}$ = 1.6 V.

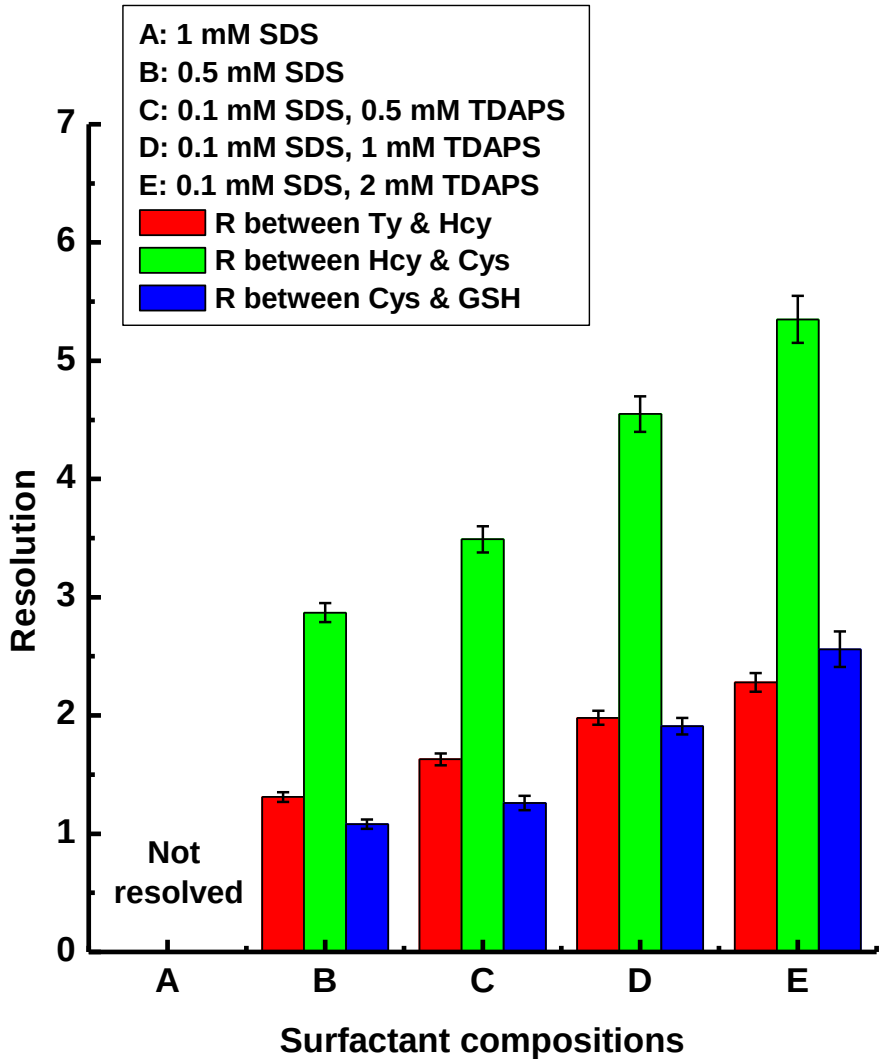


**Figure 5.4** Comparison of resolution results of Tyr, Hcy, Cys and GSH calculated from peak information in electropherograms under different surfactant conditions

**Table 5.2.** Comparisons of separation efficiency results of Tyr, Hcy, Cys and GSH under different surfactant conditions.

| | Separation efficiency (plates/m) (number in plates) | | | |
|---|---|---|---|---|
| | Ty | Hcy | Cys | GSH |
| 0.1 mM SDS, 2 mM TDAPS | 52,630 ± 4,210 (2,500 ± 200) | 50,950 ± 3,370 (2,420 ± 160) | 101,260 ± 9,050 (4,810 ± 430) | 127,160 ± 9,680 (6,040 ± 460) |
| 0.1 mM SDS, 1 mM TDAPS | 59,160 ± 3,160 (2,810 ± 150) | 69,680 ± 4,210 (3,310 ± 200) | 99,160 ± 5,470 (4,710 ± 260) | 100,840 ± 7,160 (4,790 ± 340) |
| 0.1 mM SDS, 0.5 mM TDAPS | 56,440 ± 2,600 (2,680 ± 120) | 81,680 ± 4,400 (3,880 ± 210) | 121,270 ± 7,100 (5,760 ± 340) | 91,570 ± 6,500 (4,350 ± 340) |
| 0.5 mM SDS | 43,360 ± 1,900 (2,060 ± 90) | 61,680 ± 3,160 (2,930 ± 150) | 104,210 ± 6,740 (4,950 ± 320) | 67,380 ± 4,420 (3,200 ± 210) |
| 1 mM SDS | N/A | | | |

### 5.2.2 Separation and detection of GSH in human RBCs

Glutathione is the most abundant intracellular non-enzymatic component of the antioxidant system found in healthy RBCs, existing mainly in its reduced form, and is important as a diagnostic marker of oxidative stress.[10, 11] To demonstrate the ability of the mixed SDS/TDAPS surfactant system to improve separations in real samples, the determination of GSH in human RBCs was performed using PAD with 0.1 mM SDS and 0.5 mM TDAPS in 20 mM boric acid buffer at pH 9.2. Electropherograms of this analysis are given in Figure 5.5. A main analyte peak, eluting at 131.2 s, corresponded to the GSH in the hemolysate was confirmed by spiking with 100 μM reduced GSH. Here, the analyte peak of Cys was not observed since it is present at low levels in erythrocyte hemolysate samples.[12, 13] The concentration of GSH in the 4x diluted hemolysate sample was determined by standard addition to be 379 ± 52 μM (n = 3), which corresponded to a concentration of 1.52 ± 0.21 mM GSH in RBCs. The recovery under

this condition for GSH in the RBCs was between 90.2% and 96.4%, and the measured GSH concentration was within the normal reference interval.[12-15]

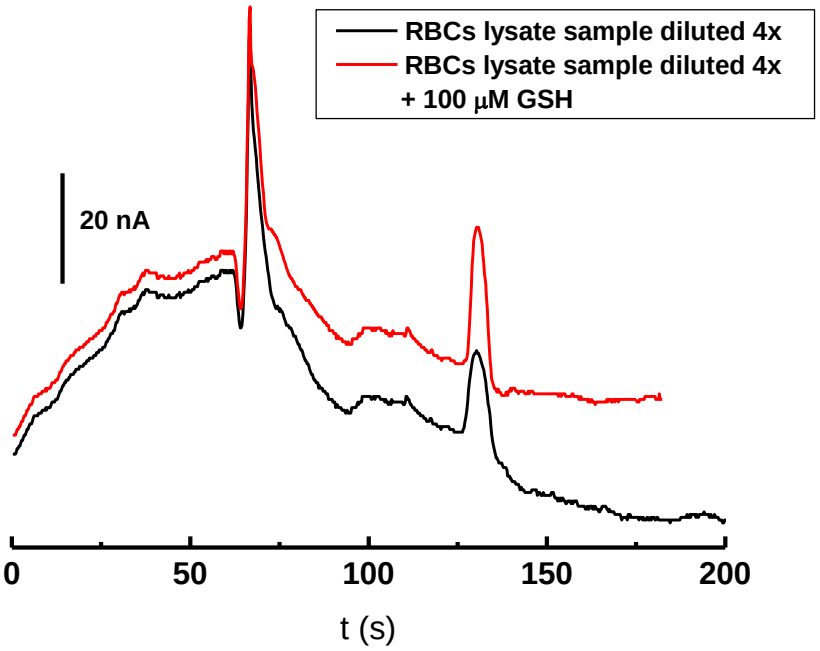


**Figure 5.5** Electropherograms of 4× diluted hemolysate samples of RBCs without and with the standard solution containing 100 μM GSH. BGE: 20 mM Boric acid, 0.1 mM SDS, 0.5 mM TDAPS, pH 9.2. Experimental conditions: separation field strength: 123 V/cm, 3-s gated injection; Detection: PAD, $E_{det}$ = 1.6 V.

### 5.2.3 Separation applications using mixed SDS/nonionic surfactant systems

Next, the BGEs containing mixed surfactants SDS/(Tween 20, Triton X-100, or PEG 400) were employed for the separation of Tyr and three aminothiols (Hcy, Cys and GSH) as part of a study aimed at measuring changes in GSH concentration in the presence of environmental

oxidants. Electropherograms for 50 μM Tyr, Hcy, and Cys as well as 150 μM GSH using various mixed surfactant compositions are shown in Figure 5.6, 5.7 and 5.8 for mixed SDS/PEG 400, SDS/Tween 20, and SDS/Triton X-100 systems, respectively. As depicted in Figure 5.6, the longest (106.3 ± 3.8, 127.5 ± 4.1, 173.0 ± 6.9, and 223.0 ± 9.9 s, n = 3) and shortest (65.8 ± 2.2, 73.5 ± 2.3, 86.3 ± 2.8, and 95.75 ± 3.0 s, n = 3) migration times were obtained for Tyr, Hcy, and Cys and GSH, using PEG 400 (2 mM) and SDS (1 mM) alone, respectively. Clear baseline separations were achieved for these four analytes with their migration times increasing as the SDS/PEG 400 ratio decreased. Additionally, analyte resolution improved as PEG 400 concentration increased, which is expected when reducing the electroosmotic flow. Among the tested mixtures of SDS and PEG, the mixture containing 2 mM SDS and 2 mM PEG 400 produced the greatest peak heights (23.2 ± 1.9, 22.1 ± 1.8, 30.5 ± 2.7, and 21.5 ± 1.5 nA, n = 3) for 50 μM Tyr, Hcy, and Cys as well as 150 μM GSH respectively, with their separation efficiencies of 50,000 ± 2,200, 50,000 ± 2,000, 80,000 ± 4,400, and 53,000 ± 2,600 plates/m (n = 3) (corresponding to 2,500 ± 110, 2,500 ± 100, 4,000 ± 220, 2,600 ± 130 plates), respectively. Resolution between adjacent analytes were 1.69 ± 0.10 (Tyr/Hcy), 2.39 ± 0.17 (Hcy/Cys), and 1.80 ± 0.12 (Cys/GSH) (n = 3). Under this surfactant condition, LODs of Tyr, Hcy, Cys, and GSH are 2.5 ± 0.7, 2.5 ± 0.6, 1.5 ± 0.4, and 10.0 ± 2.8 μM (n = 3 and S/N = 3), respectively. Similar separation performance was observed for another two mixed SDS/nonionic surfactant systems, with the migration times of four analytes increasing as a decrease in the SDS/(Tween 20 or Triton X-100) ratio. To compare these mixed surfactant systems, normalized peak area ratios of four analytes in three specific mixed SDS/nonionic surfactant conditions are shown in Figure 5.9. Here, the peak area of each analyte was normalized according to its corresponding sample injection volume based on EOF calculation and compared with that obtained using the 0.5 mM

SDS, 0.5 mM TDAPS BGE to get the final normalized peak area ratio. Larger normalized peak areas were realized for SDS/PEG mixtures compared to those in the SDS/TDAPS system, with the exception of some Triton X-100 results. The detailed mechanism underlying this single enhancement is still unclear. Considering the best combination of peak areas, migration times and resolution, the surfactant mixture containing 2 mM SDS and 2 mM PEG 400 was selected for detection of GSH in RBCs.

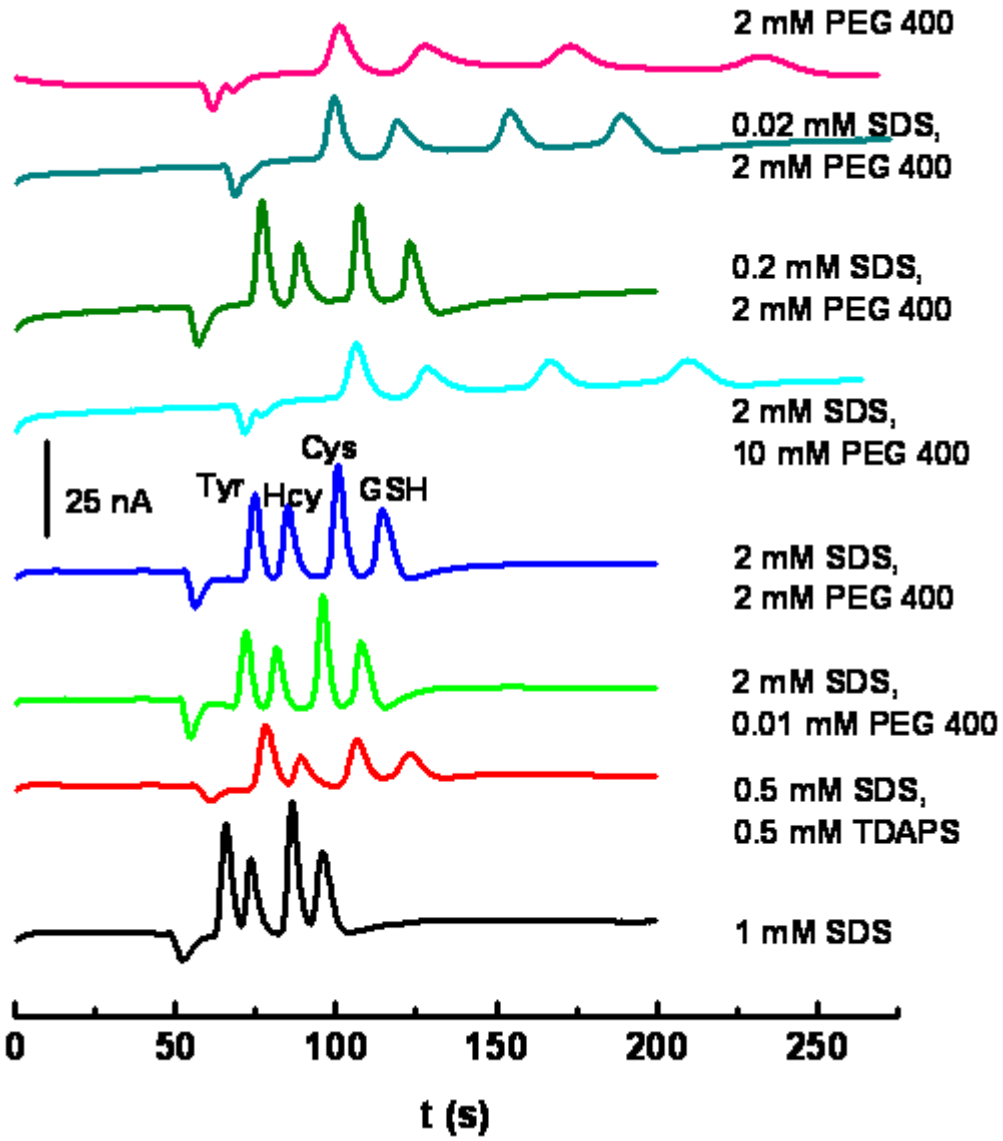


**Figure 5.6** Example electropherograms for 50 μM Tyr, Hcy, Cys and 150 μM GSH in 20 mM boric acid buffer at pH 9.2 with various surfactant conditions (mixed SDS/PEG 400 system). Experimental conditions: separation field strength: 123 V/cm; 3-s gated injection; Detection: PAD, $E_{det}$ = 1.6 V.

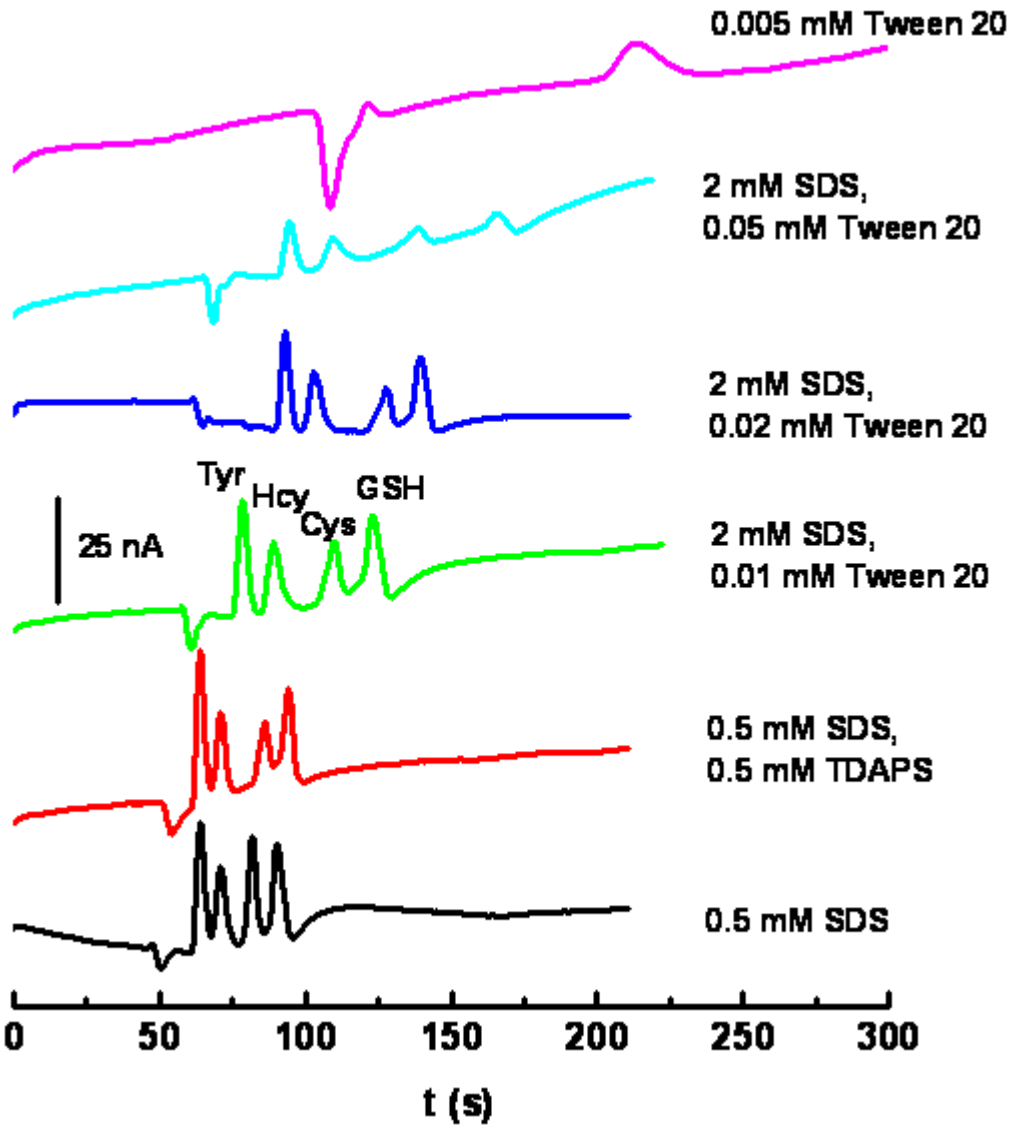


**Figure 5.7** Example electropherograms for 50 μM Tyr, Hcy, Cys and 150 μM GSH in 20 mM boric acid buffer at pH 9.2 with various surfactant conditions (mixed SDS/Tween 20 system). Experimental conditions: separation field strength: 123 V/cm; 3-s gated injection; Detection: PAD, $E_{det}$ = 1.6 V.

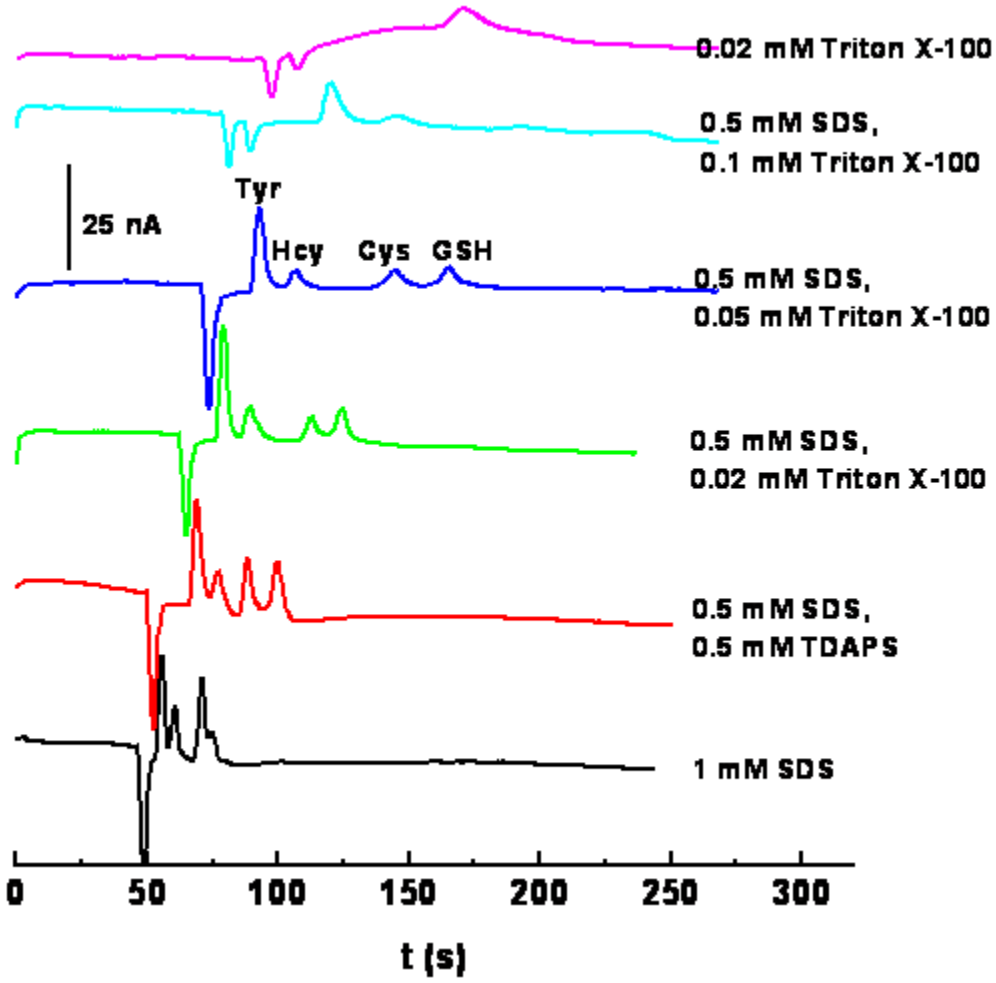


**Figure 5.8** Example electropherograms for 50 μM Tyr, Hcy, Cys and 150 μM GSH in 20 mM boric acid buffer at pH 9.2 with various surfactant conditions (mixed SDS/Triton X-100 system). Experimental conditions: separation field strength: 123 V/cm; 3-s gated injection; Detection: PAD, $E_{det}$ = 1.6 V.

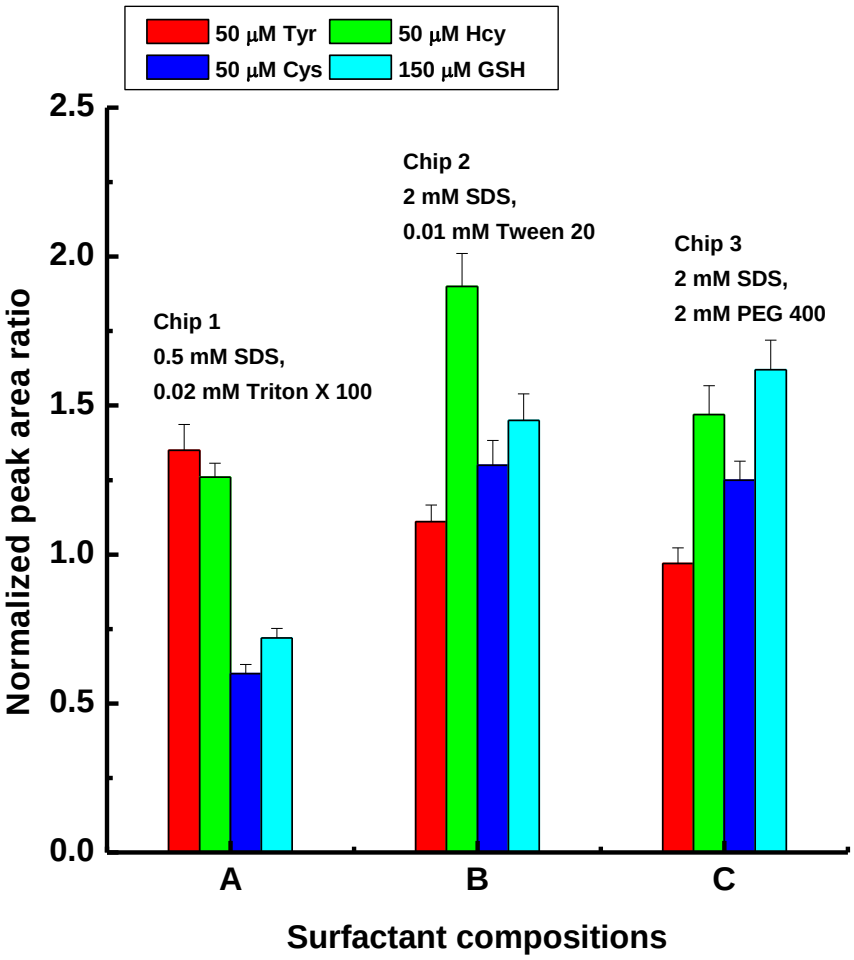


**Figure 5.9** Normalized peak area ratios of four analytes in three specific mixed SDS/nonionic surfactant (Tween 20, Triton X-100, or PEG 400) conditions.

### 5.2.4 Time study of GSH in RBCs exposed to fly ash suspension/$H_2O_2$

Here, GSH was measured as an indicator of fly ash-induced oxidative stress. Similar studies on mammals indicate that fly ash can promote production of reactive oxygen species at physiological conditions.[16] Here, time studies of GSH concentration in human RBCs exposed to fly ash suspension with or without $H_2O_2$ at 2, 4 and 6 hrs, respectively are shown in Figure 5.10. $H_2O_2$ was added to induce Fenton chemistry from transition metals associated with the fly ash

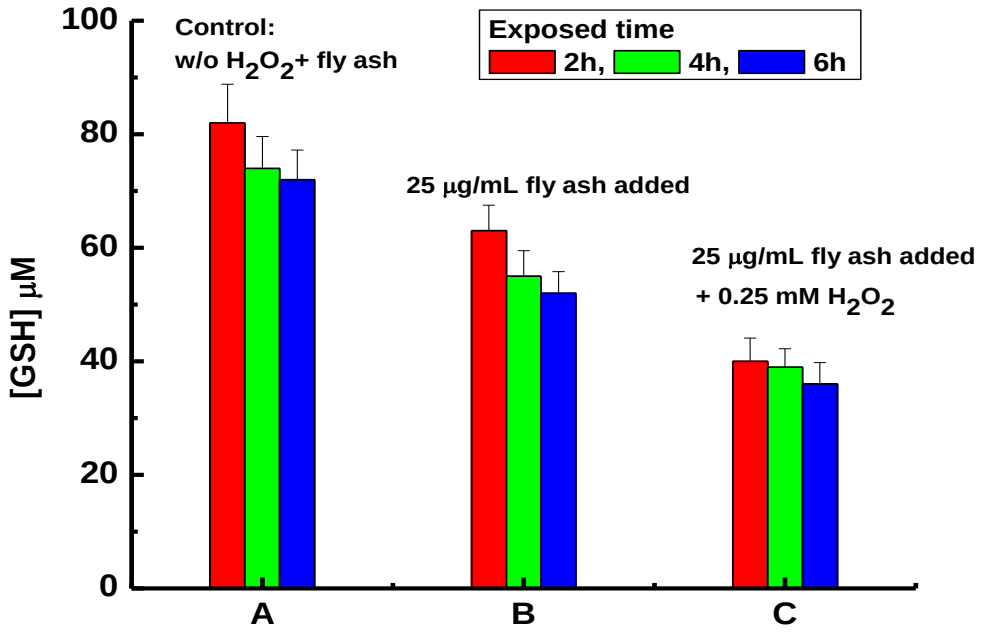


**Figure 5.10** Time study of GSH concentration in RBCs exposed to fly ash suspension with or without $H_2O_2$.

particles.[17] The determination of GSH in RBCs under each exposure condition was performed using PAD with 2 mM SDS and 2 mM PEG 400 in 20 mM boric acid buffer at pH 9.2. As shown in Figure 5.10, significant decreases in GSH concentrations in RBCs exposed to 25 μg/mL fly ash suspension with or without 0.25 mM $H_2O_2$ for 2 h (40.2 ± 4.1 μM and 63.1 ± 4.5 μM, n = 3, respectively) were obtained when compared with the control experiment at the same time period (82.3 ± 6.8 μM, n = 3). Similar behavior was observed for time studies at 4 h and 6 h with further decreases in GSH concentrations due to the extended exposure time. The results of this study demonstrates that fly ash both with and without the present $H_2O_2$ can cause cellular glutathione levels to decrease, indicative of oxidative stress. Furthermore, this result clearly shows the ability of the mixed surfactant system to provide resolution of GSH in the complex cell lysate media.

### 5.2.5 Separation application using mixed TDAPS/Tween 20 surfactant system

The use of mixed TDAPS/Tween 20 surfactant system was also demonstrated for the separation of the neurotransmitters DA, NE, E, and their metabolic precursors L-DOPA and CA. Separations of 20 μM DA, NE, E and 40 μM CA and L-DOPA in 20 mM TES pH 7.0 buffer with various surfactant concentrations were performed (Figure 5.11). The combination of 0.5 mM Tween 20 and 0.5 mM TDAPS gave the longest migration times, while the mixture of 5 μM SDS and 2 mM TDAPS gave the shortest separation times. As the TDAPS/Tween 20 ratio increases, the migration times of DA, NE and E became faster, in agreement with the EOF trend shown in Figure 4.15. This result suggests that electrophoretic mobility and electroosmotic flow are the dominant forces dictating migration time for this set of analytes. However, CA and L-DOPA co-migrated in BGEs without surfactant or BGEs containing Tween 20/TDAPS mixtures with low TDAPS concentration (0.5 mM). A baseline separation was obtained for CA and L-DOPA when using TDAPS alone or mixed surfactant systems containing TDAPS concentrations ≥2 mM. Here, the EOF without surfactant was very similar to that in the BGE with 2 mM TDAPS/0.5 mM Tween 20 mixture as evidenced by the similarity of migration times for DA, NE and E. As the concentration of TDAPS increased from 2 to 4 mM in the presence of 0.5 mM Tween 20, however, the migration time for CA and L-DOPA increased as did the separation between NE and CA peaks. The slower CA and L-DOPA migration can be attributed to interactions between these two analytes and micelles formed from the surfactant mixture. Furthermore, the resolution between CA and L-DOPA also increased ((2 mM TDAPS/0.5 mM Tween 20: 1.29 ± 0.07, 4 mM TDAPS/0.5 mM Tween 20: 1.46 ± 0.08). Determining the exact nature of the interaction and the composition of the micelles are beyond the scope of the current work, however, some insight can be gained from prior work on mixed micelles. First, the

increase in migration time for both CA and L-DOPA suggest an apparent negative charge to the micelle that would result from surface exposed sulfate groups on TDAPS. The cationic amine functionality of TDAPS would be buried in the micelle and therefore not contribute to the apparent mobility. The charge is supported by the fact that both CA and L-DOPA, which are neutral at pH 7.0, migrate slower than the electroosmotic flow based on their co-migration in the surfactant free electropherogram of Figure 5.11. Second, prior work on the separation of cationic amines using mixtures of SDS and Tween 20 showed that increases in the Tween concentration relative to the TDAPS reduced the overall interaction.[18] In the results shown here, it is reasonable to conclude based on this prior work that Tween 20 moderates the interaction between the analytes and TDAPS and thus increasing the TDAPS concentrations results in greater retention by the micelles.

The resolution between analytes for all surfactant systems was compared (Figure 5.12). The mixture of 0.5 mM TDAPS and 0.5 mM Tween 20 gave the highest resolution of 1.27 ± 0.07 and 1.10 ± 0.05 (n = 3) for DA/NE and NE/E, respectively, due to the slow EOF in this surfactant system. Unfortunately, CA and L-DOPA co-migrated in this BGE. The highest resolution where all compounds were partially resolved (DA/NE: 1.18 ± 0.05, NE/E: 0.98 ± 0.05, and CA/L-DOPA: 2.34 ± 0.09, n = 3) was obtained for the BGE containing only 2 mM TDAPS. However, the resolution (DA/NE: 1.08 ± 0.06, NE/E: 0.94 ± 0.05, and CA/L-DOPA: 1.46 ± 0.08, n = 3) obtained for the BGE with 4 mM TDAPS/0.5 mM Tween 20 mixture was statistically identical to the 0.5 mM TDAPS/0.5 mM Tween BGE but provided significantly higher peaks as shown in the Figure 5.11

The 4 mM TDAPS/0.5 mM Tween 20 BGE gave peak heights of 1.28 ± 0.11 nA for DA, 1.17 ± 0.12 nA for NE, 1.33 ± 0.12 nA for E, 0.66 ± 0.05 nA for CA, and 1.21 ± 0.13 nA for L-

DOPA (n = 3), while the mixed 0.5 mM Tween 20/0.5 mM TDAPS surfactants gave the significantly lower peak heights (DA: 0.66 ± 0.06 nA, NE: 0.54 ± 0.06 nA, E: 0.57 ± 0.05 nA, CA and L-DOPA: 0.31 ± 0.03 nA, n = 3). Differences in peak height are unlikely to be the result of differences in injection volume because hydrodynamic injection was used and the solution viscosities are all similar. The exact mechanism is not clear at this point, however, may be the result of enhanced solubility of the oxidized products in the 4.0 mM TDAPS/0.5 mM Tween 20 BGE. Prior work has shown similar results with pure alkyl sulfate BGEs.[19] Considering both peak height and analyte resolution the BGE composed of 4 mM TDAPS and 0.5 mM Tween 20 was chosen for the analysis of catecholamines released from PC12 cells. The separation efficiencies for 20 μM DA, NE, E and 40 μM CA and L-DOPA under this separation condition were 182,000 ± 8,500, 139,000 ± 7,500, 223,000 ± 12,000, 160,000 ± 9,500, and 141,000 ± 11,000 plates/m (n = 3) (corresponding to 18,200 ± 850, 13,900 ± 750, 22,300 ± 1,200, 16,000 ± 950, and 14,100 ± 1,100 plates). The LODs using this mixed surfactant system were 1.5 ± 0.1 μM, 1.5 ± 0.1 μM, 1.2 ± 0.1 μM, 3.5 ± 0.3 μM, and 2.5 ± 0.2 μM (n = 3, and S/N = 3) for DA, NE, E, CA and L-DOPA, respectively. Additional reductions in the concentration detection limit could be achieved by increasing the injection time, adjusting the channel dimensions, and/or application of sample stacking techniques.

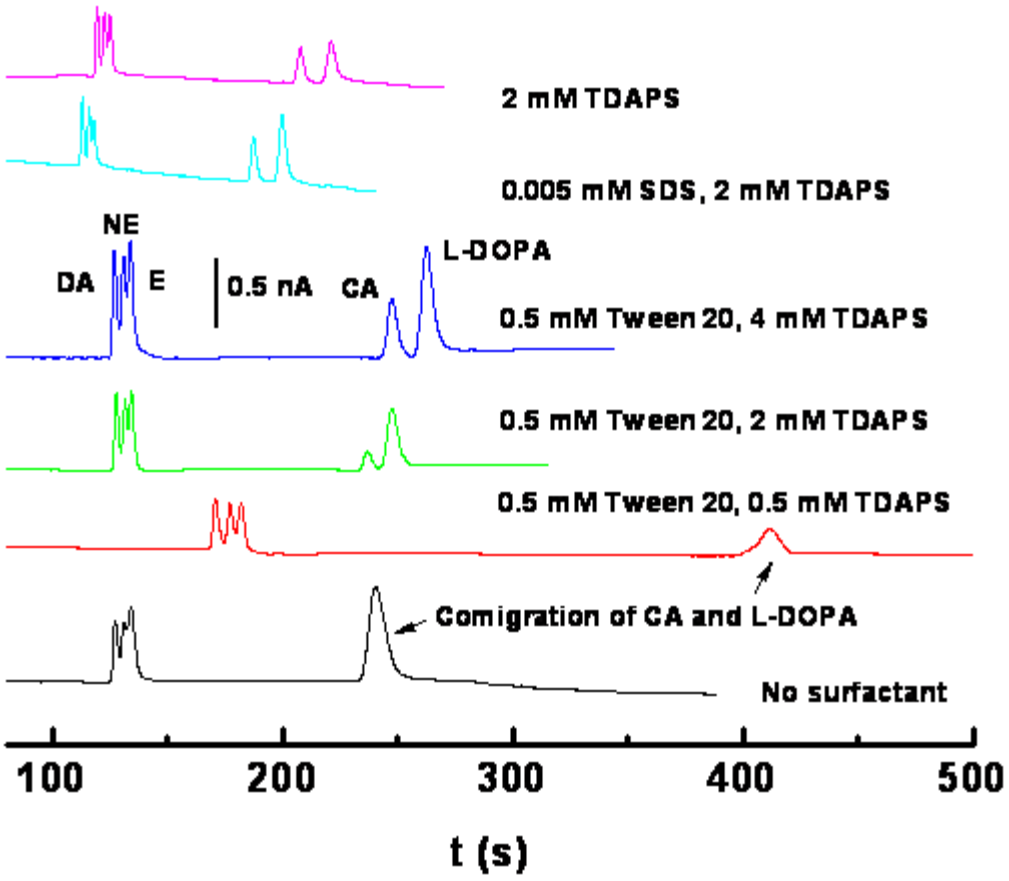


**Figure 5.11** Example electropherograms for 20 µM DA, NE, E and 40 µM CA and L-DOPA in 20 mM TES buffer at pH 7.0 as a function of surfactant composition. Experimental conditions: separation field strength: 150 V/cm; 10-s hydrodynamic injection; Detection: DC Amp., $E_{det}$ = 1.2 V.

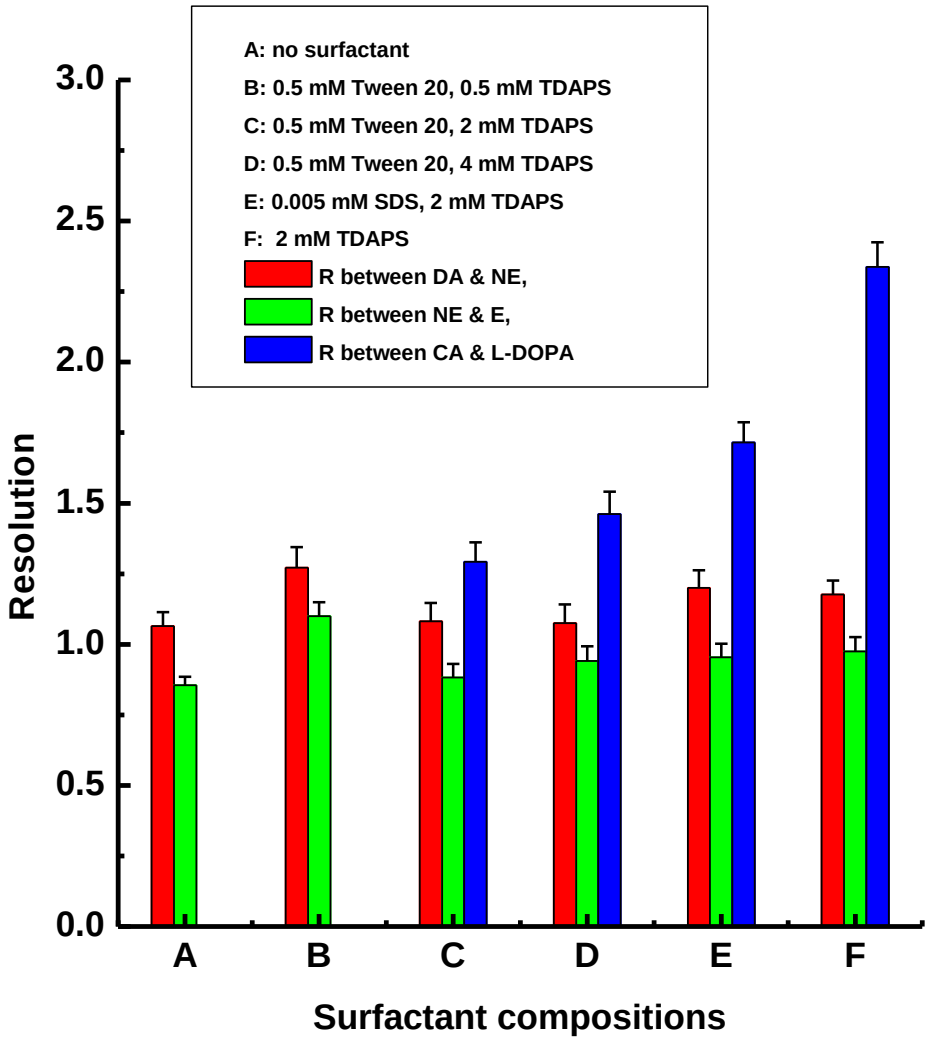


**Figure 5.12** The resolutions between analytes for all tested surfactant systems.

### 5.2.6 Catecholamine release from PC12 cells by stimulation with 80 mM $K^+$

Due to their role in the brain, neurotransmitters (catecholamines: DA, NE, and E) are of considerable interest.[20] Rat pheochromocytoma (PC12) cells have been used as a model for the developing sympathetic nerve since this clone cell line exhibits many of the physiological properties of sympathetic ganglion neurons.[21, 22] The NE/DA ratio in PC12 cells varies from

0.003 to 0.53, [23, 24] with no detectable level of E. Electropherograms of catecholamine release from a PC12 cell population by stimulation with 80 mM $K^+$ as well as the same sample spiked with standards using a BGE composed of 0.5 mM Tween 20 and 4 mM TDAPS are shown in Figure 5.13. The only detectable catecholamine released from these PC12 cells is DA according to its migration time and the increased peak height observed on addition of standards. NE may also be present here but is below our detection limit. The analyte concentration was determined to be 4.96 ± 0.25 μM (n = 3) in 2× diluted sample, corresponding to 9.92 ± 0.53 μM (64.42 ± 3.41 pM/cell) DA released from PC12 cells (1.54 x $10^5$ cells). The recovery of DA from spiking with standards is 96.3 ± 5.4%. Ewing's group reported that PC12 cell vesicles contain an average catecholamine concentration of 110 mM and release just 0.06% of this concentration, or 67 μM (190 zmol/vesicles), during exocytotic events.[25, 26] Another publication by Martin's group indicated that 20–160 μM DA (153–1230 pM/cell) following calcium stimulation was released from PC12 cells.[27] While the amount of catecholamine detected here is lower than previously published, it was in agreement with results (58.3 pM/cell) for carbon paste electrodes modified with multi-walled carbon nanotubes.

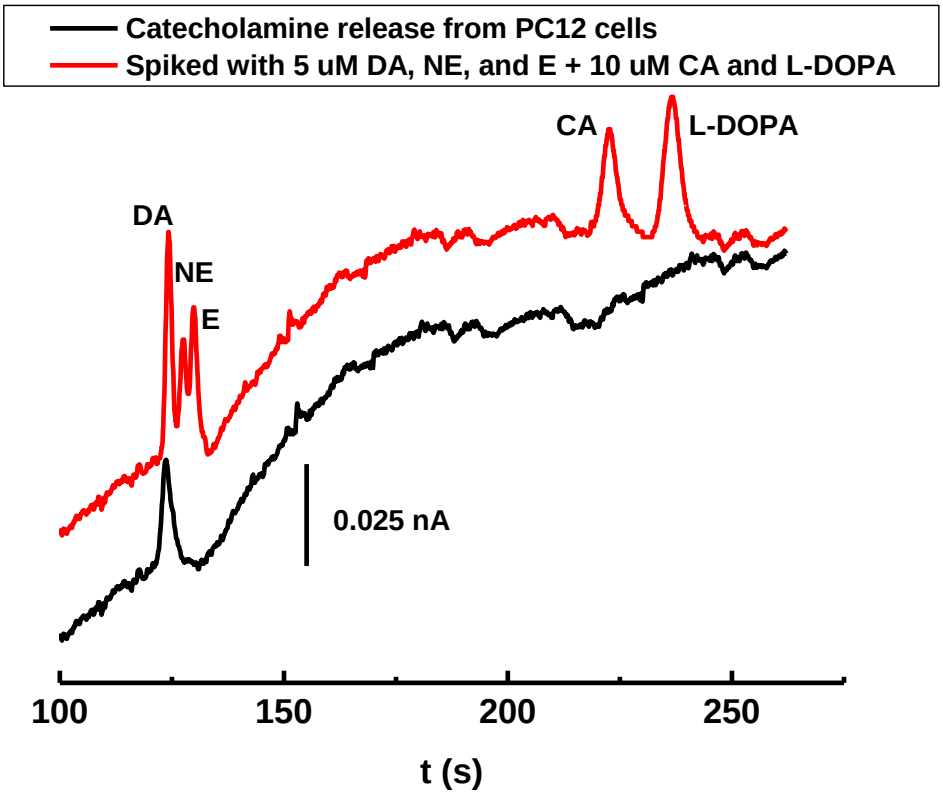


**Figure 5.13** Electropherograms of catecholamine release from PC12 cells by stimulation with 80 mM $K^+$ in 2× diluted sample and with the standard solution containing 5 μM DA, NE, E and 10 μM CA and L-DOPA. BGE: 20 mM TES, 0.5 mM Tween 20, 4 mM TDAPS, pH 7.0. Experimental conditions: separation field strength: 150 V/cm; 10-s Hydrodynamic injection; Detection: DC Amp., Edet = 1.2 V.

## 5.3 CONCLUSIONS

The use of three mixed surfactant systems (ionic/zwitterionic, ionic/nonionic and zwitterionic/nonionic) on PDMS microchips to control EOF and improve separation was reported. First, electrophoretic separation and electrochemical detection of two groups of model analytes (Group 1: DA, CA and AA; Group 2: Tyr, Hcy, Cys and GSH) using mixtures of SDS

and TDAPS surfactants was performed. Faster analysis times and/or improved resolutions for some model analytes were achieved in these mixed surfactants relative to the single surfactant system. By using the optimal mixed SDS/TDAPS surfactant composition, the concentration of GSH in RBCs was determined to be 1.45 ± 0.08 mM, which is in the normal reference interval for this analyte. Next, separation and electrochemical detection of two groups of model analytes (Group 1: DA, NE, E, CA and L-DOPA; Group 2: Tyr, Hcy, Cys and GSH) were explored using mixed zwitterionic/nonionic and ionic/nonionic surfactant systems, respectively, and compared with the above mixed SDS/TDAPS surfactants. Analyte resolution was maintained and peak height was increased in mixed surfactant BGEs containing the nonionic surfactant relative to the single surfactant system. Finally, by using a mixed surfactants composed of 0.5 mM Tween 20 and 4 mM TDAPS, the catecholamine released from PC12 cells by stimulation with 80 mM $K^+$ was determined as DA at a concentration of 64.42 ± 3.41 pM/cell, with a recovery of 96.3 ± 5.4%. GSH in RBCs exposed to fly ash suspension with or without $H_2O_2$ using the mixed surfactants with 2 mM SDS and 2 mM PEG 400 was also determined. The results of time study demonstrated that both fly ash constituents and $H_2O_2$ exposures caused cellular glutathione levels to decrease, with potential to allow oxidative stress.

## 5.4 REFERENCES


(1) Sameenoi, Y., Mensack, M. M., Boonsong, K., Ewing, R., Dungchai, W., Chailapakul, O., Cropek, D. M., Henry, C. S., *Analyst* **2011**, *136*. 3177-3184.
(2) Griffith, O. W., *Analytical biochemistry* **1980**, *106*. 207-212.
(3) McDonald, J. C., Duffy, D. C., Anderson, J. R., Chiu, D. T., Wu, H., Schueller, O. J., Whitesides, G. M., *Electrophoresis* **2000**, *21*. 27-40.
(4) Vickers, J. A., Henry, C. S., *Electrophoresis* **2005**, *26*. 4641-4647.
(5) Guan, Q., Henry, C. S., *Electrophoresis* **2009**, *30*. 3339-3346.
(6) Garcia, C. D., Liu, Y., Anderson, P., Henry, C. S., *Lab on a Chip* **2003**, *3*. 324-328.
(7) Lin, C. C., Chen, C. C., Lin, C. E., Chen, S. H., *Journal of chromatography. A* **2004**, *1051*. 69-74.
(8) Jacobson, S. C., Koutny, L. B., Hergenroder, R., Moore, A. W., Ramsey, J. M., *Analytical Chemistry* **1994**, *66*. 3472-3476.
(9) Wallingford, R. A., Ewing, A. G., *Analytical Chemistry* **1988**, *60*. 258-263.
(10) Costagliola, C., *Clinical physiology and biochemistry* **1990**, *8*. 204-210.
(11) Beard, K. M., Shangari, N., Wu, B., O'Brien, P. J., *Molecular and cellular biochemistry* **2003**, *252*. 331-338.
(12) Calvo-Marzal, P., Chumbimuni-Torres, K. Y., Hoehr, N. F., Kubota, L. T., *Clinica chimica acta; international journal of clinical chemistry* **2006**, *371*. 152-158.
(13) Luz, R. C. S., Maroneze, C. M., Tanaka, A. A., Kubota, L. T., Gushikem, Y., Damos, F. S., *Microchimica Acta* **2010**, *171*. 169-178.
(14) Weinstein, R. S., Surgenor, D. M. (Ed.), *The Red Blood Cell*. Academic Press: New York 1974.
(15) Jocelyn, P. C., *Biochemical Journal* **1960**, *77*. 363-368.
(16) van Maanen, J. M., Borm, P. J., Knaapen, A., van Herwijnen, M., Schilderman, P. A., Smith, K. R., Aust, A. E., Tomatis, M., Fubini, B., *Inhalation toxicology* **1999**, *11*. 1123-1141.
(17) Winterbourn, C. C., *Toxicology letters* **1995**, *82-83*. 969-974.
(18) Esaka, Y., Tanaka, K., Uno, B., Goto, M., Kano, K., *Analytical Chemistry* **1997**, *69*. 1332-1338.
(19) Ding, Y., Mora, M. F., Merrill, G. N., Garcia, C. D., *The Analyst* **2007**, *132*. 997-1004.
(20) Adams, R. N., *Analytical Chemistry* **1976**, *48*. 1126A-1138A.
(21) Greene, L. A., Tischler, A. S., *Proceedings of the National Academy of Sciences of the United States of America* **1976**, *73*. 2424-2428.
(22) Shafer, T. J., Atchison, W. D., *Neurotoxicology* **1991**, *12*. 473-492.
(23) Takashima, A., Koike, T., *Biochimica et biophysica acta* **1985**, *847*. 101-107.
(24) Clift-O'Grady, L., Linstedt, A. D., Lowe, A. W., Grote, E., Kelly, R. B., *The Journal of cell biology* **1990**, *110*. 1693-1703.
(25) Chen, T. K., Luo, G. O., Ewing, A. G., *Analytical Chemistry* **1994**, *66*. 3031-3035.
(26) Kozminski, K. D., Gutman, D. A., Davila, V., Sulzer, D., Ewing, A. G., *Analytical Chemistry* **1998**, *70*. 3123-3130.
(27) Li, M. W., Spence, D. M., Martin, R. S., *Electroanalysis* **2005**, *17*. 1171-1180.

# CHAPTER 6. CONCLUSIONS AND FUTURE DIRECTIONS

## 6.1 DISSERTATION SUMMARY

The focus of this dissertation has been the development of a microchip capillary electrophoresis coupled electrochemical detection (MCE-ECD) device based on our previous design with improved separation and detection performance using detection geometry, on-line preconcentration and surface modification.

The first milestone toward the overall project goal was to improve the detection sensitivity and detection limits (LODs) of our previous MCE-ECD system. The first effort for this purpose was established by an implementation of a capillary expansion (bubble cell) at the detection zone. Bubble cell widths were varied from 1× to 10× the separation channel width (50 μm) to investigate the effects of electrode surface area on detection sensitivity, LOD, and separation efficiency. Improved detection sensitivity and decreased LODs were obtained with increased bubble cell width, and LODs of dopamine and catechol detected in a 5× bubble cell were 25 nM and 50 nM, respectively. In addition, fluorescent imaging results demonstrate ~8% to ~12% loss in separation efficiency in 4× and 5× bubble cell, respectively. Considering the balance between the loss in separation efficiency and improved detection sensitivity as well as detection limit in a large bubble cell, microchips with a 4× bubble cell in the detection zone were selected for further experiments performed with sample stacking techniques or surface modification using mixed surfactants. The second effort for enhancing detection sensitivity and reducing the LOD involves using field amplified sample injection and field amplified sample stacking. Stacking effects were shown for both methods using amperometric detection and

pulsed amperometric detection (PAD) with increased peak height, decreased HPW and improved detection sensitivity. Using stacking in conjunction with a 4× bubble cell, LODs of 8 and 20 nM for dopamine by using FASI and FASS were obtained respectively. However, these stacking techniques did not significantly improve LODs for anionic analytes. The work presented in this part was published in *Electrophoresis* in 2009.[1]

The second milestone toward the overall goal of this project was to improve the separation performance of our MCE-ECD device in poly(dimethylsiloxane) (PDMS) substrate by performing surface modification using mixed surfactants. Mixed surfactant systems represent an interesting alternative to single surfactant systems and their abilities for better control of EOF and separation chemistry are presented in this thesis. Representative single and mixed surfactant systems were chosen to study their EOF behavior with a PDMS substrate. These surfactants included a single anionic surfactant (sodium dodecyl sulfate, SDS), a single zwitterionic surfactant (N-tetradecylammonium-N, N-dimethyl-3-ammonio-1-propane sulfonate, TDAPS), three nonionic surfactants, (polyoxyethylene (20) sorbitan monolaurate (Tween 20), polyoxyethylene octyl phenyl ether (Triton X-100), polyethylene glycol, (PEG 400)), and three mixed surfactant systems: ionic/zwitterionic (SDS/TDAPS), ionic/nonionic (SDS/Tween 20, SDS/Triton X-100, and SDS/PEG 400) and zwitterionic/nonionic (TDAPS/Tween 20, TDAPS/Triton X-100, and TDAPS/PEG 400). EOF measurements as a function of the surfactant concentration were first performed using the current monitoring method with SDS, TDAPS, and a mixed SDS/TDAPS surfactant system. SDS increased the EOF as reported previously while TDAPS showed an initial increase in EOF followed by a reduction in EOF at higher concentrations. The mixed SDS/TDAPS surfactant system allowed tuning of the EOF across a range of pH and concentration conditions, with higher EOF values and expanded EOF windows

as compared to a single surfactant. Also, the correlation between EOF and surfactant concentration demonstrated that EOF could be tuned over a range of values based on the surfactant ratio. In addition, SDS exhibited faster adsorption/desorption rates than TDAPS. In all cases, the initial EOF was not fully recovered after removal of the surfactant, showing a residual amount of surfactant remaining on the PDMS surface. After establishing EOF behavior, separation and electrochemical detection of model analytes using mixtures of these two types of surfactants were performed. Faster analysis times and/or improved resolution for some model analytes were achieved in mixed surfactants relative to the single surfactant system. By using the optimal mixed SDS/TDAPS surfactant composition, the concentration of GSH in RBCs was determined to be 1.45 ± 0.08 mM, which is in the normal reference interval for this analyte. Next, capacitively coupled contactless conductivity detection ($C^4D$) was introduced for EOF measurements on PDMS microchips as an alternative to the current monitoring method to improve measurement reproducibility. EOF measurements as a function of the surfactant concentration were performed simultaneously using both methods for three nonionic surfactants (Tween 20, Triton X-100, PEG 400), mixed ionic/nonionic surfactant systems (SDS/Tween 20, SDS/Triton X-100, and SDS/PEG 400) and mixed zwitterionic/nonionic surfactant systems (TDAPS/Tween 20, TDAPS/Triton X-100, and TDAPS/PEG 400). EOF for the nonionic surfactants decreased with increasing surfactant concentration. Using mixed surfactants, higher EOF values and a wider tunable EOF range was obtained as compared to BGEs containing a single nonionic surfactant. Next, separation and electrochemical detection of two groups of model analytes (catecholamines and aminothiols) were explored using the mixed surfactant systems. Analyte resolution was maintained and peak height was increased in mixed surfactant BGEs containing the nonionic surfactant relative to the single surfactant system. Finally, the

utility of these two mixed surfactant systems for analysis of biologically relevant compounds in complex sample matrixes was demonstrated in two applications. By using a mixed surfactants composed of 0.5 mM Tween 20 and 4 mM TDAPS, the catecholamine released from rat pheochromocytoma (PC12) cells by stimulation with 80 mM $K^+$ was determined as dopamine at a concentration of 9.92 $\pm$ 0.53 μM (corresponding to 64.42 $\pm$ 3.41 pM/cell), with a recovery of 96.3 $\pm$ 5.4%. Reduced glutathione (GSH) in red blood cells (RBCS) exposed to fly ash suspension with or without $H_2O_2$ was also determined using the BGE containing mixed surfactants with 2 mM SDS and 2 mM PEG 400. The results of time study demonstrated that both fly ash constituents and $H_2O_2$ exposures caused cellular glutathione levels to decrease, with potentials to induce oxidative stress while also showing the potential of mixed surfactant system to provide reproducible results in complex samples. Part of this work was published in *Electrophoresis* in 2012[2] and the remaining work has been submitted to *Electrophoresis*.

## 6.2 FUTURE DIRECTIONS

The future of this project lies in a few main areas. The first is to further enhance the stacking impact and improve LOD. The second is to expand the abilities in EOF control and improve separation chemistry by exploring the EOF behaviors of different mixed surfactant systems with different polymeric substrate materials. By integrating these changes with other improvements developed in our group, the ultimate project goal would be to develop a lab-on-a-chip device for direct metabolic profiling of multiple redox markers with highly efficient separation as well as sensitive detection reaching detection limit at nM.

For the optimization of stacking conditions in field amplified sample injection and field amplified sample stacking on MCE-ECD system, the next logical step may include using either

narrow channel, inversion of the applied electric field, or negative pressure for the introduction of large volume of low-conductivity sample solution. Additionally, other on-line sample preconcentration methods, such as solid phase extraction (SPE), can be tested for the compatibility with electrochemical detection. The LODs of catecholamines and amionthiols tested in our current MCE-ECD system are not low enough for the detection of analyte of interest with low concentrations in complex biological samples. The use of chemically modified electrodes, such as carbon paste electrodes (CPEs) modified with multi-walled carbon nanotubes (MWCNT) or cobalt phthalocyanine (CoPC) can selectively enhance the detection of specific analytes in a complex mixture.[3] The integration of both stacking techniques and chemically modified electrodes on our current MCE-ECD system will has the potential for a further decrease in LOD to reach detection limit at nM.

Besides the mixed anionic/zwitterionic, anionic/nonionic, zwitterionic/nonionic systems (EOF working window is approximately 1to 8 $\cdot 10^{4}$ $cm^{2}$ $V^{-1}s^{-1}$) discussed in this thesis, our group also studied the EOF behavior of another type of mixed surfactant systems (cationic (cetyltrimethylammonium bromide (CTAB) or tetraadecyltrimethylammonium bromide (TTAB)/zwitterionic (N-cetyl-N,N-dimethylammonium-1-propane-3-sulfonate (CDAPS) or TDAPS) and explored the utility of these systems in the separation of several cations commonly found in atmospheric aerosols. The results demonstrated the EOF can be tuned over a broad range (for example: -3 to 3 $\cdot 10^{4}$ $cm^{2}$ $V^{-1}s^{-1}$) based on the ratio of surfactant. It is worthy of testing the different combinations of cationic and nonionic surfactant in our future work for studing their EOF behavior. Numerous polymers have been used as substrate materials for MCE, including PDMS,[4] poly(methyl methacrylate) (PMMA),[5, 6] polycarbonate (PC),[7] thermoset polyester (TPE)[8, 9], and cyclic olefin copolymer (COC).[10] As compared to the long time and high cost

consumed in the fabrication of glass chips, most polymeric microchips can be fabricated outside a cleanroom environment and have a wide choice in microfabrication techniques. PDMS is the most popular used polymeric material due to its low cost, good optical clarity and elasticity,[11] while it suffer poor separation performance as a result of the hydrophobicity of the bulk materials and a fast hydrophobic recovery (< 30 min) of the microchannel surface.[12-14] In contrast with PDMS, PMMA and PC give better separation efficiencies, a more uniform surface charge and a resistance to adsorbing hydrophobic materials.[6, 7] TPE has shown promise as a merger between the ease of fabrication and cost effectiveness of PDMS with the higher separation efficiencies (~100, 000 N/m for neutral compounds) and increased stability of PMMA and PC.[8] EOF within microfluidic devices made from polymers can vary widely due to the diversity of the surface-exposed functional groups. In addition, the zeta potential of these materials that gives rise to the EOF is often less than optimal for a specific separation. Our current results demonstrate the usefulness of mixed micellar surfactant systems to affect EOF and achieve better resolution of biologically relevant compounds in complex sample matrixes. Therefore, it would be necessary to further explore the EOF behaviors with other polymeric substrate modified by either single or mixed surfactant systems. These improvements will enable our MCE-ECD device to have a potential for analysis of a variety of biomolecules with different mobilities in complex biofluids.

## 6.3 REFERENCES


(1) Guan, Q., Henry, C. S., *Electrophoresis* **2009**, *30*. 3339-3346.
(2) Guan, Q., Noblitt, S. D., Henry, C. S., *Electrophoresis* **2012**, *33*. 379-387.
(3) Sameenoi, Y., Mensack, M. M., Boonsong, K., Ewing, R., Dungchai, W., Chailapakul, O., Cropek, D. M., Henry, C. S., *Analyst* **2011**, *136*. 3177-3184.
(4) Duffy, D. C., McDonald, J. C., Schueller, O. J. A., Whitesides, G. M., *Analytical Chemistry* **1998**, *70*. 4974-4984.
(5) Henry, A. C., Tutt, T. J., Galloway, M., Davidson, Y. Y., McWhorter, C. S., Soper, S. A., McCarley, R. L., *Analytical Chemistry* **2000**, *72*. 5331-5337.
(6) Johnson, T. J., Waddell, E. A., Kramer, G. W., Locascio, L. E., *Applied Surface Science* **2001**, *181*. 149-159.
(7) Roberts, M. A., Rossier, J. S., Bercier, P., Girault, H., *Analytical Chemistry* **1997**, *69*. 2035-2042.
(8) Fiorini, G. S., Lorenz, R. M., Kuo, J. S., Chiu, D. T., *Analytical Chemistry* **2004**, *76*. 4697-4704.
(9) Vickers, J. A., Dressen, B. M., Weston, M. C., Boonsong, K., Chailapakul, O., Cropek, D. M., Henry, C. S., *Electrophoresis* **2007**, *28*. 1123-1129.
(10) Ladner, Y., Cretier, G., Faure, K., *Journal of chromatography. A* **2010**, *1217*. 8001-8008.
(11) McDonald, J. C., Whitesides, G. M., *Accounts of chemical research* **2002**, *35*. 491-499.
(12) Fritz, J. L., Owen, M. J., *Journal of Adhesion* **1995**, *54*. 33-45.
(13) Kim, J., Chaudhury, M. K., Owen, M. J., *Journal of colloid and interface science* **2000**, *226*. 231-236.
(14) Kim, J., Chaudhury, M. K., Owen, M. J., Orbeck, T., *Journal of colloid and interface science* **2001**, *244*. 200-207.